DEVELOPMENT OF AN HSV-BASED MODEL SYSTEM TO IDENTIFY EVENTS CRITICAL FOR EMBRYONIC MYOGENESIS

by

April Marie Craft

Bachelors of Science, Westminster College, 2001

Submitted to the Graduate Faculty of

School of Medicine in partial fulfillment

of the requirements for the degree of

Doctor of Philosophy

University of Pittsburgh

2007

UNIVERSITY OF PITTSBURGH

SCHOOL OF MEDICINE

This dissertation was presented

by

April Marie Craft

It was defended on

November 15, 2007

and approved by

Fred Homa, PhD, Associate Professor, Molecular Genetics and Biochemistry

Johnny Huard, PhD, Professor, Cellular and Molecular Pathology

Neil Hukriede, PhD, Assistant Professor, Molecular Genetics and Biochemistry

Paul Robbins, PhD, Professor, Molecular Genetics and Biochemistry

Thomas Smithgall, PhD, Professor, Molecular Genetics and Biochemistry

Dissertation Advisor: Joseph C. Glorioso, III, PhD, Chairman and Professor, Molecular Genetics and Biochemistry

DEVELOPMENT OF AN HSV-BASED MODEL SYSTEM TO IDENTIFY EVENTS CRITICAL FOR EMBRYONIC MYOGENESIS

April Marie Craft, PhD

University of Pittsburgh, 2007

Muscular dystrophy is a devastating disease in which no treatment or cure exists. A promising therapy for muscular dystrophy is the transplantation of cells that are able to contribute to existing muscle fibers or generate new muscle fibers. While several cell populations have been shown to demonstrate this phenomenon in mouse models, the mechanism by which these cells are able to differentiate into myogenic cells is largely unknown. The goal of this research was to (i) create HSV vectors that are useful for expressing muscle development genes in developing embryos in culture (ii) design strategies to produce and characterize large and diverse HSV vector libraries of expressed genes from different cells or tissues and (iii) design methods by which this expression vector library can be screened for expressed gene functions that participate in skeletal muscle lineage determination. The outcome of these studies were intended to provide a method for exploiting the high level infectivity and growth of HSV in ES cells and germ layer derivatives, the virus ability to accommodate large DNA inserts, and the ability to create vector libraries potentially useful in selection of lineage determining genes based on complementation of virus growth.

The engineering and characterization of a replication defective HSV vector that is useful for the delivery of genes to embryonic stem cells and their derivatives was described. The deletion of ICP4, ICP22 and the conversion of the immediate early genes ICP0 and ICP27 to the early gene class by promoter exchange generated a vector, JDββHE. JDββHE was found to be

non-toxic to ES cells and vector infection of ES cells did not interfere with germ layers formation. This vector was engineered to be dependent on a single IE gene ICP4 for replication. Gene expression from the JDββHE HSV vector, including the expression of eGFP and the early myogenic gene Pax3, was demonstrated in infected ES cells and cells of the embryoid body in a robust and transient manner.

In order to discover genes which contribute to muscle differentiation, a cDNA library was constructed within HSV viral vectors in order to be used in the identification of novel gene functions which play a role in the activation early myogenic promoters. For this purpose, the HSV genome was modified to contain BAC elements as well as the Gateway recombination system, which facilitated efficient incorporation of cDNAs into the vector genome. HSV cDNA vectors expressed gene products at the transcriptional and protein level. Functional analysis of the cDNA inserts demonstrated that the library consisted of at least 15,000 unique genes. Some of these genes have been shown to participate in biological functions related to muscle differentiation, such as Id1 and Cand2.

Finally, a conditional replication strategy was developed by which the recently produced HSV cDNA library could be used to identify genes that activate early myogenic promoters. This study exploited the characteristic of the JDββHE vector in which viral replication can be restored upon introduction of the essential viral gene ICP4. By placing this essential viral gene under the control of the early myogenic promoter Pax3, viral replication was found to be dependent on activation of this cellular promoter in a Pax3-expressing rhabdomyosarcoma cell line. In a similar manner, HSV cDNA library vectors that express a Pax3 activator will be able to replicate in the presence of the conditional ICP4 construct, thereby capturing the relevant gene product by the release of viral progeny into the supernatant.

The future use of this strategy to identify gene products that specifically activate an early myogenic promoter would lead to the testing of these gene products for their ability to induce downstream myogenic gene expression and differentiation. In this manner, a better understanding of early muscle differentiation might be achieved and applied to the use of stem cells in transplantation studies using muscular dystrophy models.

TABLE OF CONTENTS

LIST OF TABLES

LIST OF FIGURES

PREFACE

My accomplishments would not have been possible without my dissertation advisor, Joe Glorioso. His ability to think critically about scientific questions and the excitement he demonstrates for the chance to make a difference will always keep me reaching for the next level in my research and in life. Dr. Darren Wolfe was instrumental in teaching me the basic principles of experimentation and laboratory technique, and I appreciate all that I have learned from him. Thanks to all of my other "mentors," a word that I do not mention lightly, Dr. Bill Goins, Dr. David Krisky, and Dr. James Wechuck. Thank you for guiding me in the right direction and welcoming me into your lives.

I would like to express my sincerest thanks to my thesis committee members, Dr. Fred Homa, Dr. Johnny Huard, Dr. Neil Hukriede, Dr. Paul Robbins, and Dr. Thomas Smithgall, without whom I would have not progressed this far. Thank you for your continued support and advice, and keeping my best interest at heart. I will continue to aspire to be a successfully independent researcher by following your collectively good example. I am especially grateful to Dr. Thomas Smithgall and Dr. Malcolm (Tony) Meyn at the University of Pittsburgh for the training in embryonic stem cell culture, their much appreciated suggestions and discussion regarding experiments and results, and their friendship throughout the years.

I would like to acknowledge several investigators who have contributed to the work presented in this dissertation. Dr. David Krisky and Ying Jiang developed the HSV vector backbone and necessary plasmids to generate JDββHE. Dr. Darren Wolfe initiated the intellectual development and generation of the HSV cDNA library and performed and optimized the Gateway recombination reactions. Dr. Darren Wolfe also generated the necessary bacterial strain HerpesHogs that was used in the construction of the HSV cDNA library. Dr. Rahul Srinivasan and Suchita Chaudhry developed the ion channel selection scheme which resulted in the identification of several cDNA library isolates which were characterized in this dissertation. The parental HSV vectors JDQ0ZEH1 and JDD0Z1 were engineered by Dr. Darren Wolfe and Dr. David Krisky. Dr. James Wechuck optimized HSV vector purification by ion exchange chromatography. Dr. Ali Ozuer and Kyle Grant developed many of the HSV-specific quantitative RT-PCR primer and probe sequences that were used. Many thanks to all involved.

Additionally, I would like to acknowledge Simon Watkins and Sean Alber at the University of Pittsburgh Center for Biological Imaging, Dr. Andrea Gambotto at the University of Pittsburgh for the use of the Becton Dickinson FlowScan, and Dr. Alan Russell at McGowan Institute for Regenerative Medicine for the use of the Zeiss Axiovert fluorescent microscope. We received the Pax3 and Tead2 coding sequences as a gift from Dr. Jonathan Epstein, University of Pennsylvania.

I would like to thank everyone in the lab, past and present, for their friendship, their great sense of humor, and for making both labs (BST and down by the river) feel like my two homes away from home, especially Kyle Grant, Shaohao (George) Huang, Art Frampton, Rahul Srinivasan, Rocel Perez, Adriana Forero, David Clawson, Lilly Laemmle. In addition to her

valued friendship, I also thank Anna Jones for her hard work in keeping our lab running smoothly.

A final thanks to my parents and family for their love and understanding. My husband, Ben Craft, who has been with me since the beginning, has been my rock. He has encouraged me to succeed beyond all expectations and his friendship has kept me strong enough to overcome all of the unexpected hurdles that science presents. For the dedication he has given to me, I would like to dedicate this dissertation to him.

1.0 INTRODUCTION

1.1 MUSCULAR DYSTROPHY

Muscular dystrophy is a group of genetic diseases that causes progressive muscle degeneration in skeletal muscles involved in voluntary movement. The word dystrophy is derived from the Greek word *dys*, which means difficult or faulty and *troph*, which means nourish. The occurrence of muscular dystrophy was first described by physicians in the 1850s when young boys were observed to have muscle weakness, muscle damage, and died at an early age. The French neurologist Guillaume Duchenne did an extensive study of 13 boys with the most common form of muscular dystrophy, which is now referred to as Duchenne muscular dystrophy. Duchenne muscular dystrophy affects one in 3500 males worldwide, and between 400-600 live male births in the Unites States each year [1, 2]. Currently, there are no treatments for muscular dystrophy that will stop or reverse the disease and therefore, there are many efforts for new treatments and possible cures for this unfortunately common ailment.

Muscular dystrophy is caused by a genetic mutation in one of thousands of genes that are related to muscle integrity [3]. Skeletal muscles are bundles of long-multinucleated muscle fibers, made up of individual cells that fuse during development. Muscles are activated in response to a signal that is sent from the brain to the neuromuscular junction via peripheral nerves. At the neuromuscular junction, the release of acetylcholine is able to induce a series of

events that triggers the muscle to contract. To protect muscles from damage that is inflicted during the contraction and relaxation processes, muscle fibers are bound to connective tissues by an outer membrane. The outer membrane is a complex of proteins consisting of dystrophin and glycoprotein family members, and a mutation in one of the genes causes the outer membrane to lose integrity. An enzyme required for the generation of energy for muscle contraction, creatine kinase, is often leaked from the muscle fiber due to the disruption of the outer membrane. This leakage causes increased calcium uptake and eventual death of affected muscle fibers [3]. This (or similar) sequence of events is initiated by simple muscle contraction, and the regularity of this course contributes to the progressiveness of these muscle degenerative diseases.

1.1.1 Nine Major Groups of Muscular Dystrophies

The nine groups of muscular dystrophies are categorized by age of onset [3]. The earliest forms begin in early childhood and include Duchenne MD (DMD), Becker MD, Congenital MD, and Emery-Dreifuss MD. Several become evident during adolescence, including Facioscapulohumeral MD (FSHD) and Limb-girdle MD. Finally, there are three forms that occur in adults, Distal MD, Myotonic MD, and Oculopharyngeal MD (OPMD).

Duchenne muscular dystrophy is the most common form of MD overall, accounting for about half of the reported cases worldwide. DMD is caused by a recessive mutation on the X-chromosome resulting in the absence of the muscle protein dystrophin. Since inheritance is X-linked recessive, DMD primarily affects male children, although females who carry one copy of the mutated gene may show less severe symptoms [4]. An abnormally high level of creatine kinase in the blood can be detected in DMD patients at birth [5]. The degeneration of muscles begins in the upper legs and pelvis and becomes apparent when the affected child has difficulty

walking, has frequent falls, or is unable to run or jump [3]. Many children develop breathing difficulties and increased respiratory infections due to the weakening of the diaphragm muscle. Other common symptoms include lung weakness, cardiomyopathy, bone thinning, and scoliosis (curving of the spine). This devastating disease often causes children to become wheelchair-bound by age 12, and most patients die in their early twenties.

Becker MD patients have a less severe form of DMD in which the protein dystrophin is partially functional, but still insufficient. The onset of Becker MD ranges from age 10 to age 25, and the rate of progression varies greatly, with many individuals living until middle age or later. Early symptoms include walking on one's toes and frequent falls. Some patients lose the ability to walk in their early teens and others may still be able to walk in their mid-thirties. Cardiac impairments in Becker MD patients are less severe than DMD patients.

Congenital MD is a group of autosomal recessive disorders that affect both males and females at birth or by age 2 and is identified when affected children fail to achieve milestones in motor functions and muscle control. Consequential degeneration is limited to skeletal muscle, and may be mild to severe depending on the individual, with many patients unable to sit or stand without assistance. Most congenital muscular dystrophies are caused by a defect in the protein merosin, which is normally found in the connective tissue surrounding muscle fibers. Congenital MD may result in contractures (chronic shortening of the muscles and tendons near joints), a weakened diaphragm, or may affect the central nervous system causing seizures, speech and vision impairment, and structural changes in the brain. The lifespan of affected individuals ranges from infancy in the worst case to adulthood with minimal disability in the best case scenario.

Emery-Dreifuss MD has two forms, X-linked and autosomal dominant, that both primarily affect males. Symptoms are less severe than DMD patients and they include wasting of skeletal muscles, contractures that cause elbows to become locked in a flexed position, rigid spine, toe-walking, slightly elevated creatine kinase levels in the blood, and mild facial weakness. Nearly all Emery-Dreifuss MD patients develop heart problems by age 30, and many patients die from pulmonary or cardiac failure.

There are two muscular dystrophies that become apparent during adolescence. FSHD is the third most common muscular dystrophy, and affects the muscles of the face, shoulders, and upper arms. Muscle wasting in patients with FSHD is typically very slow. Individuals often have normal life expectancies; however, many live with severe disabilities. Limb-girdle MD collectively describes more than a dozen disorders in which both male and female patients lose a majority of muscle mass and exhibit weakening of muscles in the shoulders and hips. The most common symptoms include a waddling gait, difficulty rising from chairs, contractures in back muscles that make the spine appear rigid, and impairment of proximal reflexes. Life expectancy ranges among affected individuals, however, patients become severely disabled within 20 years of onset, and those having an earlier onset of clinical symptoms have faster disease progression.

Adult-onset muscular dystrophies are typically less severe than other MDs. Distal MD develops in males and females between the ages of 40-60. Distal muscles, such as those in the forearms, hands, lower legs, and feet, are affected. Patients have reduced finger dexterity, and sometimes develop heart conditions. Myotonic MD may be the most common adult-onset dystrophy, occurring in individuals around age 20-30. It is caused by an increase in the copy number of one specific codon in the inherited gene. Myotonic MD results in myotonia, the inability to relax muscles after contraction. Affected individuals may have normal life

expectancy, however, the disease will slowly progress and cause disabilities. If an expectant mother has myotonic MD, the baby may be born with a rare congenital form of the disease that can cause mental impairment as well as muscle wasting. OPMD is the final adult-onset muscular dystrophy in which men and women in their 40s or 50s begin to experience weakness in facial muscles, especially those controlling eye movement and pharyngeal muscles in the throat. Patients often have vision problems, muscle weakness in the neck and shoulder region, and cardiac irregularities. Some individuals with severe symptoms may lose the ability to walk.

There is a wide variety of muscular dystrophies in the human population. The diseases are collectively very painful and discouraging to patients who have normal mental capabilities but cannot function properly without assistance. A shortened life expectancy is an unfortunate consequence of many of these genetically linked diseases, and the lack of effective treatment has prompted many new research projects.

1.1.2 Current Treatments for Muscular Dystrophies

Currently, there is no treatment for muscular dystrophies that can stop or reverse the progression of the disease. Many available treatments prevent further disease complications or extend the time in which an affected individual is able to function independently, reviewed in reference [6]. Included in these treatments is physical therapy, which often improves movement by keeping muscles in shape for as long as possible. Dietary guidelines suggest high-fiber and protein intake coupled with a low calorie plan, which aids in preventing obesity and dehydration that can be caused by an MD patient's loss of mobility. In addition, many patients inevitably incorporate home and workplace modifications that make daily chores easier. Occupational therapy is available to those patients that would like to learn alternative job skills. These very important

treatments undoubtedly provide MD patients with a higher quality of life, and there are still more aggressive therapies that prolong the life of an individual afflicted with this disease.

The body has a natural way of healing itself that has been well characterized and includes the attraction of immune cells to the site of injury, and the systematic clearing of damaged cell debris, infectious particles, and other foreign substances. Similarly, immune cells are drawn to the muscle tissue of an MD patient as contraction and relaxation causes cell death of affected muscle fibers. There are some drug therapies that are prescribed in order to reduce the immune response and consequently delay muscle degeneration. The most widely drug used to treat DMD is a corticosteroid called prednisone, which slows the rate of muscle degeneration and allows children to remain stronger and walk independently for up to several years [7-9]. The positive effect seen in many patients may be due to the anti-inflammatory and immunosuppressive properties of prednisone. The extensive use of this drug is offset by side effects like fluid retention, which can lead to weight gain and high blood pressure, and long-term immunosuppressive effects (characteristic of other immunosuppressive drug therapies available as well). To control muscle hyperactivity and, in some patients, seizures, anticonvulsants are commonly prescribed. In addition, to compensate for the loss of an important enzyme creatine kinase, creatine can be taken as a supplement and aids in the generation of energy used for muscle contraction [10]. Many different approaches are used in drug therapy, and therapies are always tailored to each individual patient. Unfortunately, although drugs can delay muscle degeneration, they currently do not participate in the regeneration or replacement of new muscle.

Surgical approaches are often used to improve the quality of life of an MD patient. Corrective surgeries are needed to ease certain complications from MD, such as tendon or muscle-release surgery. When a contracture causes a joint to become locked in a certain

position, the tendon or muscle must be severed in order to free movement. Consequently, the use of braces or physical therapy can help the patient rebuild muscle strength or movement range. The insertion of metal rods has been performed to help correct severe cases of scoliosis, which interferes with posture and balance if the spine curvature is too great. As many MD patients develop heart problems, assisted ventilation is often needed to compensate for weakened respiratory muscles. In addition, some individuals with Emery-Dreifuss MD or Myotonic MD require a pacemaker or other assistive device in order to maintain cardiac functionality. It is especially noteworthy that MD patients most commonly die from respiratory and heart failure and assistance from ventilators and pacemakers can extend the lifespan of affected individuals.

1.1.3 Current research for the treatment of muscular dystrophies

The development of better drug therapies for muscular dystrophies is among the goals to improve treatment. Studies have been designed to identify the exact mechanisms by which current drugs, such as corticosteroids, work and/or cause unwanted side effects. Many alternative approaches are underway to identify additional drugs that have the potential to improve the quality of life for these patients. Muscle degeneration is caused by many enzymes, all which can be targeted for inhibition. Other approaches include prolonging the loss of muscle mass, and many of these drugs will be tested in combination with current drug therapies. The effects and optimal dosage of creatine protein, often administered as a dietary supplemented to MD patients, are currently being examined in humans. Similarly, the nutritional supplement CoEnzyme Q10 can protect cell membranes from oxidative injury, and is a promising supplement [11] that may be further tested in boys with DMD. Other steroids such as oxatomide, which blocks histamine release from mast cells, could prevent inflammatory damage

caused by immune cells in boys with DMD as well. Studies using controlled release of currently approved drugs may show reduced side effects with the same level of efficacy.

A recent approach to identify a more effective treatment for muscular dystrophy is to improve the body's natural muscle repair mechanism. Normal skeletal muscle is able to regenerate itself upon injury because of the presence of satellite cells [12]. Satellite cells are adult stem cells that undergo self-renewal as well as terminal differentiation to generate new muscle fibers. Perhaps there are points within this repair pathway that could be targeted for therapeutics. Targeted inhibition of myostatin, which normally blocks muscle growth, could enhance muscle repair in animal models [13]. A better understanding of the effects of these and other potential therapeutic drugs on the body's natural way of regenerating muscle will provide more insight on developing effective treatments.

In over 80 percent of DMD patients, the dystrophin gene is mis-read in a manner that causes the reading machinery to prematurely stop, generating a truncated non-functional dystrophin protein [14, 15]. Restoration of the ability to read the dystrophin gene in the correct manner would produce fully functional dystrophin protein of the correct size. These methods can involve an antibiotic, gentamicin, which causes the transcriptional machinery to ignore the nonsense mutation that confers the premature stop signal [16], and due to the success of this therapy in mouse models [17], it is thought that it could be utilized in a small percentage of DMD patients. Another approach modifies the use of naturally occurring splicing sites in the dystrophin gene that would bypass the unwanted mutation to a point where the genetic information was complete [18, 19]. This exon-skipping strategy was shown to be promising in the dystrophic mouse model [20], and could help as many as 80 percent of DMD patients.

In a much different approach, gene replacement therapy could effectively replace the mutated gene with a functional one using various methods, and is able to take advantage the fact that most muscular dystrophies are caused by a mutation in a single gene. In the case of DMD, the ability to deliver a functional dystrophin gene has been troublesome since the coding sequence is one of the largest in the human genome. Also, systemic and safe delivery of a functional gene product to all skeletal muscles, including the affected diaphragm and heart has been difficult. In attempts to generate a smaller yet functional dystrophin gene product, researchers have developed a truncated version, microdystrophin, which was shown to be as functional as the full length protein [21] yet the coding sequence was sufficiently small to incorporate into viral vectors [22, 23]. This microdystrophin gene has been delivered in a dystrophic mouse model using a viral vector, adeno-associated virus (AAV), and could effectively improve muscle function [24]. More effective and targeted delivery of therapeutic genes to affected muscle fibers using both non-viral and viral methods will continue to be a large focus of muscular dystrophy research.

Cell-based therapies have become more promising during the past few decades following the identification of adult and embryonic stem cells, which are able to regenerate many different cell types in the body. The theory behind cell-based therapy is that MD patients often are missing a critical muscle protein that normal cells, when transplanted into the affected muscles, can produce and replace. The production of the missing protein by the transplanted cells could restore muscle function in MD patients. An explosion of stem cell research in the past decade has shown promising results that could potentially be translated into humans (see Cell-based therapies section below). Further studies are absolutely necessary in order to design the safest and most effective cell-based treatment.

1.1.4 Skeletal muscle differentiation

Embryonic myogenesis depends on both temporal and spatial signals from three areas of the developing embryo including axial tissues, lateral plate mesoderm, and the overlying ectoderm. Skeletal muscle is derived from paraxial mesoderm in vertebrates, which becomes segmented into somites [25]. The first skeletal muscle mass formed in the embryo develops from the dorsal parts of somites and is termed the dermomyotome. From this structure, both epaxial dermomyotome (back) and hypaxial dermomyotome (limb and body) muscle are formed. Epaxial muscle formation initiates first, about 12 hours after the onset of somitogenesis, followed by hypaxial muscle formation, which begins 1 to 2 days later. Muscle precursor cells present in the dermomyotome express transcription factors Pax3 and Pax7 [26, 27] and are maintained in a proliferative state by a balance of signals secreted from the lateral plate mesoderm and surface ectoderm [28, 29]. Wnt proteins are able to induce and maintain the expression of dermomyotome markers Pax3 and Pax7 in somitic tissue culture explants in the absence of the overlying ectoderm [30]. Conversely, the addition of bone morphogenic proteins (BMPs) has been shown to mimic the signals from the lateral plate mesoderm and effectively prevent the activation of downstream muscle genes [29] before the cells reach their niche.

Near the limb buds of the animal, muscle progenitor cells delaminate from the hypaxial dermomyotome and migrate into limb fields where dorsal and ventral muscle masses first form. This migrational process depends on many signals in the developing embryo, namely the presence of c-met, a tyrosine kinase receptor that is able to guide the migrating limb muscle precursor cells to the limb bud using the gradient of its ligand HGF (hepatocyte growth factor) which is produced by non-somitic cells [31]. The expression of c-met is dependent on the homeo- and paired-domain containing transcription factor Pax3 [32], and mice deficient in either

c-met [33] or Pax3 [34] fail to develop limb muscles. A summary of the sequential cascade of myogenic gene expression is shown in Figure 1.

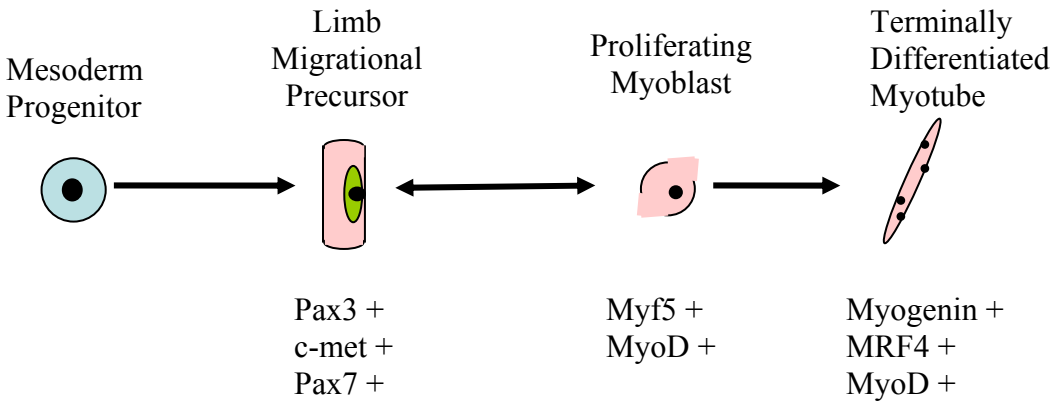

Figure 1. Sequential gene expression during embryonic muscle differentation.

A population of mesoderm progenitor cells, present in the somitic tissue of the organism upregulates Pax3, which stimulates migration of progenitor cells into the limb field. In the limb field, MyoD and Myf5 expression are upregulated in a cell population called myoblasts, which proliferates extensively to generate the muscle mass. Terminal muscle differentiation is characterized by the fusion of myoblasts into large multi-nucleated myotubes that express myogenin and MRF4.

As muscle precursor cells enter the limb bud, two cell populations arise to create a superficial layer of Pax3 expressing cells that continually proliferate and a deep layer of differentiating myoblasts that express MyoD and other muscle proteins [35]. Signals from the dorsal ectoderm stimulate myogenesis by inducing MyoD expression, which is one of several myogenic regulatory factors (MRFs). It is unclear the exact signals that are provided by the overlying ectoderm, however, it has been shown that Wnt proteins can mimic its function in the absence of this embryonic tissue [36]. Pax3 has also been shown to indirectly activate MyoD and Myf5 using embryonic explants [34, 37].

Muscle fibers are formed by the fusion of myoblasts with one another [38]. The regulated expression of myogenic regulatory factors (MRFs), including the basic helix-loop-helix (bHLH) family of muscle transcription factors MyoD, Myf5, myogenin, and MRF4, can be used to distinguish steps in this fusion process (Figure 1). Myf5 and MyoD are expressed in proliferating myoblasts prior to differentiation; myogenin and MRF4 are expressed in terminally differentiated multi-nucleated muscle cells [39, 40]. In double MyoD and Myf5 mutant mice, the muscle precursor population is absent and therefore no skeletal muscle is able to form [41].

Pax3 has been shown to be expressed before this known muscle-specific gene cascade, and its activity induces myogenesis in pluripotent stem cells [42, 43]. Pax3 directly activates several genes, most of which have myogenic function such as c-met and Six1 [32, 42]. Pax3 also indirectly regulates gene expression of muscle-specific factors such as MyoD [37]. Human heterodeficiencies in Pax3 cause Waardenburg syndrome, characterized by cranio-facial anomalies and pigmentation defects [44]. Mice deficient in Pax3, also called s*plotch* mutants, fail to develop limb muscles [34, 45]. This may be, in part, caused by the lack of migration due to the absence of c-met expression [46]. Further evidence that Pax3 is an important regulator of myogenesis shows that a dominant negative splice variant of Pax3 prevents the formation of skeletal muscle by inhibiting the function of the full length Pax3 protein [47].

1.1.5 Cell-based therapies for muscular dystrophy

The simple idea behind the application of cell based therapies is to provide cells that are able to replenish the missing muscle protein in muscular dystrophy patients by either fusion with existing muscle fibers or the generation of new muscle fibers. An ideal cell type would replenish a particular population of muscle progenitor cells in addition to providing the missing muscle

function such as dystrophin. Cell transplantation can be done using autologous stem cells, which originate from the patient thereby minimizing the immune response in MD patients. However, a patient's cells must be modified genetically in vitro in order to correct or replace the mutated gene(s), and this process may cause undesirable permanent changes to chromosomal DNA. In addition, many primary cells have limited capacity to proliferate in vitro. Alternative sources of cells for transplantation are considered allogenic stem cells, originating from an individual capable of producing a functional dystrophin gene product. These cells are not subject to genetic alteration because they naturally contribute to muscle function, but they have been shown to induce an immune response in the MD patient. The following cell types, originating from both muscle and non-muscle tissues of adults and embryo-stage animals, may provide insights for the generation of novel therapeutic cell-based treatments for MD (reviewed in [48], see also Table 1).

Normal skeletal muscle has the ability to repair itself upon injury due to the presence of satellite cells. Satellite cells are located adjacent to mature muscle fibers and account for approximately 2-5% of nuclei associated with muscle fibers [49, 50]. These cells are multipotent in vitro and are able to differentiate into myogenic, osteogenic, chondrogenic and adipogenic cells [51, 52]. After normal skeletal muscle is injured, satellite cells will proliferate and give rise to a population of cells that regenerate muscle tissue via differentiation and fusion. In patients with muscular dystrophy, continued degeneration and consequent regeneration eventually depletes the body's natural satellite cell population [53]. Replacement of these naturally occurring cells would give MD patients a population of cells that can self-renew as well as contribute to new and healthy muscle fibers. However, satellite cells are scarce and are difficult to isolate, and therefore have not been used directly in cell transplantation studies.

Progeny of satellite cells, called primary myoblasts, can be maintained in a self-renewing state in vitro and they have a highly proliferative characteristic [54, 55] which allows for easy genetic modifications and the generation of large quantities for cell transplantation. Transplantation of myoblasts from several sources into mdx mice, a dystrophic mouse model, as well as human MD patients has resulted in transient dystrophin expression, however these experiments fail to show a physiological improvement in muscle function [56-65]. This may be due to the limited migration capacity of myoblasts, poor survival, the inability to contribute to long-term regeneration, and the need for repeated injections into multiple muscles, including the heart and diaphragms of MD patients.

Table 1. Cell-based therapies for the treatment of muscular dystrophy.

Cell Type	Advantages	Disadvantages
Satellite Cells	Multipotent, Naturally regenerate muscle	Scarce, difficult to isolate
Myoblasts	Highly prolilferative, Committed to muscle	Limited migration, poor survival, repeated injections, No physiological improvement
Side Population Cells (SP) – bone marrow and muscle	Widespread distribution via bloodstream	Low 5-8% engraftment rate, no long term regeneration
Muscle Derived Stem Cells (MDSC)	Multipotent, Migration, Proliferative, Restore dystrophin in mdx mice	No physiological improvement, origin unidentified
Mesoangioblast Cells	Mesodermal, isolated from adult, widespread distribution, functional restoration of MD mouse model	Requires enhanced delivery and further optimization
Hematopoetic Stem cells	Restore dystrophin in mdx mice	No physiological improvement, mechanism unknown
Mesenchymal Stem Cells	Multipotent, Ectopically induced skeletal muscle incorporated into injured rat muscle	Mechanism of Notch-induced muscle differentiation is unknown, population is heterogeneous
Embryonic Stem Cells	Proliferate indefinately, Pluripotent, Generates skeletal muscle in vitro	Differentiation is hetergeneous, transplanted ES cells cause teratomas, unknown mechanisms of differentiation

There are other types of stem cells that exist in various normal adult tissues that may be potential sources for cell transplantation into MD patients. Side population (SP) cells can be isolated from both bone marrow and muscle [66, 67] and have been tested for their ability to contribute to muscle regeneration in vivo. Although SP cells are able to migrate from the bloodstream to the muscle, allowing widespread distribution, these cells were only shown to have a 5-8% muscle engraftment rate [68]. In addition, SP cells did not participate in long-term muscle regeneration for unknown reasons. Currently, these cells are not considered to be a viable source of cells for transplantation into MD patients.

Muscle-derived stem cells (MDSC) are a heterogeneous population of progenitor cells that are isolated from skeletal muscle using a preplate technique [69]. These cells have been shown to differentiate into myogenic, hematopoetic and other cell lineages in vitro [70, 71]. When transplanted into the limb muscle or into the circulation of mdx dystrophic mice, MDSCs are able to regenerate muscle and dystrophin expression is elevated by more than 10 fold compared to myoblast transplantation [69, 72]. However, like most transplantation results, this experiment failed to show physiological improvement. These cells have proven to be useful due to the ease of migration, their proliferative nature, and their multipotency. The uncertain origin of MDSCs, and their absolute characterization prevents their current use in MD patients.

Vascular derived cells such as embryonic mesoangioblasts are mesodermal in nature and are able to differentiate into many mesoderm tissues including muscle in vitro [73]. Similarly, cells that express similar marker genes to pericytes and endothelial cells have been isolated from adult blood vessels, and when transplanted into a mouse model for limb girdle muscular dystrophy (α-sarcoglycan-null) were able to functionally restore the dystrophic phenotype [74]. The widespread distribution of these cells in recipient animals is likely due to their origin (the

walls of blood vessels) and the ability to be transported via capillary networks. Human cells that express similar genetic markers to mesoangioblasts (pericytes) have been isolated from skeletal muscle and when transplanted into mdx dystrophic mice, were able to generate many dystrophin positive muscle fibers [75]. Furthermore, cells isolated from human DMD patients have been genetically corrected using the mini-dystrophin gene which demonstrates the versatility of this cell type with respect to cell based treatments for muscular dystrophy.

Hematopoetic stem cells have long been considered as a source of transplantable cells for numerous applications. Transplantation of bone-marrow derived cells into the mdx mouse is able to partially restore dystrophin expression, however the amount of muscle that is regenerated is not therapeutically useful [76]. In addition, the mechanism by which bone-marrow derived cells contribute to muscle regeneration is not known, as some research suggests a fusion event with a patient's muscle cells, rather than an inherent ability of bone marrow cells to differentiate into myogenic lineages. Later studies conclude that bone marrow derived cells are able to participate in skeletal muscle regeneration [77] and may be therapeutically useful in the future, and optimizing a method of transplantation is crucial.

Mesenchymal stem cells (MSCs) are pluripotent progenitor cells that are derived from the bone marrow and are able to differentiate into osteoblasts, chondroblasts, adipocytes, and skeletal muscle [78]. MSCs can be committed to the skeletal muscle lineage using ectopically induced Notch signaling, which has been previously linked to satellite cell activation and muscle differentiation [79]. Transplantation of myogenic cells, derived from MSCs using Notch, into injured rat muscle has resulted in their incorporation into newly formed myofibers [80]. Further characterization of the muscle specific gene expression of this population suggests that it is heterogeneous, containing both myogenic progenitor cells and partially differentiated cells, and

may need further clarification. Furthermore, the use of Notch signaling to induce myogenic differentiation may be highly efficient, however the mechanism by which myogenesis has been triggered must also be made clear prior to translation into humans.

Finally, embryonic stem cells have been thought of as a source of therapeutic cell populations since they are able to proliferate indefinitely, have the capability to generate cells of all tissue types, and are easily genetically modified. ES cells are able to generate skeletal muscle in vitro [81] amongst various other cell types in a heterogeneous population. Unfortunately, there is currently no way to efficiently harness ES cells that have differentiated into skeletal muscle or muscle precursor cells. For this reason, ES cells are most often used as a tool to study early molecular events of myogenesis, and will undoubtedly provide relevant information to be applied in the future.

1.2 EMBRYONIC STEM CELLS

1.2.1 Embryonic stem cell definition

Embryonic stem (ES) cells are derived from the inner cell mass of an embryo at the blastocyst stage. Murine (mouse) embryonic stem cells were first cultured in 1981 by Evans and Martin [82, 83], while human ES cells were first derived in 1998 [84]. Murine ES cells are able to generate cells of many lineages [85, 86], and they can also be maintained indefinitely in a self-renewing state one of two ways: on a feeder layer of irradiated primary mouse embryonic fibroblasts (MEFs) or in culture with leukemia inhibitory factor (LIF) [87, 88]. LIF-mediated signaling activates the canonical Jak/Stat pathway, in which Stat3 activation has been reported to

be sufficient for maintenance of pluripotency in murine ES (mES) cells [89]. In the absence of serum, however, LIF-mediated Stat3 activation is not sufficient to sustain the self-renewal of mES cells. Investigators have found that the addition of BMP4, a member of the TGFβ superfamily, enables LIF to maintain self-renewal of mES cells without serum [90].

Human embryonic stem (hES) cell pluripotency is regulated by different signaling pathways. Unlike mES cells, whose self-renewal can be maintained in the presence of LIF, LIF cannot maintain hES cells in a self-renewing state. Alternatively, pluripotent hES cells are cultured on fibroblast feeder cells with basic fibroblast growth factor (bFGF), whose signaling appears to be important for hES cell self-renewal [91, 92]. Also unlike murine ES cells, hES cells are induced to differentiate into trophoblast or primitive endoderm like cells in the presense of BMP4 [93]. Consequently, the addition of Noggin, a BMP4 signaling antagonist, contributes to the maintenance of hES cell pluripotency [94].

There several characteristics that define undifferentiated ES cells. Morphologically, ES cells appear in culture as very round colonies with a glassy appearance (Figure 2A). The appearance of flattened cell colonies or flattened cells surrounding the glassy round ES colonies signify differentiated cell contamination. Undifferentiated ES cells express high levels of alkaline phosphatase activity [95] as well as telomerase activity [96], unlike differentiated cells that downregulate these activities.

Murine ES cells express a network of transcription factors that are responsible for blocking differentiation (for review of self-renewal maintenance see reference [97]). Oct3/4 is a POU family transcription factor that is one of the main transcriptional regulators of self-renewal [98]. Interaction of Oct3/4 with Sox-2 [99], a Sox (SRY-related HMG box) family member, has been shown to partially regulate Nanog [100, 101], an NK-2 class homeobox transcription factor.

Overexpression of Nanog in mES cells has been shown to maintain pluripotency in the absence of LIF [102, 103]. These transcription factors maintain pluripotency by blocking the activation of differentiation-inducing gene products.

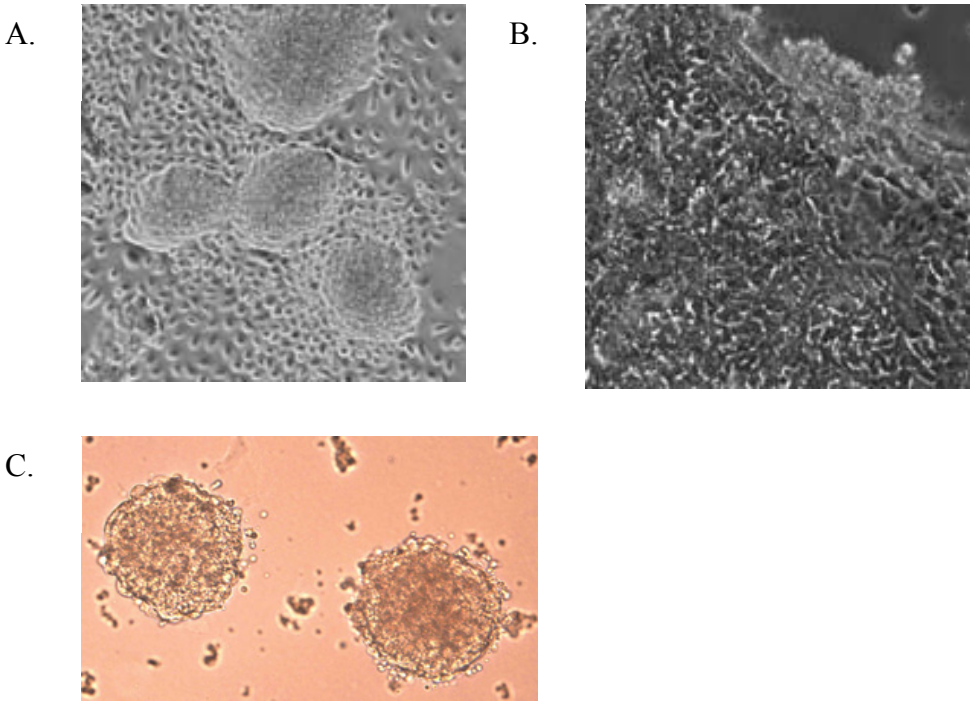

Figure 2. Embryonic stem cell and differentiated cell morphology.

Embryonic stem cells can be maintained in a self-renewing state on a layer of irradiated mouse embryonic fibroblast feeder layers (A) or in the presence of LIF without feeder cells. ES cell colonies are round and glassy in appearance. When LIF or the feeder layer is removed, confluent ES cells spontaneously differentiate into cell types of all three germ layers, shown by the loss of ES cell colonies and the emergence of various flattened cell types (B). Embryoid bodies are derived from ES cells in the absence of LIF and feeder cells (C., 4-day old embryoid bodies formed by single cell suspension in high density media).

1.2.2 Differentiation of ES cells

Embryogenesis is a complex process in which several pathways are involved in the proliferation, migration, and differentiation of embryonic stem cells in the developing embryo. ES cell lines

have the capability to differentiate into cells of all three germ layers, however, specification of certain lineages is often difficult. The simplest ways to induce differentiation of ES cells is to remove LIF from the culture media or allow ES cell cultures to become confluent. The lack of self-renewal pathway activation by LIF allows the ES cells to spontaneously differentiate into cells of all three germ layers in an unorganized manner (Figure 2B). This method is not a reliable way to study the molecular events of differentiation, therefore more specialized methods of ES cell differentiation have been explored, such as embryoid body formation.

ES cells are able to recapitulate many early events of the embryo during embryoid body formation (Figure 2C). Most differentiation protocols follow in-suspension or hanging drop [104] method of embryoid body (EB) formation to obtain cells of particular interest, then subsequent plating to allow outgrowth. To form embryoid bodies, ES cells are plated at a low density with or without methyl cellulose [85] on non-adherent culture dishes to allow each ES cell to proliferate into a dense cell mass in suspension. Alternatively, 600-800 ES cells may be placed onto the lid of a Petri dish in a volume of approximately 20 μl, where gravity causes the cells to collect at the bottom of the hanging drop. The cells proliferate and interact to form EBs and cells of all three germ layers, providing scientists with a good in vitro model for embryonic development.

Embryoid bodies have been shown to express developmental genes in a regulated manner, similar to that of the developing embryo. During the first two to four days of embryoid body formation, endoderm forms on the outer layer of the ES cell aggregate. These early differentiating bodies are termed simple embryoid bodies. The next stage of embryoid body formation occurs around day 4, when a central cavity is formed. These embryoid bodies resemble embryos that are at the egg-cylinder stage [83, 85, 105, 106]. Embryoid bodies will

form endodermal, mesodermal, and ectodermal cells in continued cell culture, and additional cell lineages will appear at later stages that resemble primitive streak and somite-stage embryos. These lineages include neuronal cells [107-109], hematopoetic cells [110-115], cardiac [116-118], and skeletal muscle cells [81, 119]. A study of the temporal and spatial expression patterns of several developmental marker genes has shown that EBs have strikingly similar gene expression patterns to the early mouse embryo [120]. It has therefore been concluded that embryoid body formation can be used as an in vitro model of early embryogenesis.

Embryoid body formation provides an indispensable tool for understanding how these germ layers and the differentiation of subsequent cell lineages are induced and maintained. Many developmental markers have been established to demonstrate germ layer induction and lineage specification in the embryoid body. Brachyury (T) is a representative marker of mesoderm [119], whose expression peaks during gastrulation and primitive streak formation *in vivo* as well as day 4 during EB formation [121]. Nodal is expressed in the epiblast and during embryonic gastrulation [122, 123] and represents primitive endoderm in day 2.5 EBs [121]. Flk-1 (Kdr) is an early hematopoetic and endothelial cell marker [124]. Understanding the cues and signals that an embryonic stem cell requires to differentiate into specific cell types will provide valuable information and potential targets for regenerative medicine and tissue engineering based therapeutics.

1.2.2.1 Specialized differentiation of mouse ES cells

Significant effort has been put towards the generation of specific cell lineages from stem cells in order to develop novel cell-based treatments for several prominent diseases in the human population including Parkinson's disease, diabetes, and liver disease.

Specific cell lineages may be induced or enhanced from ES cells and embryoid bodies using various methods. These include but are not limited to: the addition of growth factors and cytokines to the culture media, co-culture with other cell types [125], microdissection of cell types from embryoid body outgrowths [126], genetic modification of ES cell lines using drug selection [127] or a fluorescent marker gene [121], cell sorting, or a combination of methods.

Cells that are able to regenerate the vascular system were derived from murine ES cells by the use of cell sorting, in which green fluorescent protein (GFP) was targeted to the Brachyury locus. Cells that expressed GFP (and Brachyury) were sorted based on the expression of GFP and an additional cell surface marker Flk1, which is one of the earliest endothelial and hematopoetic genes expressed. Brachyury and Flk1 positive cells regenerated both endothelial cells and erythrocytes upon the addition of mixture of cytokines [121]. In a similar experiment, branching structures that are typical of blood vessel formation were formed from Flk1-positive ES-derived progenitor cells that were exposed to VEGF [128]. Injection of the Flk1 positive cell population in stage 16-17 chick embryos resulted in the formation of both endothelial cells and mural cells around blood vessels [129], demonstrating that this progenitor population can contribute to both components of the vascular system *in vivo*. Zandstra has been able to generate hematopoetic cells from mES cells in a scalable manner by encapsidation of EBs under hypoxic conditions [130].

Neuronal cells have been obtained from embryonic stem cells in efforts to develop novel treatments for neurodegenerative diseases such as Parkinson's and Alzheimer's. Murine ES cells have been differentiated into dopamine-releasing midbrain neurons as well as hindbrain neurons that release serotonin [131]. Similarly differentiated cells can be further enriched for neuronal fates using genetically modified ES cells expressing Nurr1. Neurons derived in this manner

were grafted into a rat Parkinsonian model and grafted animals showed marked improvement in motor skills [132].

ES cells can also be directed towards endodermal cell types such as pancreatic islet cells [133] and hepatic cells [134]. In the case of hepatocyte generation, ES cells were sorted based on the expression of several endodermal and mesodermal markers, such that cells that express Brachyury, Foxa2, and c-kit were induced to differentiate into an early hepatoblast stage by exposure to BMP-4, bFGF and activin A [134]. These signals are similar to the signals that induce hepatocyte generation in the embryo, and were administered in a biologically relevant manner. Furthermore, this early hepatoblast population was injected into two mouse models of liver deficiency, and was able to generate new hepatocyte clusters as well as endothelial cells in grafted animals.

The generation of skeletal muscle precursor cells from embryoid bodies has been somewhat problematic since EBs always form heterogeneous mixtures of cells. When cells of the EB are cultured in the presence of 1% DMSO [104] or low concentrations of activin A [119], a higher percentage of cells will differentiate into skeletal muscle cells, allowing for a more reliable control model of myogenesis. The previously described ES cell line containing GFP under the control of the mesoderm marker Brachyury was used to enhance skeletal muscle in the presence of activin A. Unfortunately, these methods only provide an enrichment of skeletal muscle in the heterogenous cell population, and since these studies, there have been very limited attempts to derive skeletal muscle precursors from ES cells and embryoid bodies.

Differentiated cells that have been obtained by genetic modification and/or drug selection of ES cell lines are less likely to be approved for tissue regeneration or cell transplantation studies in humans. Most importantly, these methods of inducing or enhancing specific cell

lineages have not yet provided a means of generating a truly homogenous population of cells that can subsequently be used in cell transplantation studies.

1.2.3 Gene transfer methods for ES cells

Gene transfer tools for ES cells will facilitate functional studies to identify and understand differentiation into specific lineages. Gene transfer is often inefficiently used to direct ES cells toward a certain lineage, such as with MyoD, whose expression has been shown to induce several downstream muscle genes in ES cells, but environmental conditions are required for complete skeletal myoblast differentiation [135-137]. Valuable information is attainable from ES cells by expressing developmental genes in a homogenous manner without the time-consuming generation of stable cell lines, the risk of contamination from other cell types, or cell sorting [119, 121].

A variety of non-viral and viral approaches have been used to express genes in ES cells, each with their advantages and disadvantages. Non-viral gene transfer methods, commonly used to create stable cell lines, are generally simplistic. These methods require high DNA concentrations and large numbers of cells due to toxicity [138], and result in low efficiencies of gene transfer to ES cells. Nucleofection has shown to have improved transduction, but cell death is still observed [138, 139]. Lipofectamine-mediated gene transfer is less toxic, requires less DNA and cells, but only transduces 10% of mES cells [140]. The lack of efficient transgene delivery has been a barrier to the application of non-viral gene transfer methods to large populations of ES cells.

Viral vector systems have generally improved efficiency compared to non-viral methods, but are typically more labor-intensive. Each viral vector system is useful for different

applications based on transduction efficiency, inherent toxicity, ease of manipulation and vector integration. Adenoviral vectors are able to express transgenes in murine ES cells, but MOIs of nearly 3000 are necessary for a nominal transduction efficiency [141]. Integrating vectors such as retroviruses or lentiviruses are commonly used to create stable cell lines [142], a time-consuming and labor-intensive task. In these cases, integration, in addition to drug selection required for stable cell lines, may alter endogeneous gene transcription and may be silenced. Adeno-associated virus-2 (AAV2) transduces ES cells at even lower efficiencies (0.02%), and requires a much higher MOI of greater than 10^6 [143]. Herpes simplex viral (HSV) vectors offer an additional vector system that may provide a potential solution inefficient transduction of ES cells. HSV has been shown to infect a wide variety of cell types with high efficiency and HSV amplicons have been previously used as a gene delivery vector for ES cells. Amplicons, however, are not widely accepted due to low titers and the lack of expression in the absence of helper virus. Each of these approaches has their own distinct advantages yet there remains an outstanding need for an efficient, uniform, and non-toxic gene delivery to ES cells.

1.3 HERPES SIMPLEX VIRUS-1

HSV-1 belongs to the Herpesviridae family, a group of enveloped DNA viruses ranging from 120nm-200nm in diameter. Viruses in the Herpesviridae family have four main structural components including the envelope, the tegument, the nucleocapsid, and a core. Viral encoded glycoproteins are embedded into the cell membrane-derived envelope and are used for attachment and entry of the virion into a host cell. The tegument is an amorphous structure that contains several viral proteins and enzymes that are released into the host cell upon infection.

The nucleocapsid is icosadeltrahedral in shape with 162 capsomers. The double-stranded viral DNA, ranging from 120-200 kilobases (kb) in size, is wound in a toroidal shape in the core, and encodes 60 to 120 genes. Herpesviruses replicate in the nucleus of a variety of vertebrate hosts, including humans, and a few invertebrate hosts.

There are three subfamilies in the Herpesviridae family, alpha-, beta- and gamma-herpesviruses. Herpesviruses are categorized into these subfamilies based on genome size and content, host range, pathogenicity, and where latency is established in the host. The human alpha-herpesvirus family members, HSV-1, HSV-2, and Varicella Zoster virus (VZV), have a wide host range and are highly cytolytic with a characteristically short replication cycle (12-15 hours). Alpha-herpesviruses cause localized lesions, associated with the skin (HSV-1) or mucosa of the respiratory tract or genitals (HSV-2). VZV is the causative agent of chicken pox. Alpha-herpesviruses are neurotrophic and are able to establish latency in the nervous system. Beta-herpesviruses, including human cytomegalovirus (HCMV), HHV-6 and HHV-7, are lymphotrophic and infect primarily T- or B- cells. The life cycle of beta-herpesviruses is longer than alpha-herpesvirus replication (several days) and tends to enlarge the infected cell rather than cause cell lysis, as in the case of HCMV. Beta-herpesviruses may remain latent in secretory glands, kidneys, and lymph tissue, among others.

Gamma-herpesviruses include Epstein Barr virus (EBV) and Kaposi's Sarcoma associated herpesvirus (KSHV or HHV-8). These viruses are lymphotrophic and infect primarily B-cells and endothelial cells and may establish latency in lymphocytes. Gamma-herpesviruses are capable of transforming a cell into a cancerous phenotype such as the case with KSHV which causes Kaposi's sarcoma.

1.3.1 HSV-1 Productive (Lytic) Life Cycle

Replication of HSV-1 is a multi-step process, depicted in Figure 3, which is initiated by the attachment of the HSV-1 virion particle to the host cell membrane. Viral glycoproteins embedded in the envelope mediate fusion of the envelope with the cellular membrane, which releases the contents of the tegument and the nucleocapsid into the cytoplasm. Viral DNA is released from the nucleocapsid and is transported to the nucleus where viral gene expression occurs in a cascade fashion. Transcription of immediate early (IE, α) genes occurs first, followed by early (E, β) gene expression, and finally late (L, γ) gene expression. Expression of early genes precedes viral DNA replication, which occurs in the nucleus of the cell. Assembly of the viral DNA core and nucleocapsid also occurs in the nucleus, and this structure is enveloped at the nuclear membrane and transported through the endoplasmic reticulum and Golgi apparatus. Mature virions are transported to the outer cell membrane through the use of cellular vesicles. Host cell lysis releases progeny virus.

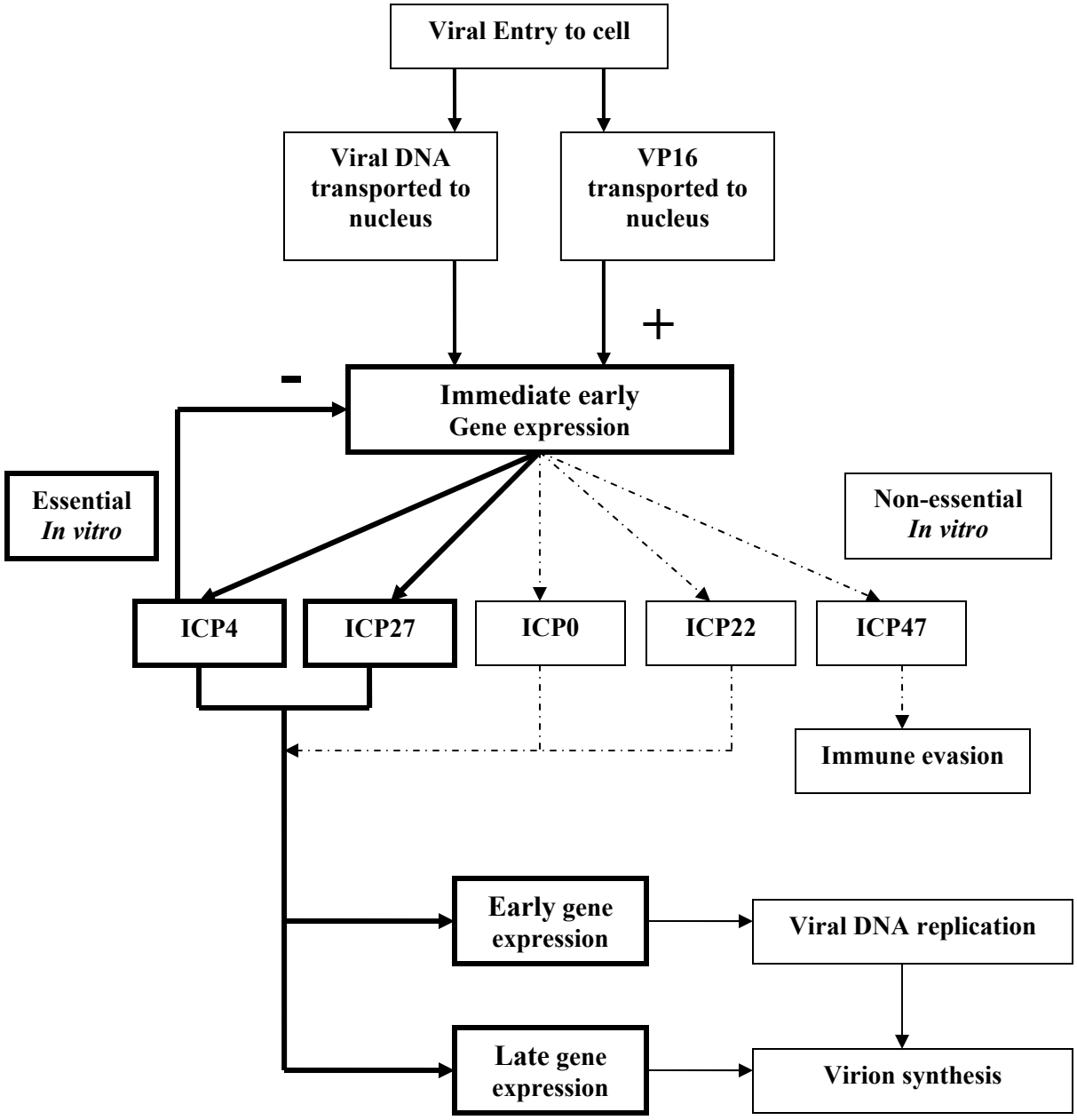

Figure 3. Replication cascade of HSV-1 in permissive cells.

HSV-1 lytic replication occurs in a temporally regulated cascade. Upon entry to a permissive cell, viral DNA and a tegument protein VP16 are transported to the nucleus. VP16 facilitates the high level of immediate early gene expression by 3 hours post infection (p.i.). Immediate early gene expression causes the activation of early genes by 6 hours p.i., which are involved in the process of viral DNA replication. Early gene expression, and for a subset of late viral genes the completion of viral DNA replication, triggers late gene expression from which the structural components of the virion are synthesized. Two immediate early genes, ICP4 and ICP27, are required for initiation of the rest of the viral gene expression cascade and are therefore essential for viral replication in vitro. The deletion of one or more of these essential genes renders an HSV viral vector replication-defective in non-complementing cells. Figure adapted from Burton et al. [144].

1.3.2 HSV-1 Genome Configuration

HSV-1 is a large double-stranded DNA virus whose genome encodes over 80 proteins. The genome is quite large (~152kb) and is partitioned into the unique long (U_L) and unique short (U_S) segments divided by inverted repeat elements (TR_L/IR_L and IR_S/TR_S) termed joints (Figure 4). The U_L (108 kb) and U_S (13 kb) segments can be positioned in both forward and inverted orientation in the HSV genome, resulting in four isoforms of the HSV-1 genome. Two origins of replication are contained within the HSV genome, including one copy of Ori_L within the U_L segment and two copies of Ori_S contained within the inverted terminal repeat elements adjacent to the U_S segment. The guanine/cytosine content of HSV-1 genome is 68.3%. The repeat elements flanking the U_L segment encode for the IE gene ICP0, and the repeat elements flanking the U_S segment encode for the IE gene ICP4. Many HSV-1 encoded genes resemble cellular genes with respect to the presence of a promoter, a 3' untranslated region, an open reading frame, and a signal for poly-adenylation. Most HSV-1 encoded genes differ from cellular genes due to the lack of introns, with the exception of gamma34.5, ICP0 and UL15.

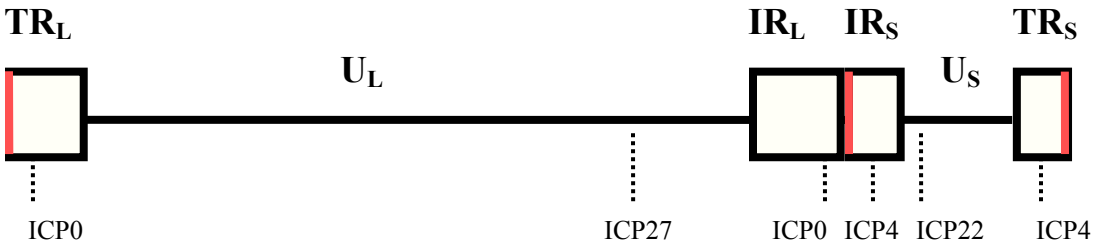

Figure 4. HSV-1 genome configuration.

A diagram of the 152 kb HSV-1 genome is depicted. The unique long (U_L) and unique short (U_S) segments are flanked by inverted repeat elements (TR_L/IR_L and IR_S/TR_S). Relevant immediate early gene loci are indicated.

1.3.3 Cascade of HSV gene expression

HSV-1 gene expression follows the typical herpesvirus cascade of immediate early (α) genes, followed by early (β) gene expression, and finally late (γ) gene transcription (Figure 3) [144]. There are five IE genes in HSV-1, including infected cell protein (ICP) ICP0, ICP4, ICP22, ICP27, and ICP47. The promoter structure of the IE genes differs from E or L gene promoters, where IE gene promoters contain TAATGA(R)AT sites that specifically bind the viral transcription factor VP16, a tegument protein that is transported to the nucleus upon infection of the host cell and E/L gene promoters do not. ICP4 functions to transactivate viral genes at the promoter level, while ICP27 aids in viral mRNA processing and transport [145, 146]. Both of these genes are essential for viral replication. ICP22 and ICP0 are not essential for viral replication but they enhance the transactivation of viral genes and viral growth [147]. ICP47, the final immediate early gene, is an immune evasion gene that affects the cellular TAP protein by interfering with its ability to load MHC class I molecules with antigen. The generalized function of IE genes is to activate other viral genes in the cascade, including early genes, which are generally responsible for viral DNA replication [147, 148]. Late genes are transcribed after both IE gene expression and DNA replication have occurred, and these genes mainly encode for structural components of the virion [147, 148].

1.4 REPLICATION DEFECTIVE HSV VECTORS

The cascade of HSV viral gene expression depends on the expression of the IE genes, and deletion of one or more of these genes can affect the virus's replicative competence. Restoration

of viral replication is achieved by the generation of cell lines that provide the missing essential IE gene(s) in trans. The current availability of complementing cell lines that provide various combinations of IE genes has contributed to the ability to produce high titer purified stocks of severely deleted HSV recombinant vectors. These deleted vectors are then suitable for delivery of transgenes to a variety of cell types in vitro and in vivo.

Replication defective HSV-1 vectors have several attractive qualities and provide an ideal system for the delivery of genes to many cell types. The 152 kb genome can be deleted for several essential and non-essential genes, which leads to a reduction in toxicity to the host cell. The genome is easily modified genetically and may be engineered to contain large and multiple expression cassettes. HSV infects a wide variety of cells, including cells that may be derived during cellular differentiation. Equally important, the HSV genome remains episomal in infected cells and will not permanently alter the host cell or interfere with endogenous gene expression, a side effect commonly seen with integrating viral vectors.

There is a delicate balance between the deletion of toxic or replication essential IE genes and the amount of transgene expression from the viral genome as a result of those deletions. ICP4 and ICP27 are essential for viral replication and are often removed in order to prevent additional viral gene expression. ICP0 and ICP22 are also involved in transcriptional regulation of viral genes and function to enhance expression and growth of the virus. ICP22 modifies RNA polymerase II to promote late gene expression [147], while ICP0 has many functions in HSV infected cells, including the targeted degradation of a variety of proteins [149] involved in antiviral responses to infection. The expression of all four immediate early genes (excluding ICP47, which plays a role in vivo) must be modified to achieve sufficient transgene expression

and the least amount of toxicity, and HSV mutants are least toxic when there is little to no viral gene expression.

1.4.1 Role of ICP0 in gene expression from HSV vectors

Although ICP0 is not required for viral replication in vitro, recombinants deleted of the ICP0 function display significantly reduced replication capabilities [150, 151]. ICP0 has long been characterized as a promiscuous transactivator of viral genes, although it does not possess DNA binding activities [152]. Instead, ICP0 has many functions that consequently create a permissive intracellular environment for viral gene expression, such as its interaction with ND10 components. ND10 nuclear bodies are a reservoir of proteins involved in the innate immune response that silence gene expression from incoming foreign DNA. The proteasome-dependent degradation of PML, one of several protein components of ND10 bodies that is targeted by ICP0, has been linked to the activation of input HSV genomes and subsequent increase in replication [153, 154].

ICP0 also targets the degradation of several other proteins that are theorized to aid in the host cell's attempt to repress the viral gene expression and replication. The centromeric proteins CENP-A [155] and CENP-C [156] are degraded by ICP0 which causes perturbations in cell cycle progression, as well as the catalytic subunit of double-stranded DNA repair protein DNA-PK [157]. Proteasome-dependent degradation of these proteins by ICP0 requires the intact RING-finger domain of ICP0, similar to the RING-finger of E3 ubiquitin ligases. ICP0 has since been shown to function as an E3 ubiquitin ligase, and may function by stimulating the addition of ubiquitin to host proteins targeted for degradation [158, 159].

While ICP0 has various detrimental effects on cells, its expression is correlated with elevated transgene expression from the viral genome. A replication defective HSV vector that expresses wild type ICP0, such as d95, illustrates this correlation as it is capable of high transgene expression, yet also induced host cell cycle arrest [160]. On the other hand, HSV vectors deleted for ICP0 are less toxic to infected cells, but as expected, they have notably less transgene, early, and late gene expression [161-164] than those with ICP0. This raises the conundrum that ICP0 is required for transgene expression from HSV vectors, yet its expression is toxic to infected cells.

ICP0's extensive involvement with both cellular processes as well as viral gene expression [164, 165] has prompted studies with varying ICP0 levels. Deluca and colleagues have shown that a modest level of ICP0 expressed from an adenoviral vector was able to disperse PML bodies, or ND10 nuclear bodies, without inducing cell cycle arrest, thereby rescuing the ICP0 deletion phenotype [166]. This research and others led us to hypothesize that reduced levels of ICP0 expression from the HSV genome, in combination with other genome modifications, would provide an attractive platform for gene delivery to embryonic stem cells.

2.0 RATIONALE

There currently exists no effective treatment for the millions of patients with muscular dystrophy. Preliminary studies using cell-based therapies in animal models have been somewhat successful, and provide much hope for future research and a potential cure for this devastating disease. As of today, the underlying mechanisms by which progenitor cells, adult or embryonic, are able to differentiate into muscle and contribute to long-term muscle regeneration are not clear. Further knowledge in this field is likely to aid in the development of novel treatments for muscle degenerative diseases such as muscular dystrophy.

The ability to deliver developmentally regulated genes to embryonic stem (ES) cells and their derivates would provide a method of evaluating the role of individual genes during ES cell differentiation. The first objective of this study was the design and characterization of a replication defective HSV vector that infected ES cells with high efficiencies, was non-cytotoxic, and was able to express gene products in ES cells without disturbing ES cell biology. This vector provided high levels of the early myogenic gene Pax3 to ES cells and differentiated cells derived during embryoid body formation in a transient and developmentally relevant manner. In addition, this highly defective vector was dependent on a single essential viral gene for lytic replication which was utilized in conditional replication studies described below.

Undoubtedly, there are many unknown elements involved in ES cell differentiation. For this reason, the second objective of this study sought to incorporate a cDNA library into HSV vectors to generate a pool from which relevant gene products could be identified. This goal was accomplished by the introduction of a bacterial artificial chromosome (BAC) and the highly efficient Gateway recombination system (Invitrogen) into the HSV genome. For proof of principle and to aid an additional project in the lab, the first source of cDNA material was the neuronal PC12 cell line. We confirmed gene expression and complexity of the HSV cDNA library by microarray analysis. HSV library isolates expressed cDNAs at the mRNA and protein level. HSV was not only shown to be an efficient method of introducing the cDNA library into relevant cell types, but the viral life cycle also provided a mechanism for capture of a functionally active gene product.

The final objective was to develop a system by which the newly generated HSV cDNA library could be applied to the identification of novel myogenic factors. We exploited the natural biology of HSV by engineering viral replication to be dependent on the expression of the single essential viral gene ICP4. To determine whether viral replication could be dependent on the activation of an early myogenic promoter by host cell factors, the missing essential viral gene was placed under the transcriptional control of the Pax3 promoter and transiently transfected into human rhabdomyosarcoma cells, which express high levels of a Pax3 fusion protein. Activation of the Pax3 promoter in this construct by factors present in the host cell provided sufficient ICP4 expression to induce viral DNA replication. In a similar manner, vectors from the HSV cDNA library that express a Pax3 activator in the presence of this construct will be able to replicate, thereby capturing the relevant gene product by the release of virus progeny.

In conclusion, we have developed a selection system by which genes that activate early myogenic promoters could be selected from a pool of cDNAs incorporated into HSV viral vectors. The versatility of this system can be broadly applied to many other lineages, in which the ICP4 gene is placed under the control of any differentiation-related promoter in a stable cell line or the viral genome. This system has a great potential to contribute to the vastly growing field of embryonic stem cell research and to the development of novel therapeutic treatments for muscular dystrophy.

3.0 GENERATION AND CHARACTERIZATION OF A NON-CYTOTOXIC REPLICATION-DEFECTIVE HSV VECTOR THAT IS CAPABLE OF GENE EXPRESSION IN ES CELLS WITH HIGH EFFICIENCY

3.1 ABSTRACT

Gene transfer tools provide a means to dissect the complex process of embryonic stem cell differentiation into different lineages. Here we describe a non-cytotoxic, replication-defective HSV-1 vector, JDββHE, for gene delivery to murine ES cells. JDββHE is deleted for the immediate early (IE) genes ICP4 and ICP22, while the IE genes ICP0 and ICP27 have been converted to early, or β genes. This vector is thus dependent on a single IE gene, ICP4, for virus replication. In the absence of ICP4, the βICP0 is expressed at highly reduced levels and does not affect infected ES cell viability. In contrast a similar gene vector JDD0Z1, which has been deleted for ICP4 and ICP22, expresses ICP0 from its IE gene promoter and is highly cytotoxic. JDββHE can activate expression of eGFP under control of the HCMV promoter located in the ICP4 locus. This vector is capable of efficient transduction and moderate transgene expression at multiplicities of 15. A Pax3 JDββ expression vector provided transient Pax3 expression in ES cells and cells of the embryoid body, a result of genome loss during cell division. At very high multiplicity (MOI=100), JDββHE did not inhibit embryoid body formation or alter the endogenous expression of representative germ layer markers during embryoid body formation.

The ability of this vector to provide transgene expression at high multiplicity without affecting ES cell gene expression or pluripotency suggests that it will be useful for studies of ES cell differentiation in model systems.

3.2 INTRODUCTION

Embryonic development involves complex processes that result in the ordered proliferation, migration, and differentiation of stem cells. Lineage determination relies in part on transcriptional control of genes that participate in these processes. The ability to evaluate the contribution of individual genes to ES differentiation can be approached using gene transfer methods which underscore the need for suitable vectors for this purpose. While various viral and non-viral vector systems have been exploited, limitations remain. These include vector integration and continued inappropriate transgene expression, vector toxicity, and poor infectivity and transduction efficiency.

The most common non-viral gene transfer methods used are technically simple, but require high DNA concentrations and large numbers of cells. Compared with conventional non-viral gene transfer methods such as electroporation [167] or nucleofection [138, 139], both cell viability and transduction efficiency are greatly improved using viral vectors [143, 168]. Integrating vectors based on lentivirus or retrovirus require the establishment of permanent cell lines and generally involve continued transgene expression. As a result, stringent control of gene expression levels post-integration is not always feasible, and constitutive expression of a developmentally related gene product may disrupt the events critical to differentiation processes and prevent terminal differentiation. Moreover, transgene expression can be subject to cellular

silencing mechanisms [142]. Thus it may be necessary to control the expression levels of stably integrated transgenes by the use of an inducible promoter or the addition of hormones to the culture media. DNA viruses such as Adenovirus or adeno-associated vectors infect ES cells very poorly and demonstrate low transduction efficiency. At high MOIs, these viruses also induce DNA damage responses which will likely affect ES cell viability and function. AAV and retroviruses also have a limited transgene capacity, which may inhibit the inclusion of multiple transgenes or an inducible or developmentally regulated promoter.

In this study, we describe the engineering and characterization of a highly defective HSV gene delivery vector designated JDββHE that is suitable for transgene delivery and expression in both undifferentiated and differentiated ES cells. By deleting ICP4, a key essential immediate early (IE) gene that is required for all lytic gene expression, this vector can be complemented with a single viral function. In addition, the essential ICP27 and non-essential ICP0 IE genes were converted to early (E) genes by E promoter substitution for their respective IE gene promoters, thus rendering these genes responsive to ICP4. Finally the vector was modified to remove the ICP22 IE gene and the repeat elements comprising the joint (J) sequences separating the U_L and U_S portions of the genome. These deletions provided ample room for insertion of foreign sequences and also enhanced the stability of the vector genome which does not undergo isomerization as observed with wild type virus. In the absence of ICP4, we observed a low level (1%) of ICP0 expression that proved to be sufficient to escape genome silencing that normally occurs in vectors completely deficient for ICP0 [162, 164]. This level of ICP0 expression was sufficient to allow transgene expression without the toxicity normally associated with ICP0 activity. The vector genomes were lost during cell division thereby providing the transient transgene expression, a feature desirable for expression of functions required transiently during

the differentiation process. JDββHE and a Pax3 equivalent expression vector were capable of efficient transduction of ES cells and their derivatives without interference with self-renewal or formation of embryoid bodies including the expression of normal differentiation markers during this process.

3.3 MATERIALS AND METHODS

Cell Culture. Vero, U2OS, & 4BLA.4 cells were cultured in DMEM supplemented with 10% FBS (Gibco), penicillin, and streptomycin. Murine D3 ES cells were obtained from ATCC & maintained in a self-renewing state in DMEM supplemented with 10^3 U/mL leukemia inhibitory factor (LIF, Chemicon), 15% fetal bovine serum (FBS, Gibco), 1% Non-essential amino acids (Specialty Media), 1mM Sodium Pyruvate, 2mM L-glutamine (Gibco), 0.1 mM β-mercaptoethanol on gelatin coated dishes. To form embryoid bodies, self-renewing ES cells were dissociated with 0.25% trypsin (Gibco), infected in suspension when indicated, then resuspended in high density media in the absence of LIF.

4BLA.4 cells are ICP4-complementing Vero cells that were engineered by transfection of Vero cells with plasmid 4bla. Plasmid 4bla contains the ICP4 coding sequence under the control of its natural IE promoter and the blasticidin resistance gene. Blasticidin resistant cell colonies were observed after several days and the clonal isolate 4BLA.4 was selected and expanded based on support of virus replication.

Embryoid Body Formation Assay. Briefly**,** 500,000 actively dividing murine ES cells were incubated with vector at the indicated MOI for 1.5 hours in suspension with rotation at 37°C. A

minimum of 100,000 cells were plated on gelatinized 6-well plates for flow cytometry analysis. Remaining cells were plated at 10^4 cells/mL in ultra low-adherence tissue culture dishes (Corning) in IMDM + 1% methyl cellulose without growth factors according to manufacturer's instructions (Hematopoetic Manual, Stem Cell Technologies). Plates remained in 37°C, 5% CO_2 humidified incubator until RNA harvest or EB quantification. For EB quantification, a minimum of three 60 mm plates per sample were manually observed 7-10 days after plating and analyzed using colony counting Quantity One software (BioRad). Results are representative of three independent experiments.

Vector Construction. JDββHE was engineered in three steps by homologous recombination in complementing Vero cells by transfection and infection methods described previously [169].

First, the βICP0 gene cassette was engineered into a quadruple IE (ICP0, ICP4, ICP27, ICP22) gene deleted vector, JDQ0ZEH1, which has also been deleted for one copy of reiterated sequences, referred to as the joint. 7b Vero cells were transfected with plasmid β0 and infected with JDQ0ZEH1, usually grown on 104.2 Vero cells, to create plaque purified recombinants termed JDT0Zβ0. Plasmid β0 was generated by insertion of a *Bgl*II fragment containing the ICP0 coding sequence into the *Bgl*II site downstream of the tk promoter in TK28B. The ICP0 coding sequence fragment is from an *Nco*I to *Hpa*I blunt ended fragment that was ligated to *Bgl*II linkers. The tk promoter (*Pvu*II to *Bgl*II) fragment was cloned into the *Sma*I to *Bgl*II sites in pSP72 to create 72TKP. From 72TKP, the newly generated *Bgl*II to *Bam*HI fragment containing the tk promoter and cloned into 28B to make TK28B. The recipient plasmid 28B was produced by a *Stu*I to *Hpa*I deletion of plasmid 28.1 and insertion of a *Bgl*II linker into this site. Plasmid 28.1 consists of the *Dra*I fragment of pSG28, which contains the *Eco*RI "EH" fragment of HSV-

1, cloned into the *Sma*I/*Eco*RV digested NSKP. Plasmid NSKB was created by a two step modification of pBSSK in which the *Not*I and Asp718 sites were changed to *Pme*I sites by linker ligation.

Second, JDT0Zβ0 was engineered to contain βICP27. 4BLA.4 Vero cells were transfected with plasmid EBT1 (β27) and infected with JDT0Zβ0. Recombinant vectors were plaque purified and termed JDD0Zβ27β0, abbreviated JDββ. Plasmid EBT1 was created by cloning the *Bgl*II fragment of BTK27 into the *Bam*HI site of plasmid EB1. BTK27 was produced by modification of the *Pvu*II site in TK27 to a BglII site by linker ligation. TK27 was created by cloning the *Pvu*II to *Bgl*II tk promoter fragment into the *Pvu*II to *Bam*HI site of p727. p727 contains the *Pme*I to *Sac*I fragment of the ICP27 coding sequence from PD7 cloned into the *Sma*I to *Sac*I sites of pSP72. Plasmid PD7 was created by cloning the *Bgl*II to *Bam*HI fragment of plasmid p2727.5, containing the *Bam*HI to *Sac*I ICP27 sequences with the *Drd*I site changed to a *Pme*I, into the *Bam*HI site of plasmid EB1 in the native orientation. EB1 was produced by cloning the *Eco*RV to *Bam*HI fragment of 5' ICP27 sequences from pXE [170] into the *Pme*I to *Bam*HI site of pNSK. pNSK is a modified pBSKK- (Stratagene, La Jolla, CA) with the *Not*I site deleted and changed to a *Pme*I site.

Finally, the HCMV IE promoter driving eGFP cassette was engineered into the ICP4 locus of JDββ. 4BLA.4 cells were transfected with plasmid SAE and infected with JDββ. Plaques that were positive for eGFP expression were purified. The resulting vector is termed JDD0Zβ0β27HE, abbreviated JDββHE. Plasmid SAE is an ICP4 targeting plasmid in which eGFP was cloned as a *Bam*HI fragment into the *Bgl*II site that lies between the ICP4-locus targeting flanks.

JDββ-Pax3 was engineered by homologous recombination between JDββHE and plasmid SAS-Pax3, an ICP4-targeting plasmid containing murine Pax3 cDNA under the control of the HCMV promoter, in complementing 4BLA.4 cells. Phenotypically clear plaques were selected based on the loss of eGFP expression that was previously at the ICP4 locus of JDββHE, plaque purified, and tested for Pax3 expression by quantitative RT-PCR and western blot analysis.

JDββHE, JDββ-Pax3, and JDD0Z are propagated on 4BLA.4 ICP4-complementing at low multiplicity. Cells and supernatant were salt-treated (final concentration 0.45M NaCl) for 1 hour at RT with agitation, followed by clarification by centrifugation. The viral pellet was resuspended in PBS, purified on an anion-exchange column, and stored in 10% glycerol at -80°C.

JDββHE, JDββ-Pax3, JDQ0ZEH1, and JDD0Z were titered by transgene expression on U2OS cells and quantified as transduction units per mL. Transduction was quantified by either flow cytometry for eGFP expression or by counting β-gal-expressing cells 24 hours post infection.

Southern Blot Analysis. Two million 4BLA.4 cells were infected with JDββHE or JDD0Z at MOI=6. Viral DNA was harvested from cells 24 hours post infection by Proteinase K (Invitrogen) digestion at 50°C overnight, followed by a phenol/chloroform extraction and isopropanol precipitation. Viral DNAs and plasmids were digested with restriction endonucleases (NEB, www.neb.com) overnight at specified temperatures. The tk promoter probe (*Pvu*II to *Bgl*II fragment from plasmid pUX) was biotinylated using Pierce North2South probe biotinylation kit according to manufacturer's instructions. Pierce North2South hybridization reagents and protocol were followed. To verify recombinant JDββHE virus

sequences, the tkp-ICP0 and tkp-ICP27 junctions were amplified by PCR and subjected to DNA sequencing analysis (data not shown).

Western Blot Analysis. Vero, 4BLA.4, or D3 ES cells (500,000) were infected with virus at MOI of 10. Cell lysates were harvested 24 hours post infection in RIPA lysis buffer supplemented with protease inhibitors (Sigma). Protein from approximately 100,000 cells were resolved on 4-12% SDS-page gel (Invitrogen), and transferred to PVDF or nylon using NuPAGE reagents and protocols. Primary αICP0 antibody (produced in our laboratory) and αICP27 antibody (Fitzgerald 10-H44) were incubated overnight at a concentration of 1:1000 at 4°C. Secondary HRP-conjugated goat α-rabbit IgG (Sigma) was incubated at a concentration of 1:10,000. Secondary HRP-conjugated goat α-mouse (Sigma) was used at concentration of 1:1000. Results were visualized using SuperSignal West Pico Chemiluminescence Substrate (Pierce).

Flow Cytometry. Immediately after infection (or mock), ES cells or Vero cells were plated onto a 6-well plate and allowed to incubate for 24 hours. After visual inspection, cells were trypsinized with 0.25% trypsin, washed once in PBS, and resuspended in a maximum concentration of $1x10^6$ cells/mL for flow cytometry analysis (Becton Dickinson FlowScan) for eGFP expression. A minimum of 100,000 cells were collected for each sample. Data analysis was performed with the CellQuest software program, typically setting mock infected cells at <3% GFP-positive.

RNA Extraction & Quantitative RT-PCR Analysis. Total RNA was harvested from ES cells and embryoid bodies using Qiagen RNEasy kit with in-column DNase treatment (Qiagen). Trypsinized ES cells were washed once with PBS before RNA isolation. Embryoid bodies forming in methyl cellulose media were diluted 1:10 with PBS and allowed to settle for 10 minutes. Media/PBS was aspirated, followed by a gentle PBS wash, and centrifugation before the first step in Qiagen RNEasy protocol. Reverse transcription of 1-5 μg RNA was performed in 20 μl reaction volume using SuperscriptIII (Invitrogen) and supplied protocol. 1/20 of each RT reaction was used for quantitative PCR.

Quantitative PCR (Q-PCR) analysis was performed using Taqman Universal master mix and Gene Expression Assays (Applied Biosystems). Primers and probes for ICP0 and 18S were developed in our laboratory (primer sequences provided upon request). Primer and probe master mixes for murine GAPDH and Pax3 were obtained as Gene Expression Assays from Applied Biosystems. Q-PCR was done on a BIO-RAD iCycler IQ with the following thermal cycle: 95°C for 3 minutes, 40 cycles through 95°C for 30 seconds, and 60°C for 30 seconds. Duplicate wells for each sample were averaged. Changes in expression were calculated from threshold cycle (Ct) values where relative gene expression = $2^{-\Delta\Delta Ct}$ [171]. Expression levels were normalized to internal control 18S or GAPDH [172]. There was no amplification from negative controls without reverse transcriptase enzyme, indicating no contamination from genomic DNA (not shown).

Statistical Analysis. Error bars represent ± standard error of the mean (SEM)

3.4 RESULTS

3.4.1 Vector Genome Confirmation.

Homologous recombination with appropriate targeting plasmids was used to derive the vector JDββHE from a previously constructed recombinant virus termed JDQ0ZEH1, as detailed in Materials and Methods. JDQ0ZEH1 is deleted for the IE genes ICP0, ICP4, ICP22, and ICP27, as well as for the internal repeat sequences referred to as the joint (JD, joint deletion) (Figure 5A). Due to the absence of all regulatory IE genes, JDQ0ZEH1 is not cytotoxic but is silent for transcription of nearly all viral genes, including transgenes under the control of strong promoters such as the HCMV IE gene promoter. JDQ0ZEH1 can be grown on ICP4/ICP27-complementing cells, but the yields are limited due to the absence of ICP0. This vector was used as a negative control for vector toxicity and ICP0-dependent transgene expression. We rescued the ICP0 and ICP27 genes in this vector to create JDD0Z1. This vector is toxic to infected cells thus providing a positive reference for ICP0 and/or ICP27-induced toxicity.

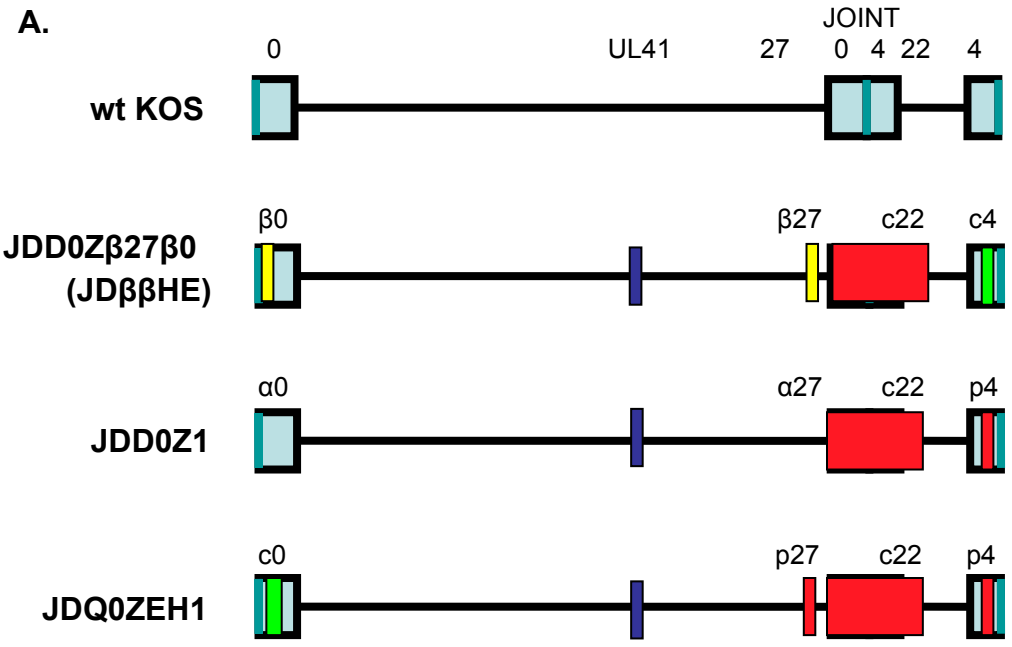
A.
JOINT
0
UL41
27
0 4 22
4
wt KOS
β0
β27
c22
c4
JDD0Zβ27β0
(JDββHE)
α0
α27
c22
p4
JDD0Z1
c0
p27
c22
p4
JDQ0ZEH1

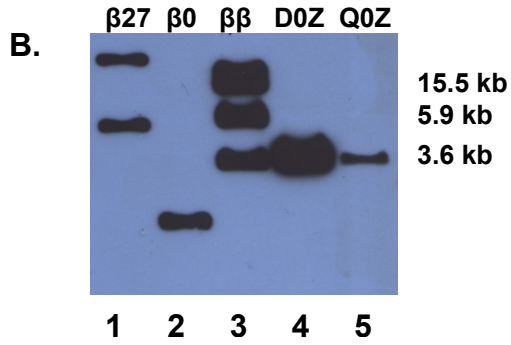
B.
β27 β0 ββ D0Z Q0Z
15.5 kb
5.9 kb
3.6 kb
1 2 3 4 5

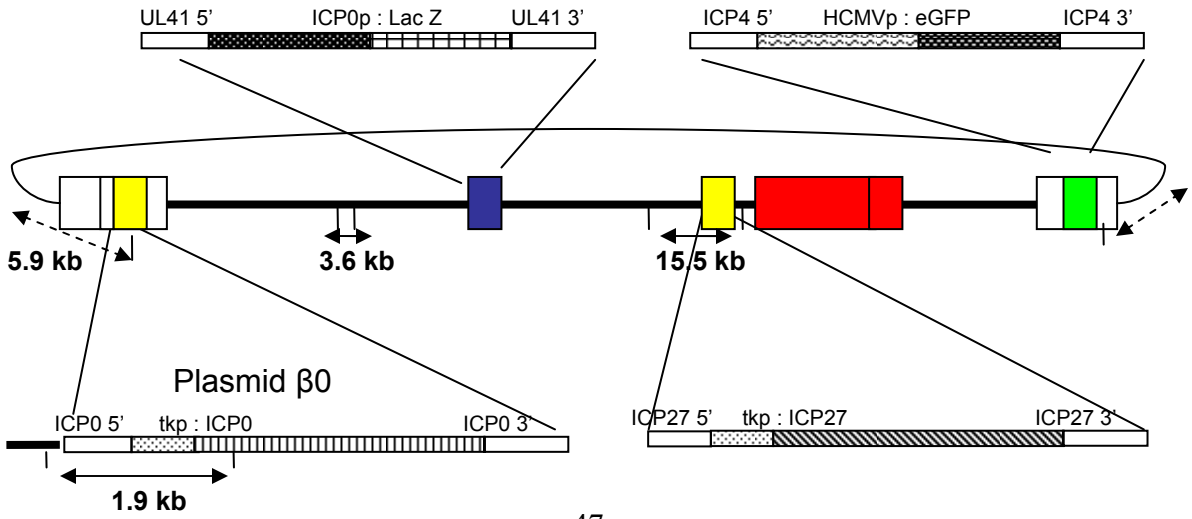
UL41 5'
ICP0p : Lac Z
UL41 3'
ICP4 5'
HCMVp : eGFP
ICP4 3'
5.9 kb
3.6 kb
15.5 kb
Plasmid β0
ICP0 5'
tkp : ICP0
ICP0 3'
1.9 kb
ICP27 5'
tkp : ICP27
ICP27 3'

Figure 5. Description and verification of HSV recombinant vectors.

Virus genomes are schematically shown in A. Immediate early genes are labeled at the approximate locations in the vectors. Partial (p) and complete (c) IE gene deletions are depicted in red. The U_L/U_S joint deletion extended from UL56 through US2. IE to E gene promoter substitutions (β) are shown in yellow and deletions substituted with transgenes are shown in green (eGFP) or blue (lac Z). Southern blot confirmation of JDββHE genome structure are presented in B. Southern blots analyses of JDββHE showed that the tk promoter was substituted for ICP0 and ICP27 IE gene promoters. Viral DNA was digested with *Bam*HI (lane 3, JDββHE; lane 4, JDD0Z1; lane 5, JDQOZEH1). Blots were probed with an internal tk promoter sequence. *Bam*HI-digested JDββHE DNA (lane 3) showed the tk promoter positioned upstream of the ICP0, ICP27 and tk genes (see *Bam*HI fragments 5.9 kb (dashed line), 15.5 kb and 3.6 kb respectively). The plasmid β27 (lane 1) does not contain a *Bam*HI site and resolved as a relaxed and supercoiled plasmid, and plasmid β0 (lane 2) contains an additional *Bam*HI site, resulting in a 1.9 kb *Bam*HI fragment. The promoter substitutions and deletions were confirmed by DNA sequence analyses.

We designed JDββHE for vigorous replication in ICP4-complementing cells along with increased transgene expression in non-complementing cells. To these ends, the ICP0 and ICP27 structural genes were restored in the parent JDQ0ZEH1 vector under transcriptional control of the viral thymidine kinase (tk) early (β) promoter (tkp). While this promoter is ICP4 dependent, we anticipated a low level of ICP4-independent activity (leakiness) which could increase transgene expression without adverse effects on cell viability. To enable detection of transgene expression in live infected cells, the gene for enhanced green fluorescent protein (eGFP) under control of the HCMV promoter was introduced at the site of the ICP4 deletion in the remaining repeat element flanking the unique short (Us) region (Fig. 5A). JDββHE, like JDQ0ZEH1 and JDD0Z1, also contained an ICP0 promoter-lac Z expression cassette in the UL41 locus which allowed for comparison of transgene expression between the different viral backgrounds. As confirmed in this study, the HCMV promoter requires ICP0 to function in the context of the HSV genome, while the ICP0 promoter is active in the absence of viral IE gene products.

Southern blots confirming the replacement of the natural ICP0 and ICP27 promoters with the tk gene promoter are presented in Fig. 5B. Control vector JDD0Z1 is isogenic with JDQ0ZEH1 for the ICP4, ICP22 and joint deletions, but is wild-type at the ICP0 and ICP27 loci

(Fig. 5A). Using a tkp fragment as a probe, three *Bam*HI fragments were detected in JDββHE DNA, but only the 3.6 kilobase pair (kb) fragment associated with the native tk locus was held in common with JDD0Z1 and JDQ0ZEH1 DNA. The 5.9 kb JDββHE band is diagnostic for the tkp-ICP0 boundary, which is excised from the circular viral genome, and the 15.5 kb fragment spans the tkp-ICP27 construct. The targeting plasmid β27 included as a control does not contain a *Bam*HI site and thus resolved as relaxed and supercoiled forms (>10 kb and 5 kb). The second targeting plasmid, β0, contains two *Bam*HI sites yielding a 1.9 kb hybridizing fragment. One of these sites is in the plasmid backbone and was thus lost during recombination into JDββHE. The promoter substitutions and deletions were confirmed by DNA sequence analyses (data not shown).

3.4.2 Virus growth

JDββHE was designed to rely exclusively on ICP4 complementation for critical IE gene expression and growth. To determine whether JDββHE replication was compromised by the promoter conversions of ICP0 and ICP27, ICP4-complementing 4BLA.4 cells were infected with JDββHE or JDD0Z1 at an MOI of 1, and allowed to replicate for 5 days. The supernatant and cells were harvested every 24 h, and standard plaque assays were performed on 4BLA.4 cells. Peak yields of JDββHE were more than 1 log lower than for JDD0Z1 and were obtained one day later (Figure 6). At this multiplicity (1 pfu/cell), JDD0Z1 infection reached CPE (>95% of the cells showing cytopathic effects) by 3 days post infection (p.i.), while JDββHE did not show CPE. Typical production of JDββHE, using an MOI of 5-10 in the presence of the HDAC inhibitor trichostatin A (TSA), requires the addition of nutrients every 2-3 days in order to observe CPE in >95% of the cells by 7 days p.i.. TSA has been previously shown to have an

effect similar to ICP0 expression on host permissivity to gene expression from the viral genome [173]. This protocol yields comparable titers to JDD0Z1 grown under standard conditions (data not shown).

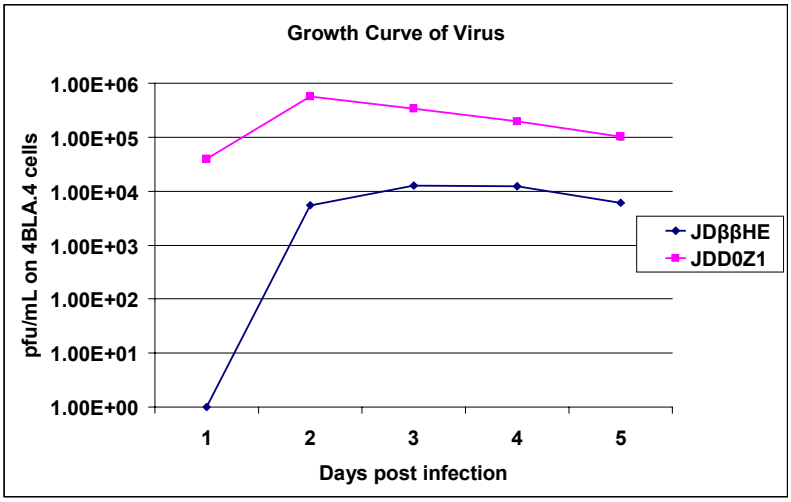

Figure 6. Growth Curve of recombinant HSV vectors on ICP4 complementing cells.

5×10^5 ICP4-complementing 4BLA.4 cells were infected with indicated vector at an initial MOI of 1. Cells and supernatant were harvested in duplicate every 24 hours and salt-treated (final concentration, 0.45M NaCl) for 1 hour. Samples were then plaque assayed on 4BLA.4 cells.

The amount of JDββHE that can be produced on ICP4-complementing cells far exceeds that of JDQ0ZEH1, which requires both ICP4 and ICP27 complementation. A typical JDQ0ZEH1 growth experiment on 7b cells, which provide ICP4 and ICP27, does not reach CPE, and the yields are less than 0.01 viral particles per cell (data not shown). Yields of JDββHE were approximately 2 viral particles per cell using high MOI and TSA, therefore, the conversion of ICP0 and ICP27 to early kinetics in JDββHE, in lieu of deletion, improved viral growth. The ICP4-complementing 4BLA.4 cell line lacks sequence overlap with the JDββHE genome to avoid rescue of replication-competent virus by homologous recombination. Thus, we achieved robust replication of JDββHE in ICP4 complementing cells without the risk of generating replication-competent virus.

3.4.3 Viral Gene Expression

To confirm that JDββHE expressed ICP0 and ICP27 as ICP4-dependent genes, we analyzed infected cells with and without ICP4 complementation by Western blot. Expression of both genes was observed in ICP4-complementing 4BLA.4 cells (Fig. 7A), showing that the β promoters controlling these genes were active in the presence of ICP4. In contrast, neither viral gene product was observed in JDββHE-infected Vero cells (Fig. 7B). The absence of ICP0 protein in Vero cells infected with JDββHE was further confirmed by immunofluorescence analysis (Fig. 7C). As a positive control, expression of ICP0 and ICP27 from their native IE promoters in JDD0Z1 was readily detected in both 4BLA.4 and Vero cells.

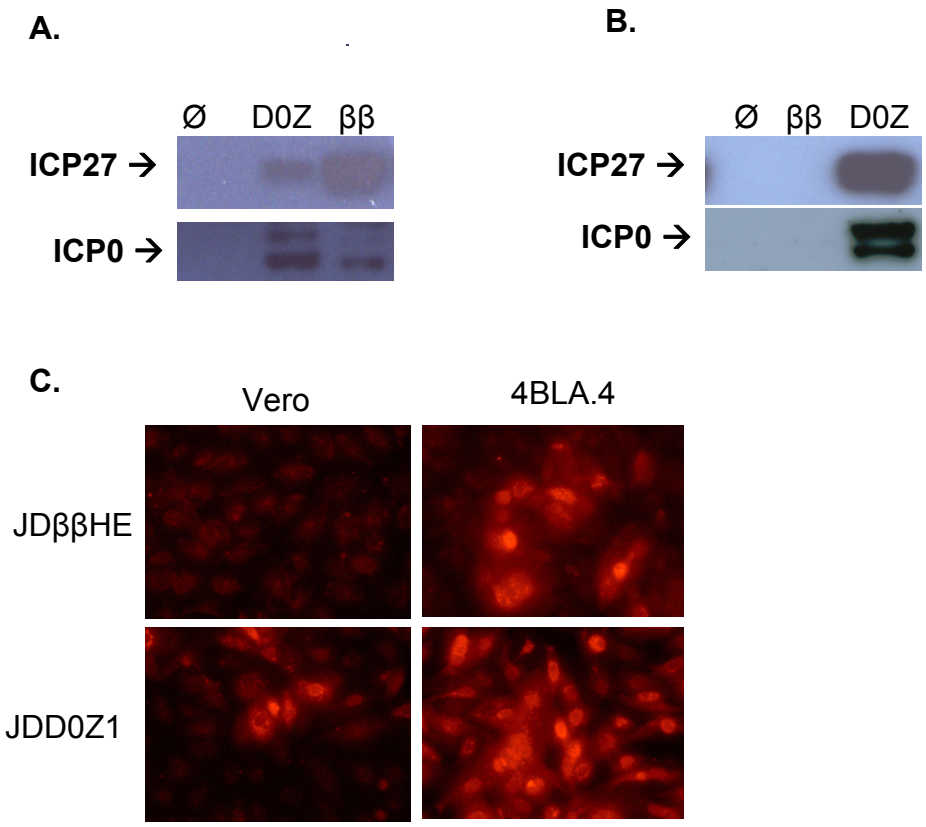

Figure 7. Expression of ICP0 or ICP27 from JDββHE is dependent on ICP4 complementation.

(A.) Protein Expression in ICP4-Complementing cells (4BLA.4). 4BLA.4 cells were infected with indicated vectors at MOI of 3 and protein was harvested at 24 h p.i. Western blots were performed using antibodies to HSV proteins. (B.) Protein expression in non-complementing Vero cells. Vero cells were infected with indicated vectors at MOI of 3. Protein was harvested at 24 h p.i., and western blots were performed using HSV antibodies. ICP0 and ICP27 are not detected in Vero cells infected with JDββHE. (C.) Immunofluorescence for ICP0 in infected cells at 24 h p.i. Vero and 4BLA.4 cells were mock infected or infected with indicated vectors at MOI of 3. IF using antibodies specific for ICP0 was performed 24 h p.i. ICP0 is not detected from JDββHE in non-complementing Vero cells (panel resembles mock or no primary antibody control – data not shown).

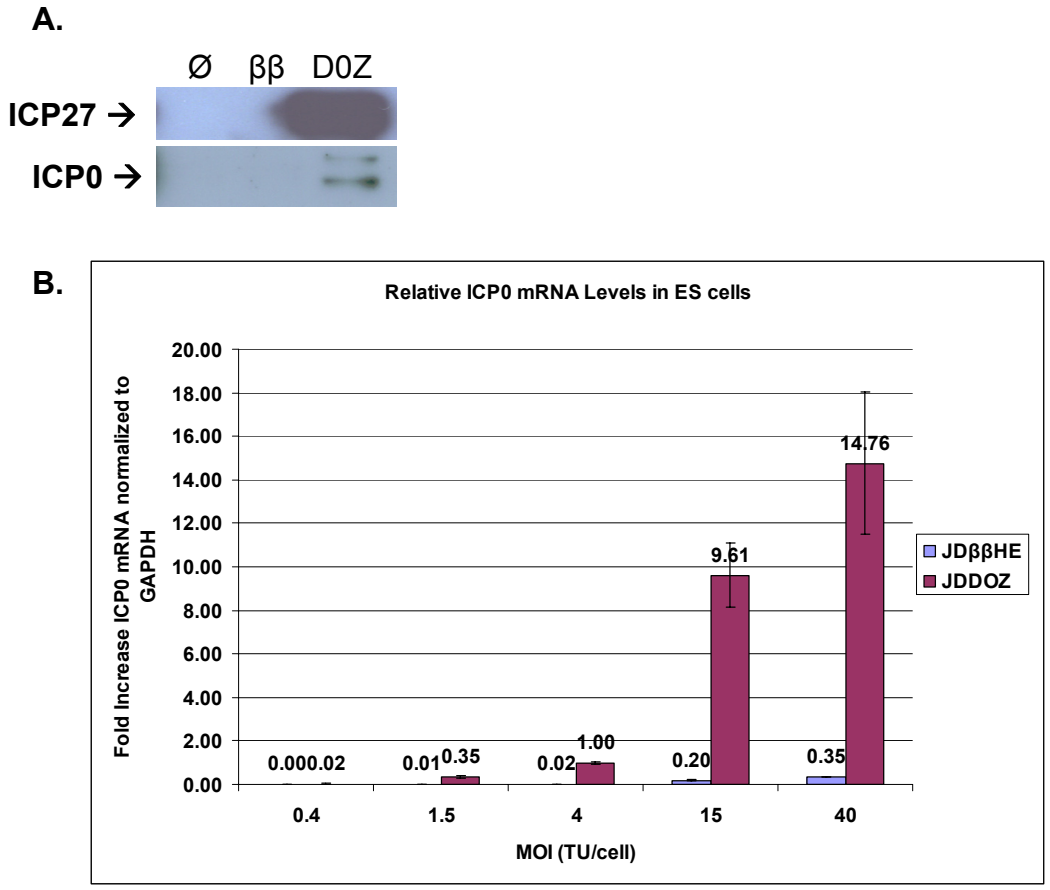

Figure 8. Viral gene expression in ES cells.

(A.) Expression of IE proteins in ES cells. ES cells were mock infected or infected with indicated vectors at an MOI of 3. Protein was harvested at 24 h p.i. and western blots were performed using antibodies specific for HSV proteins. ICP0 and ICP27 are not detected in ES cells infected with JDββHE. (B.) Relative amount of ICP0 mRNA detected at 24 h p.i. in ES cells. ES cells were infected at various MOIs with JDββHE and JDD0Z1. RNA was harvested from infected cells and reverse transcribed as described in Materials and Methods. Quantitative RT-PCR was performed using primers and probes specific for ICP0. The RT-PCR product was normalized to an RT-PCR product derived from GAPDH mRNA. DNA from the same infection was harvested and Q-PCR was performed on 200 ng of DNA per well for UL1, a single copy HSV gene. These results confirmed that the same amount of viral DNA was introduced into cells by either vector (data not shown). The relative amount of ICP0 mRNA increased with multiplicity but the amount of JDββHE produced message was approximately 1-5% of the ICP0 message produced by JDD0Z1.

We next examined the expression of ICP0 and ICP27 in infected ES cells to verify that this environment did not alter the gene expression characteristics of these vectors. While JDD0Z1 infection resulted in detectable levels of both proteins, neither ICP0 nor ICP27 was

observed in JDββHE-infected ES cells (Fig. 8A). Because even low levels of ICP0 may stimulate transgene expression, we used reverse transcription PCR (RT-PCR) as a highly sensitive assay to assess the transcriptional activity of the tkp-ICP0 gene in JDββHE-infected ES cells compared to that of the native ICP0 gene in JDD0Z1-infected cells. The results, normalized to GAPDH RNA levels determined on the same samples, showed that the amount of ICP0 RNA produced by JDββHE at 24 h p.i. was approximately 1-4% of the amount generated by JDD0Z1 (Fig. 8B). Quantitative PCR for the HSV single-copy U_L1 gene demonstrated that the amount of viral DNA introduced into the cells was the same for the two viruses at each MOI (data not shown). Hence the lack of detectable ICP0 protein in JDββHE-infected cells was most likely due to reduced transcriptional activity resulting from the conversion of the IE (α) ICP0 promoter in JDD0Z1 to the β tk promoter in JDββHE. Importantly, however, the tkp-ICP0 gene was not completely transcriptionally silent, consistent with the possibility of a low level of ICP0 production in JDββHE-infected ES cells.

3.4.4 Transgene Expression in ES Cells

To monitor the ES cell transduction efficiency of JDββHE, we took advantage of the two reporter genes in the vector, lac Z under transcriptional control of the HSV-1 ICP0 promoter in the UL41 locus and eGFP controlled by the major IE promoter of human cytomegalovirus (HCMV) in the remaining ICP4 locus. The ICP0 promoter is responsive to the tegument protein VP16 while the HCMV promoter is only responsive to cellular transcription factors. To allow comparison between viruses, we used viral titers based on transduction units (TU) determined as eGFP or lac Z expression in a human osteosarcoma cell line, U2OS, which complement viral

ICP0 deficiency for growth and transgene expression regardless of the transgene promoter [174, 175]. Following infection of ES cells at an MOI of 20 TU, JDββHE expression of eGFP was readily detectable by fluorescent microscopy at 24 h p.i. (Fig. 9A) while no fluorescing JDQ0ZEH1-infected cells were observed even at an MOI of 100 TU (data not shown). We compared the transduction efficiencies of JDββHE on Vero, U2OS and ES cells at increasing MOIs by flow cytometry at 24 h p.i. The transduction of all 3 cell lines was dose-dependent and an MOI of 15 TU was sufficient to achieve at least 95% fluorescing ES cells (Fig. 9B). The level of ES cell transduction was similar to that of Vero cells, which are widely used for HSV studies. The transduction efficiency was higher on U2OS cells, as expected from the ICP0-complementing characteristics of these cells. Expression of eGFP in JDββHE-infected ES cells was highest at 24 h p.i., reduced at 48 h p.i., and undetectable at 72 h p.i., thus demonstrating that expression was transient (data not shown). This result could be attributable to vector genome silencing or dilution of vector genomes during cell division as HSV genomes remain episomal after infection. We observed that the number of ES cells was increased 3-fold at 2 days p.i., similar to mock-infected cells (Fig. 9C), while the number of genome copies per cell was reduced up to 4-fold at this time (Fig. 9D). These data demonstrated that ES cell division was not inhibited by JDββHE infection and indicated that this unimpaired cell division was responsible for the reduction in the number of vector genomes per cell observed over time. Thus our results were consistent with the conclusion that the transient nature of eGFP transgene expression in ES cells was due at least in part to continued division of the transduced cells resulting in dilution of vector genomes.

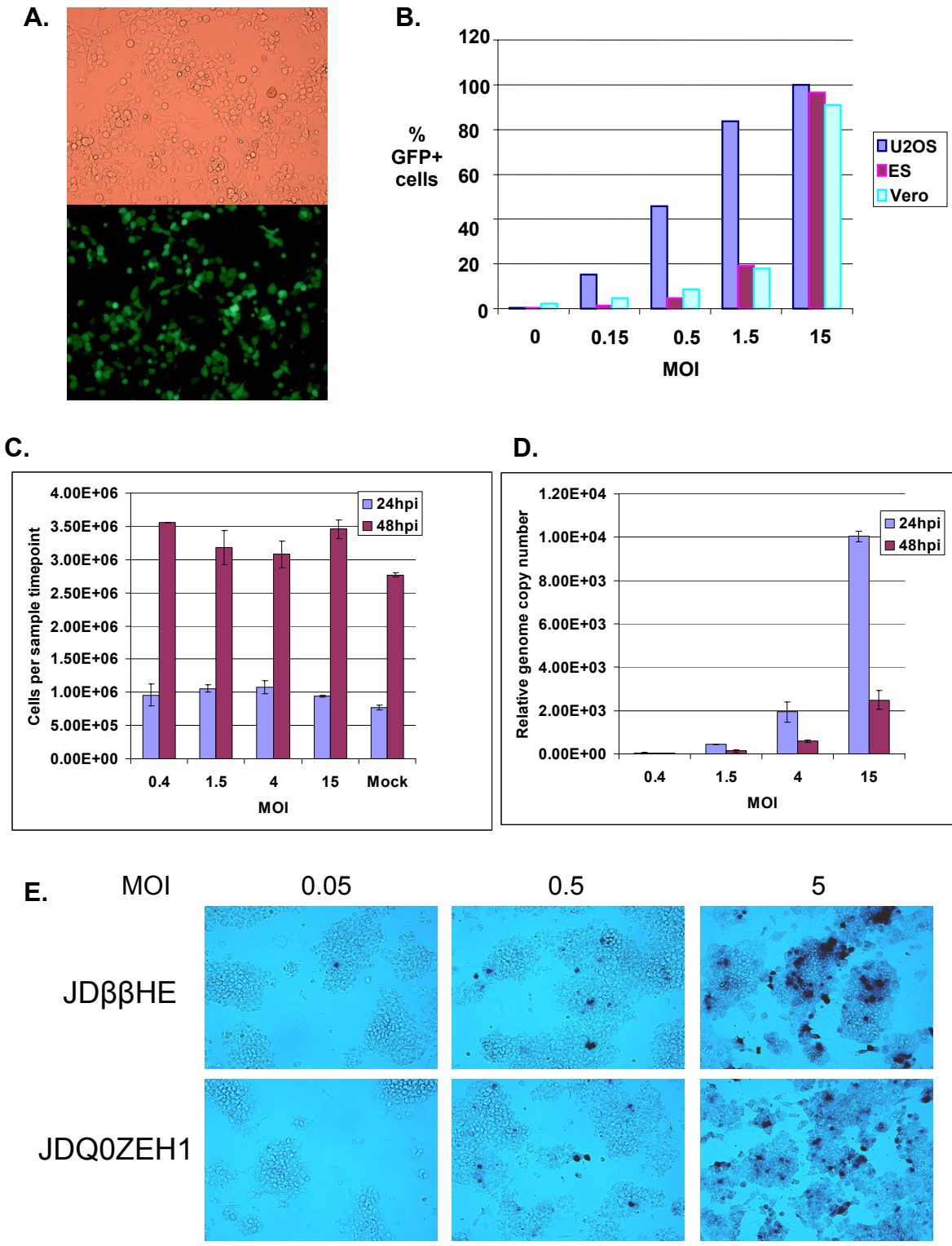

Figure 9. HSV vector behavior in ES cells.

(A.) eGFP expression controlled by the HCMV IE promoter was observed from JDββHE in ES cells at 24 h p.i. at an MOI of 20 TU. (B.) JDββHE transduces non-complementing cells in an MOI-dependent manner. U2OS, ES,

and Vero cells were infected with JDββHE at indicated MOI. Cells were trypsinized 24 h p.i. and flow cytometry was used to measure the percentage of cells expressing eGFP. (C.) ES cell division was not inhibited by JDββHE. Five hundred thousand ES cells were infected with JDββHE at indicated MOI. At 24 h p.i. and 48 h p.i., duplicate wells were counted for the number of cells by trypan blue staining. At least three rounds of cell division were detected for all infections. (D.) HSV genomes were diluted as ES cell division progressed. Five hundred thousand ES cells were infected with JDββHE at indicated MOI. DNA from duplicate infections (the same infections as Figure 5C.) were harvested and the relative level of UL1 molecules was detected per 200 ng total DNA by quantitative PCR. (E.) The ICP0 IE promoter is active in both the JDββHE and JDQ0ZEH1 viral backbones. Five hundred thousand ES cells were infected with JDββHE or JDQ0ZEH1 at indicated MOI (TU). β-gal expression was observed after X-gal staining at 24 h p.i.

We next compared the ability of JDββHE and JDQ0ZEH1 to express the lac Z gene from the ICP0 promoter in ES cells. Following infection at increasing MOIs based on U2OS TU titers, similar MOI-dependent lac Z expression was observed for both vectors (Fig. 9E). These results indicated that the ICP0 promoter remained responsive to VP16 carried into the cells with the infectious virus particles and that this response did not require any IE gene functions. This is in contrast to the situation described above for eGFP expression from the HCMV promoter, which was detectable in JDββHE-, but not in JDQ0ZEH1-infected ES cells. Thus the HCMV and ICP0 promoters, while both active in ES cells in the context of JDββHE, are controlled by distinct mechanisms. This quality offers the possibility of independently regulated expression of two transgenes from the same vector.

3.4.5 JDββHE does not interfere with ES cell differentiation during embryoid body formation

As described above, we found that JDββHE neither reduced the viability of ES cells nor prevented ES cell division. To expand these results, we sought to determine whether this vector affects the ability of stem cells to undergo differentiation expressed as embryoid-body (EB) formation. ES cells were infected with JDββHE or JDD0Z1 and then suspended as single cells in

high density media in triplicate tissue culture dishes. Eight to ten days later, EBs were counted using Quantity One software (Bio-rad). Even at excessive HSV particles per ES cell (40 TU), JDββHE did not inhibit EB formation, whereas JDD0Z1 reduced EB formation by more than 90% compared to mock-infected control cultures (Fig. 10A). While some inhibitory effect of JDββHE infection was observed at the highest MOI (100 TU), these results showed that JDββHE did not grossly interfere with EB formation and indicated that this could be ascribed to the highly reduced expression of ICP0 and perhaps ICP27 from JDββHE compared to JDD0Z1.

A.

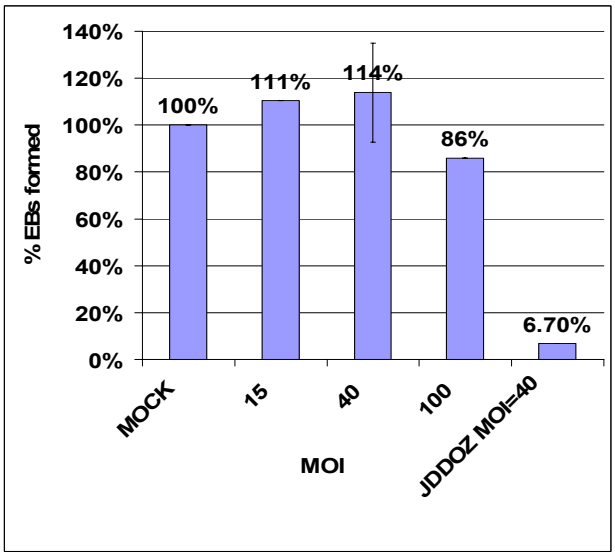
140%
120%
100%
80%
60%
40%
20%
0%
% EBs formed
100%
111%
114%
86%
6.70%
MOCK
15
40
100
JDDOZ MOI=40
MOI

C.

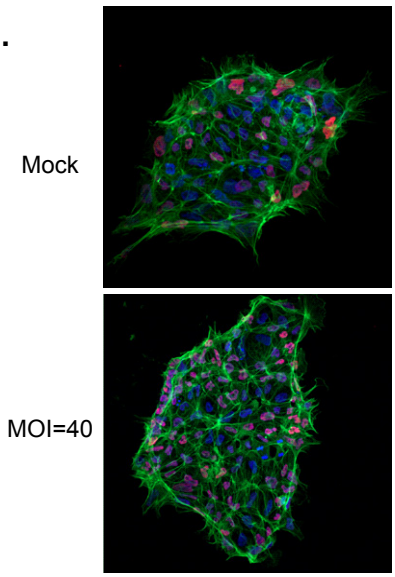
Mock
MOI=40

B.

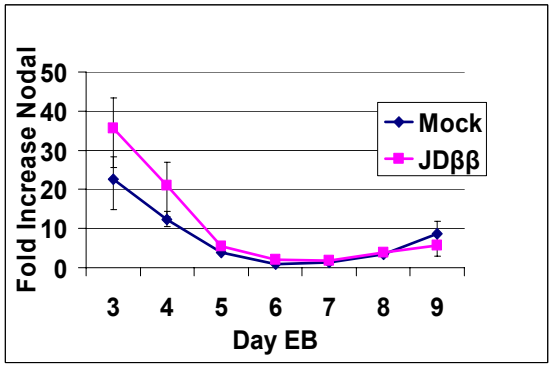
Fold Increase Nodal
50
40
30
20
10
0
3 4 5 6 7 8 9
Day EB
Mock
JDββ

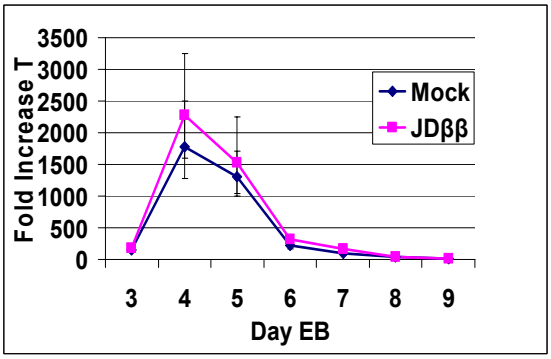
Fold Increase T
3500
3000
2500
2000
1500
1000
500
0
3 4 5 6 7 8 9
Day EB
Mock
JDββ

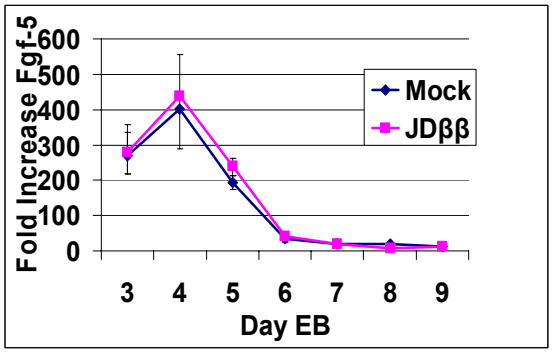
Fold Increase Fgf-5
600
500
400
300
200
100
0
3 4 5 6 7 8 9
Day EB
Mock
JDββ

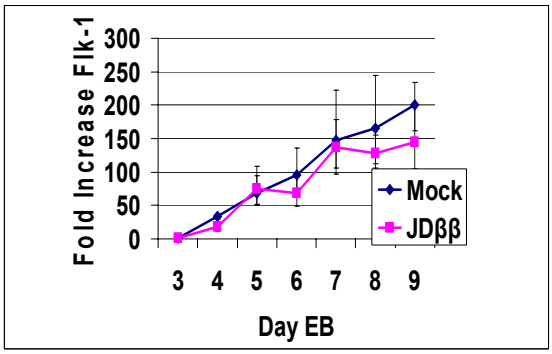
Fold Increase Flk-1
300
250
200
150
100
50
0
3 4 5 6 7 8 9
Day EB
Mock
JDββ

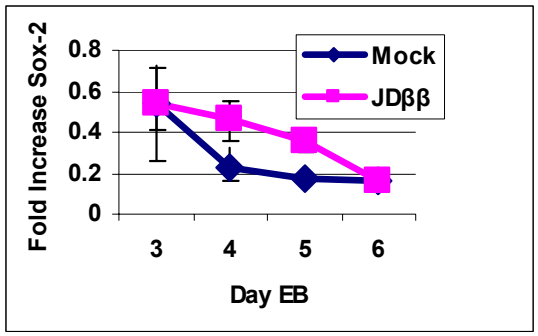
Fold Increase Sox-2
0.8
0.6
0.4
0.2
0
3 4 5 6
Day EB
Mock
JDββ

Figure 10. JDββHE does not affect ES cell differentiation or the expression patterns of developmental markers.

(A.) JDββHE does not inhibit EB formation. ES cells were mock infected or infected with JDββHE at indicated MOI or with JDDOZ at an MOI of 40 in suspension and then seeded in bacterial petri dishes in methyl cellulose for 10 days in the absence of LIF. The number of EBs were quantified using Quantity One software (Bio-RAD). Each bar represents an independent comparison between infected and mock performed in triplicate (3 EB plates), with the exception of JDββHE MOI=40 which represents two independent experiments, each compared to its respective mock infection. **(B.)** JDββHE does not alter the endogenous expression of developmental markers in EBs. ES cells were mock infected or infected at an MOI of 100, then plated in methyl cellulose as described above. Quantitative RT-PCR was used to show the expression patterns of representative germ layer and extraembryonic tissue markers between day 3 and day 9 of EB formation. (Brachyury (T), mesoderm; Fgf-5, embryonic ectoderm; Nodal, visceral endoderm; Flk-1, hematopoetic and endothelial) or between day 3 and day 6 of EB formation for Sox2 (self-renewal marker). **(C.)** Localization of Brachyury protein is similar in day 4 EB cells derived from either mock-infected or JDββHE-infected ES cells. EBs were plated on gelatin coated 8-well slides in ES media on day 3. IF for Brachyury was performed on day 4. Red, Brachyury; Blue, draq5 (nuclear); Green, Phalloidin.

To determine whether JDββHE produced more subtle effects during EB development, expression of marker genes representing normal differentiation processes was assessed by quantitative RT-PCR analysis. Expression levels were compared between EBs formed in high density media from single-cell suspensions of mock-infected ES cells or ES cells infected with JDββHE at a TU-based MOI of 100. The temporal expression patterns and levels on days 3-9 of EB formation for several germ layer and extraembryonic tissue markers, Nodal (visceral endoderm), Brachyury (mesoderm) [119], and Fgf-5 (embryonic ectoderm) [85, 176], were very similar between EBs formed from virus-infected and mock-infected ES cells (Fig. 10B). In addition, immunofluorescence for Brachyury protein showed that the level and distribution of this protein were similar between 4-day old EBs derived from mock- and JDββHE-infected ES cells (Fig. 10C). We also measured the expression of a self-renewal marker Sox-2 during ES cell differentiation. Expression of Sox-2 decreases as EBs differentiate and we detected no significant differences in Sox-2 expression between mock EBs and EBs derived from infected ES cells (Fig. 10B). The expression of vascular endothelial growth factor receptor 2 (Flk-1) was measured as a lineage-specific marker. Unlike the patterns observed for the three germ-layer markers, Flk-1 expression increased over the course of the experiment, as expected since

hematopoietic precursor cells become prominent during EB development. However, the pattern of Flk-1 expression was not markedly different between EBs derived from uninfected and JDββHE-infected ES cells (Fig. 10B). Together, these results demonstrated that JDββHE does not inhibit EB formation or alter the normal induction of representative markers of developmental processes or the hematopoetic lineage.

3.4.6 Expression of Pax3 in ES cells and EBs.

The ability to provide ES cells and cells of the embryoid body with a pulse of gene expression is potentially useful for mimicking the transient expression patterns of many developmentally regulated genes. To determine whether our HSV vector was capable of expressing a developmentally regulated gene, we engineered a derivative of JDββHE in which the eGFP cassette was replaced by Pax3 (Figure 11). This vector was used to infect ES cells and we examined the levels of Pax3 RNA by quantitative RT-PCR. Both JDββHE and JDββ-Pax3 possessed the lac Z gene under control of the ICP0 promoter and thus lac Z expression could be used to control for differences in transduction efficiencies between the two vectors.

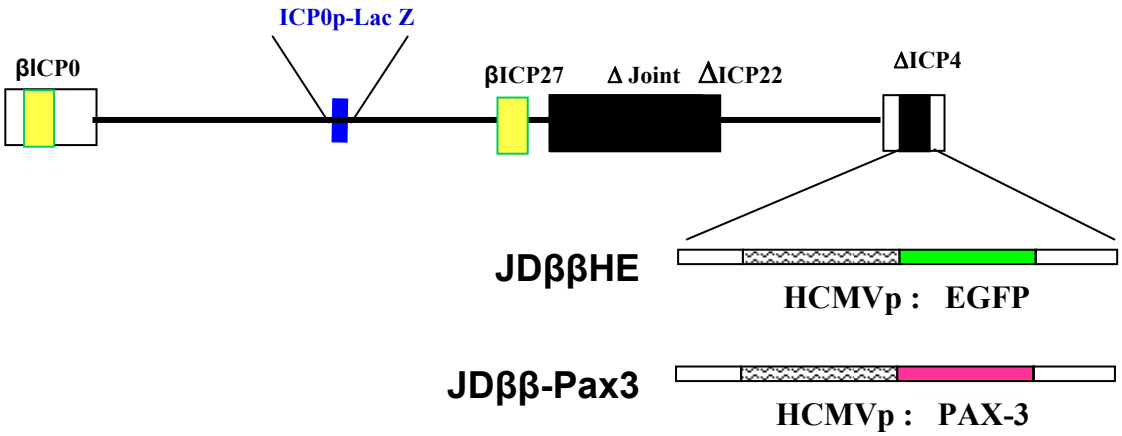

Figure 11. Diagram of JDββHE and a Pax3 expressing JDββ vector.

The Pax3 expression vector was engineered by replacing the eGFP transgene in JDββHE with the murine Pax3 coding sequence. The two vectors are otherwise isogenic and contain the lac Z reporter gene at the UL41 locus as previously described.

Using β-galactosidase (β-gal) activity as a measure of lac Z gene expression, the ES cell transduction efficiencies of the two vectors were similar on infection at 20 TU (Fig. 12A; TU titers based on β-gal expression in U2OS cells). Pax3 RNA levels were essentially the same in mock- and JDββHE-infected ES cells at both 24 h p.i. and 48 h p.i., indicating that the vector did not induce endogenous Pax3 gene expression (Fig 12B). However, at 24 h p.i. Pax3 RNA abundance was more than 3 orders of magnitude higher in ES cells infected with JDββ-Pax3. As observed earlier for eGFP protein in JDββHE-infected ES cells, the amount of Pax3 RNA in JDββ-Pax3-infected cells was reduced at 48 h p.i. Western-blot analysis using Pax3-specific antibody detected Pax3 protein at 24 h p.i. in ES cells infected with the Pax3 vector, but not in mock-infected cells or cells infected with JDββHE (Fig. 12B, *insert*); U2OS cells transfected with the Pax3 expression construct were used as positive control. Thus our vector was capable of expressing a developmentally regulated gene in ES cells.

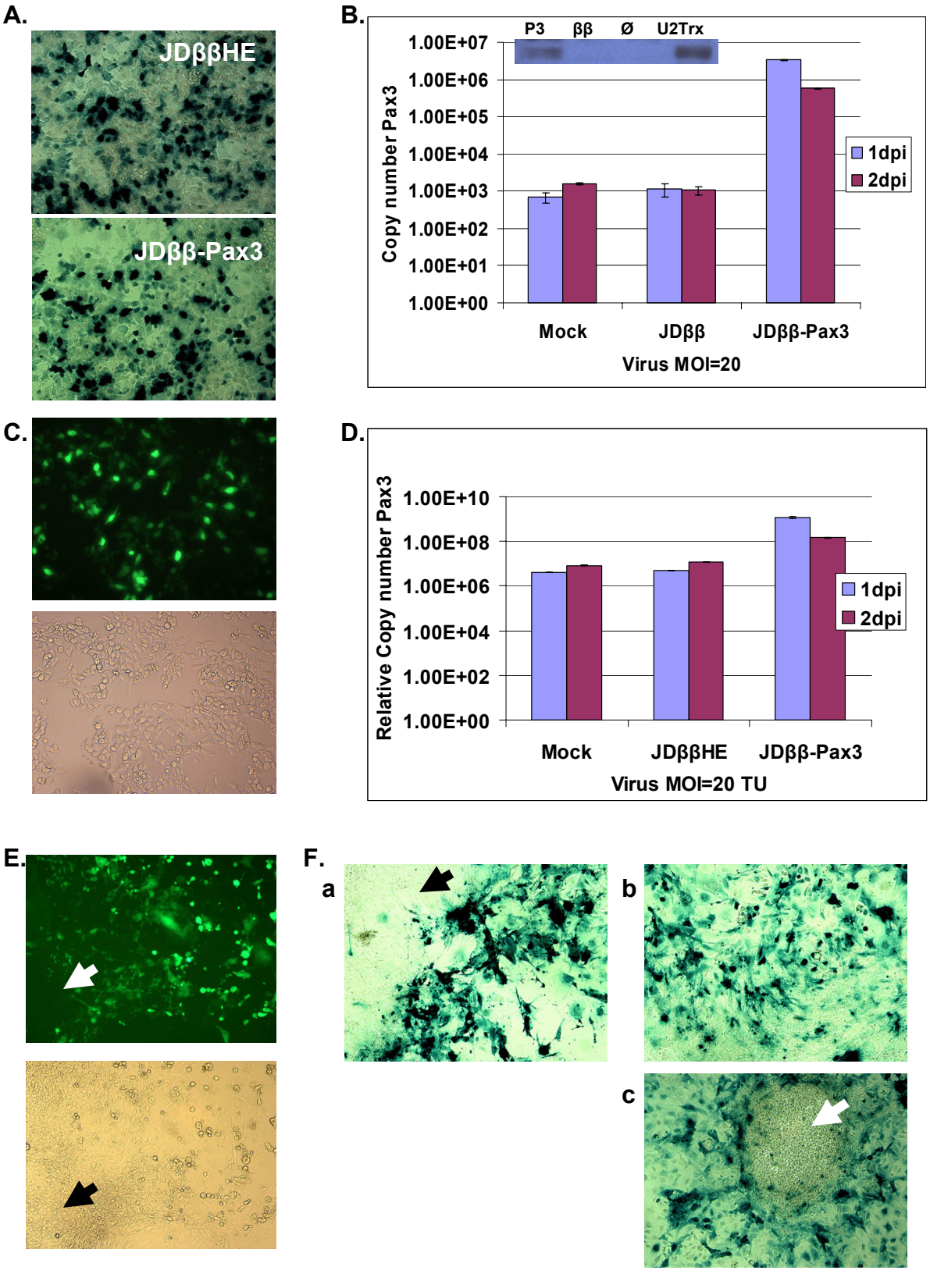
A.
JDββHE
JDββ-Pax3
B.
P3
ββ
Ø
U2Trx
1.00E+07
1.00E+06
1.00E+05
1.00E+04
1.00E+03
1.00E+02
1.00E+01
1.00E+00
Copy number Pax3
1dpi
2dpi
Mock
JDββ
JDββ-Pax3
Virus MOI=20
C.
D.
1.00E+10
1.00E+08
1.00E+06
1.00E+04
1.00E+02
1.00E+00
Relative Copy number Pax3
1dpi
2dpi
Mock
JDββHE
JDββ-Pax3
Virus MOI=20 TU
E.
F.
a
b
c

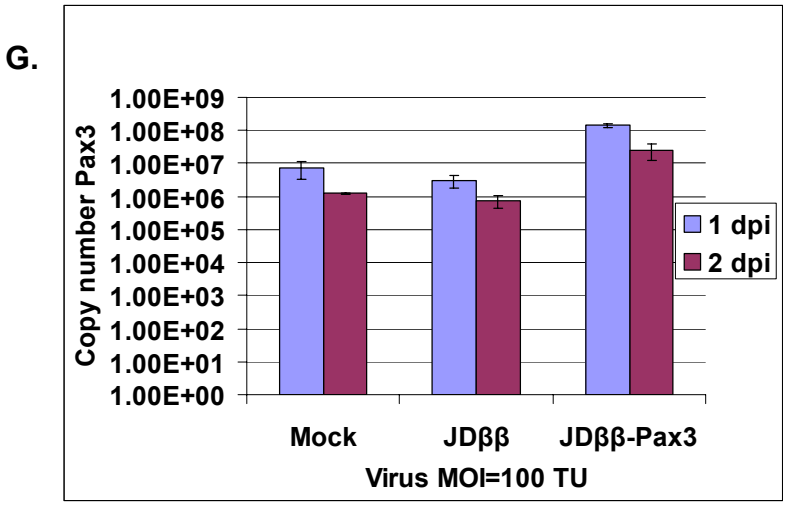

Figure 12. Transgene expression from JDββHE is robust and transient in ES cells and embryoid body cells.

(A.) ES cells were infected with JDββHE or JDββ-Pax3 at MOI of 20 TU. Similar levels of β-gal expression were detected from each vector at 24 h p.i. after X-gal staining. (B.) Pax3 expression in ES cells is transient. 500,000 ES cells were infected with virus at an MOI of 20 TU. Total RNA was harvested at 24 and 48 h p.i., reverse transcribed, and relative copy number of Pax3 mRNA was determined by quantitative RT-PCR normalized to GAPDH. Pax3 mRNA was not induced in ES cells infected with JDββHE, however Pax3 mRNA level was increased by at least three logs in JDββ-Pax3 infected ES cells. The level of Pax3 mRNA was reduced by approximately 7 fold by 48 h p.i. Pax3 protein was detected in JDββ-Pax3-infected ES cells at 24 h p.i. at an MOI of 20, as well as U2OS cells that were transfected with a Pax3 expression construct (inset). (C.) JDββHE efficiently transduced dissociated day 4 embryoid body cells. Day 4 EBs were dissociated by trypsin and infected with JDββHE at an MOI of 50. eGFP expression was detected by fluorescence microscopy at 24 h p.i. (D.) Transgene expression from JDββ-Pax3 was transient in day 4 EB cells. Day 4 embryoid bodies were dissociated by trypsin and infected with virus at an MOI of 20 TU. Total RNA was harvested at 24 and 48 h p.i., reverse transcribed, and relative Pax3 mRNA was detected by quantitative RT-PCR. The level of Pax3 mRNA was increased by approximately 2.5 logs in JDββ-Pax3 infected EB cells compared to mock or JDββHE infected EB cells. Pax3 expression was reduced by almost one log by 48 h p.i. (E., F., G.) Transgene expression in 2 week old EBs infected in monolayer. Embryoid bodies were formed in suspension for 5 days and plated onto gelatin-coated 24 well plates at 7-8 EBs/well. On day 12 of EB formation, 24-wells that contained beating cardiac areas were inoculated with $1x10^7$ TU/well using JDββHE or JDββ-Pax3. (E.) High levels of eGFP expression from JDββHE were observed by fluorescence microscopy at 24 h p.i. in embryoid body cells that are at the periphery of the dense EB mass. (F.) β-gal expression was observed in day 13 embryoid body cells that are at the periphery of the dense body of cells at one day post infection (a, JDββHE MOI=100 TU; b,c, JDββ-Pax3 MOI=100 TU). (G.) Pax3 expression in 2 week old peripheral EB cells was transient. Total RNA was harvested from infected EBs at 24 and 48 h p.i., reverse transcribed. Relative copy number of Pax3 mRNA was determined by quantitative RT-PCR. The level of Pax3 mRNA in JDββ-Pax3 EBs increased by 1-1.5 logs compared to mock or JDββHE-infected EBs, and Pax3 expression was reduced at 48 h p.i. by approximately 7 fold.

Previous reports have shown that 3 to 4 day old EBs are at a critical stage for the generation of many endoderm and mesoderm lineages and express high levels of the mesoderm marker Brachyury [119, 121]. Based on the broad host range of HSV, we anticipated that a

substantial number of the different cell types comprising EBs at this stage would be susceptible to transduction by JDββ-based vectors. To test this prediction, 4 day old EBs expressing high levels of the mesoderm marker Brachyury (Fig. 10B, T) were dissociated and infected with JDββHE or JDββ-Pax3. eGFP expression was detected by fluorescence microscopy at 24 h p.i. in EB cells infected with JDββHE at 50 TU (Fig. 12C). Pax3 RNA in JDββ-Pax3-infected EB cells (20 TU) was increased by more than 2 logs compared to mock- or JDββHE-infected cells at 24 h p.i., and this level was reduced approximately 8 fold by 48 h p.i. (Fig. 12D). These results demonstrated that a model gene-transfer vector based on JDββHE is suitable for transient transgene expression in day 4 EB cells.

In a similar experiment, we sought to express Pax3 in later-stage EBs, which were allowed to develop in suspension for five days and then plated on gelatin coated tissue culture dishes to allow outgrowth of differentiated populations. This method of ES cell differentiation results in the generation of many cell lineages such as cardiac muscle and skeletal muscle by day 14 [81]. The heterogeneous population of cells at 12 days was infected in a monolayer with JDββHE at 100 TU and transduction was detected as eGFP fluorescence. We did not observe transduction of all cells of the EB at 24 h p.i. In particular, while the outgrowing EB cells were infected and expressed eGFP (Fig. 12E), the dense mass of the EB (Fig. 12E, arrow) displayed little if any fluorescence. Likewise, following infection of 13 day old EB cells with JDββHE (a, Fig 12F) or JDββ-Pax3 (b,c, Fig 12F) at 100 TU, staining for β-gal activity at 24 h p.i. showed expression of the lac Z reporter gene only in cells at the periphery of the dense mass of EB cells (Fig. 12F, arrows). Pax3 RNA was detected in 13 day old EB cells infected with JDββ-Pax3 (same MOI) at 1.5-2 log higher levels than in mock or JDββHE-infected EB cells (Fig. 12G). The lack of uniform transduction throughout the entire embryoid body, which may be attributed

to an inability of the virus to permeate the dense mass of cells, is likely responsible for the lower level of Pax3 expression from JDββ-Pax3 observed here compared to that recorded earlier in ES cells and day 4 EB cells. Together, we conclude from these data that the JDββHE vector and the isogenic Pax3 expression vector are able to transduce both ES cells and differentiated EB cells. Furthermore, the Pax3 vector expressed a developmentally relevant gene product in a transient manner, suggesting that this vector platform will be useful in studies to examine the roles of specific genes and gene combinations in lineage determination.

3.5 DISCUSSION

In this report, we describe the engineering and characterization of a replication-defective HSV vector that is capable of efficient MOI-dependent transduction of > 95% of ES cells and transgene expression was observed in ES cells at a relatively low MOI. This vector is non-toxic to ES cells and does not inhibit EB formation or the formation of the three germ layers. These observations demonstrate that neither the introduction of the viral genome nor the expression of a reporter gene disrupts normal induction of differentiation markers.

Replication defective vectors have previously been used as vehicles for long-term transgene expression in neurons *in vitro* [169] and *in vivo* [177-179]. In non-neuronal cell types, vectors deleted for ICP4 and ICP27 remain toxic due to elevated expression of two of the other viral IE genes, ICP22 and ICP0 [160, 180]. In some cell types, deletion of ICP22 does not significantly affect the expression or growth of ICP4/ICP27 null viruses [160], but in others ICP22 is important for virus growth [181]. Although ICP0 is not an essential gene, viruses that are deleted for this function grow very poorly in all cell types at low MOI [165]. More

importantly for vector development, the presence of ICP0 is required for transgene expression in the absence of ICP4 and ICP27; when all three genes are deleted, the genome is essentially silent [161]. In addition to promoting viral gene expression, ICP0 is highly cytotoxic due to its ability to induce cell-cycle arrest and apoptosis [169, 173]. This raises the conundrum that a viral gene product that is required for transgene expression is simultaneously destructive to the host cells. We therefore sought to reduce the amount of ICP0 produced by our replication defective HSV vector, in lieu of deletion of the gene, in order to arrive at a more favorable balance between these two ICP0 activities. A similar strategy was previously reported in which an adenoviral vector expressing low levels of ICP0 was able to induce transgene expression from a highly defective HSV vector resident in cells in culture [166]. Likewise, deletion of the VP16-responsive element from the ICP22 promoter has been shown to convert this gene to one with early kinetics, resulting in highly reduced expression in the absence of ICP4 and ICP27 [161]. This study also demonstrated that ICP22 function in support of virus replication was restored in ICP4/ICP27-complementing cells.

Similar to previous studies which have demonstrated that low levels of ICP0 can promote transgene expression from severely deleted HSV vectors as well as the observation that gene expression from the viral tk E promoter in an ICP4-deficient background is low, we achieved a reduced level of ICP0 by substituting the ICP0 IE promoter with the viral tk promoter. Furthermore, by placing the ICP27 gene under the same promoter control, we eliminated all cytotoxic IE gene expression, yet could grow the virus by providing just a single complementing IE gene, ICP4. We have shown that this vector is capable of transgene expression in non-complementing ES cells from two different promoters without induction of cell death or disturbance of the ES cell differentiation program. Control vectors that either lacked the ICP0

and ICP27 genes or expressed both from their native IE promoters failed to combine these two properties. The strict replication dependence of our vector on ICP4, which controls the expression of both ICP0 and the essential ICP27 gene, raises the possibility of powerful selection protocols, as discussed further below.

ES cells provide an unlimited source of pluripotent cells that can potentially be used one day to generate specific cell lineages for cell transplantation studies. For example, it is possible to obtain a semi-pluripotent lineage-precursor population, such as day 4 EB cells that have been sorted based on the expression of the mesoderm marker Brachyury [121]. These partially committed pluripotent cells can be manipulated further to enhance or induce more specialized cell lineages using methods such as the addition of specific growth factors or cytokines to the cell media. Gene transfer at the different stages will provide a way to study the function of developmentally regulated genes and help identify the key players at the various lineage branch points. Our vector provides a promising tool toward this end. We have shown that infection at high multiplicities does not interfere with EB formation or alter the natural expression of the differentiation-specific markers Nodal, Brachyury, and Fgf-5. Our vector directed transient expression of a gene (Pax3) that is normally under developmental control, and expression was observed whether the cells were infected prior to or at various times after the induction of EB formation. Thus our vector meets the core requirements of a gene transfer vehicle suitable for the study of embryonic development.

We observed that both the HCMV promoter and the ICP0 promoter were active in JDββ-infected ES and EB cells whereas the HCMV promoter was silent in a similar vector that was deleted for the ICP0 and ICP27 genes. This result indicates that the JDββ backbone provides a factor, most likely ICP0, which prevents the repression of foreign promoters. Based on this

finding, we anticipate the possibility of using the JDββ backbone for selection of developmentally important transactivator genes from cDNA libraries cloned into the virus under the control of the ICP0 promoter. Libraries can be prepared from ES/EB cells at various early stages of development. Selection of replicating viruses will be afforded by conditional activation of the promoter for a known developmentally regulated gene, such as Pax3, engineered into the JDββ ICP4 locus in front of an intact copy of the ICP4 coding sequence. To account for the possibility that multiple stage-specific factors are required for activation of the target promoter, we intend to test this approach not only on established cell lines, but also on ES cells at varying stages of differentiation. While researchers have used techniques such as microarray analysis as a global approach to the identification of downstream events in differentiation, the JDββ vector system may help unravel earlier developmental events that are less tractable by currently available procedures.

4.0 GENERATION OF HSV-BASED GENOMICS TOOLS FOR THE IDENTIFICATION OF NOVEL GENE FUNCTIONS

4.1 ABSTRACT

Replication defective herpes simplex virus type 1 (HSV-1) vectors have been used extensively as a gene transfer vehicle for a wide variety of cell types, including embryonic stem cells. In an attempt to generate a pool of genes from which novel muscle-related genes as well as ion channel regulators can be selected, a library of HSV vectors that express cDNAs from pheochromocytoma (PC12) cells was constructed. The construction of cDNA bearing HSV vectors required the insertion of BAC elements (origin of replication and chloramphenicol resistance) and the Gateway recombination system, which facilitated efficient unidirectional recombination of cDNAs into the HSV genome. Microarray analysis demonstrated the presence of at least 15,000 unique genes, and functional analysis of the genes revealed many molecules involved in tumor cell growth and cell signaling, among other functions. The availability of a diverse cDNA library contained within infectious viral particles will likely contribute to the study of gene functions in vitro and in vivo.

4.2 INTRODUCTION

Muscular dystrophy (MD) is a prevalent genetic disorder that affects one in 3500 males

worldwide. MD is often caused by a single gene mutation in one of several genes involved in muscle integrity, which leads to the progressive degeneration of muscles and patients have shorter life expectancies due to cardiac or respiratory failure. The lack of an effective treatment or cure for MD has prompted the development of novel therapeutic approaches. One of the more promising lines of treatment is cell-based therapy, which strives to replace or regenerate new and functional muscle fibers by transplanting myogenic cells or progenitor cells into the patient. Several stem cell populations have been shown to contribute to the generation of new muscle fibers in a dystrophic (mdx) mouse model [57, 182-184], however, in order to progress these studies into human patients, the mechanism by which these cells are able to differentiate into the muscle lineage and contribute to improved muscle function in vivo must be clearly understood.

Embryonic myogenesis is extremely complex, and involves numerous pathways in the proliferation, migration, and differentiation of various cell types. The functions of many genes have been elucidated using transgenic animals, however disruption of genes with various functions in cellular differentiation can cause embryonic lethality, and does not allow for study of abolished gene function in adult tissues. In vitro models of muscle differentiation, such as myoblast cell lines or embryonic explants, have been useful in dissecting the signaling molecules involved in the activation of muscle specific genes. However, these models do not address the substantial amount of unknown regulatory gene products that are involved in this process. Furthermore, a method to identify genes that lie upstream of the earliest myogenic markers, such as Pax3 [42], does not currently exist. A clear and concise understanding of early muscle differentiation is critical in order to progress the development of cell-based therapies for muscular dystrophy. For these reasons, we sought to generate a comprehensive pool of expressed genes from which relevant myogenic genes could be identified.

Herpes simplex viral (HSV) vectors have been extensively engineered as a delivery vehicle for introducing genes into many somatic cell types, adult stem cells, embryonic stem (ES) cells, and cells that are derived through embryoid body formation (Figure 12). By eliminating essential viral genes such as ICP4 or ICP27, HSV vectors are unable to replicate in cells, however, the ability to express developmentally relevant genes in a transient manner remains in the presence of low levels of the viral gene ICP0 (Figures 8 and 12). In addition, robust viral replication is restored when the missing essential viral genes are provided in trans. There are many advantages to using HSV as a gene delivery vector including high transduction efficiencies in non-complementing cells, the ability to generate high titer purified stocks, and the HSV genome does not integrate into the host chromosomal DNA, thereby reducing the risk of altered endogenous gene expression or vector silencing. We sought to generate a library of expressed genes in HSV vectors since these vectors can be immediately applied to study gene function in various systems, both in vitro and in vivo.

Here we report methods to engineer HSV vectors containing a combined cDNA library derived from PC12 cells with and without differentiation using nerve growth factor (NGF). PC12 cells were chosen as the initial source of expressed genes in order to demonstrate that the construction of an HSV-based cDNA library was feasible. The cDNA library was introduced into the viral vector using a directionalized recombination system, Gateway (Invitrogen), and the vectors propagated in bacteria as bacterial artificial chromosomes. Recombinant viruses carrying the gene library were produced by transfection of complementing animal cells in culture with the BAC recombinant plasmids. The virus particles were capable of delivery and expression of the gene library in tissue culture cells. Library diversity was estimated by gene expression microarray analysis of cells infected with pools of gene-bearing vectors, and also microarray

analysis of cDNA inserts (in the form of PCR products generated directly from genomic library-containing DNA). It is estimated that this HSV cDNA library contains 15,000 unique gene products, of which approximately 5000 have known functions. The use of viral vector libraries that deliver and express the diversity of active genes in specific cells or tissues provides a powerful genomics tool to discover gene products that participate in a wide variety of cellular functions.

4.3 MATERIALS AND METHODS

Plasmids and Vector construction. BAC elements (origin of replication and chloramphenicol (CM) resistance gene) were engineered into the HSV vector d106 [173] genome, replacing the tk coding sequence using gancyclovir sensitivity to identify viral recombinants, and further confirmed by transformation of purified viral DNA into bacteria using chloramphenicol resistance. Thymidine kinase (tk) targeting plasmid was engineered using BAC elements from pBeloBACII and a plasmid containing homologous sequences which flank the tk locus. The resulting HSV BAC, (also referred to as DBAC), was propagated in 7b complementing cells as infectious virus, or in DH10B *E. coli* as a plasmid. HSV BAC DNA was purified from bacteria using Large-Construct DNA purification kit (Qiagen).

The ICP27-targeting plasmid containing the Gateway cassette was constructed by cloning the *Eco*RV fragment from plasmid BZPme3 (1.6 kb containing the *att*R1 site, *Pme*I site, zeo, *ccd*B, *att*R2 site) into plasmid Pme2 at the *Pme*I site. The resulting plasmid, HgatePme, contained the HCMV promoter, *att*R1, zeo, *ccd*B, *att*R2, poly A on a 2.3 kb *Bgl*II fragment. Plasmid Pme2 is EGFP-N1 (Clontech) with several modifications: *Bam*HI-*Bgl*II deletion, *Ssp*I

site converted to *Bgl*II by linker ligation, conversion of *Ase*I to *Bgl*II by linker ligation, and *Age*I/*Not*I deletion converted to *Pme*I by linker ligation. The *Bgl*II Hgate fragment was inserted into the *Bam*HI site of plasmid PXE [170]. Plasmid PXE is pBluescript cloning vector containing ICP27 flanks between *Eco*RI and *Xba*I restriction sites. Functionality of PXE-Hgate with respect to the gateway cloning system was confirmed using plasmid pENTR-gus and methods provided by Invitrogen.

DBAC was engineered to contain the Gateway cassette using homologous recombination in complementing 7b cells by transfection with plasmid PXE-Hgate. Phenotypically correct clear plaques underwent three rounds of plaque purification in 7b cells, verified by DNA sequencing analysis, expanded, aliquoted and stored at -80 until further use.

The Gateway cassette "Hgate" was derived from a commercially available destination vector (Invitrogen) and was modified to contain the zeocin coding sequence by the following modifications. 72GateA was generated by cloning the *Eco*RV fragment from Gateway conversion plasmid A into the *Eco*RV site of pSP72. The zeo coding sequence was obtained from pEM7zeo by blunting the *Xho*I to *Eco*RI fragment. The blunted *Xho*I to *Eco*RI fragment containing zeo coding sequence was cloned into the blunted *Not*I to *Mlu*I sites of 72GateA, in which the orientation of zeo was opposite relative to Gate to generate plasmid 72GateAZ1. 72GateAZ1 was cut with *Eco*RV and the gateway fragment was isolated, blunted, and then cloned into PC6 *Cla*I to *Xba*I blunted vector. Plasmid PC6 was generated from plasmid pPXE, an ICP27 targeting plasmid, in which the HCMV promoter and a poly-adenylation sequence was cloned between the ICP27 targeting flanks.

Generation of *ccd*B resistant DH10B based bacterial strain, HerpesHogs. To generate the necessary bacterial strain, we first introduced the *ccd*B containing plasmid pENTR-1A into GeneHogs bacteria (Invitrogen). Transformation of GeneHogs with pENTR (*ccd*B and kanamycin resistance) resulted in low numbers of colonies that were grown in Kanamycin (40 μg/ml) media and plasmid purified by Qiagen column. Restriction analysis revealed two bacterial strains that harbor a plasmid indistinguishable from pENTR and conferred resistance to *ccd*B. Retransformation of these plasmids into *ccd*B sensitive GeneHogs confirmed the functionality of the *ccd*B gene. Thus, in these two bacteria strains, there must have been a spontaneous mutation that renders *ccd*B resistance. Unfortunately, loss of the pENTR plasmid was required to utilize these strains for further gateway cloning. For this purpose, plasmid ETRS was generated, containing two positive selectable markers kan and CM, as well as two negative selectable markers *ccd*B and SacB. Mutagenesis of Genehogs using MNNG increased the number of dual-resistant clones ~500 fold. Two bacteria strains that were phenotypically correct (kanamycin and CM resistant in presence of plasmid ETRS, *ccd*B resistant and SacB sensitive in absence of plasmid ETRS) were chosen for HSV BAC propagation, termed HerpesHogs.

Bacterial Propagation. 2x YT (Yeast Tryptone) media were used for growth of bacterial strains in liquid culture. Luria-Bertain (LB) was used for solid media with the addition of 1.3% Agar. Selective agents included Ampicillin (200 μg/mL), Chloramphenicol (12.4 μg/mL), kanamycin (40 μg/mL), and sucrose (5% w/v). All bacterial strains were grown at 37˚C.

cDNA Library Construction in entry clones. Poly adenylated RNA was isolated from equal parts undifferentiated PC12 cells and PC12 cells that were differentiated in the presence of NGF using Qiagen's RNeasy Mini Kit according to manufacturer's protocol.

Generation of a cDNA library in the context of Gateway compatible plasmids was accomplished using the CloneMiner cDNA Library Construction Kit (Invitrogen). Briefly, mRNA purified from PC12 cells was reverse transcribed using SuperScriptIII and poly-thymine oligo primers containing the *att*B2 recombination site (first strand cDNA synthesis). After a second strand cDNA synthesis, the other recombinational site *att*B1 was ligated to the 5' end of the cDNAs overnight. T4 DNA polymerase was used to blunt the cDNA ends, followed by a phenol/chloroform extraction and ethanol precipitation to isolate the cDNA. The cDNA pool was size fractionated using the provided Sephacryl S-500 HR resin column to make cloning of larger inserts more probable. Adjacent fractions were pooled together to contain 150 ng of cDNAs, and were precipitated using ethanol. These pools of cDNAs flanked by *att*B recombination sites were then used in Gateway's BP recombination reaction to put them into a donor plasmid.

The BP recombination reaction was used to create plasmids with random cDNAs flanked by unique *att*L sites, to be used in the subsequent LR reaction described below. The BP reactions facilitated recombination between *att*B sites flanking cDNAs and *att*P sites in the donor plasmid (pDONR222). A total of 150 ng of pooled cDNA and 250 ng of pDONR222 plasmid was added to the BP Clonase enzyme mix and incubated at 25°C for 16-20 hours. Following proteinase K inactivation, DNA was ethanol precipitated and transformed into DH10B *E. coli* that were *ccdB* sensitive and kanamycin resistant. Electroporation parameters were as follows: 2.0kV, 200Ω, and 25μF. To verify cDNA insertion, twenty random colonies formed on the

overnight plate were chosen and the plasmids were isolated using Qiagen's Miniprep Kit. The plasmids digested with restriction enzyme *BsrG*I, for which sites are present in *att*L sites of the cDNA library and releases the cDNA fragment.

The pDONR:cDNA containing bacteria was pooled together and grown in LB-kan broth to an OD_{600} of 1.0. A Qiagen Maxiprep Kit was employed to retrieve and purify the cDNA library from the bacteria, using TE buffer pH 8.0 to elute the DNA. A PEG precipitation followed and the DNA was diluted to 25 ng/μl in preparation for the LR recombination reaction.

Generation of HSV cDNA library. The LR recombination reaction was used to recombine the cDNA library into the HSV BAC genome purified from HerpesHogs. The LR reaction facilitated recombination between the *att*R sites flanking the Gateway cassette in the HSV genome and the *att*L sites flanking the random cDNAs in the donor plasmids, recreating the original *att*B sites. Transformation of the resulting recombination reaction into *ccd*B sensitive DH10Bs selected for those HSV BAC Gate molecules that have incorporated a random cDNA. HSV BAC cDNA library DNA was purified using Qiagen Large construct Kit. To generate infectious virus, purified DNA was transfected into complementing 7b cells and the infection was allowed to progress to CPE. Cells and supernatant were salt treated (0.45M NaCl final concentration), aliquoted, and stored at -80 for further analysis.

Subpools of HSV BAC cDNA vectors were generated in order to test for library diversity. Five individual HSV BAC library vectors were obtained during the titration of the original DBAC library transfection stock. These five vectors were expanded individually on 7b cells. Equal amounts of pfu per each vector were mixed to generate a subpool of 5 known cDNA containing vectors. The subpool of 5 vectors was expanded once more on 7b cells. An

additional subpool of 100 cDNA vectors was expanded once more on 7b cells. Subpools and parental virus was aliquoted, titered on 7b cells, and stored at -80 for further use.

Gene Expression Microarray Analysis. Two million Vero cells were infected with the parental DBAC vector DAP, DBAC:Subpool 5, and DBAC:Subpool 100 at an MOI of 10 in duplicate. One day post infection, total RNA was harvested using RNEasy (Qiagen) and stored at -80 degrees Celsius until shipment to Cogenics.

Five hundred nanograms of total RNA was converted into labeled cRNA with nucleotides coupled to Cy3 fluorescent dye using the Low RNA Input Linear Amplification Kit (Agilent Technologies, Palo Alto, CA) following the manufacturer's protocol. Cy3 labeled cRNA (1.65 ng) from each sample was hybridized to an Agilent Whole Rat Genome Oligonucleotide Microarrays in 4 pack format. The hybridized array was then washed and scanned and data was extracted from the scanned image using Feature Extraction version 9.1 (Agilent Technologies).

Pearson correlation values were calculated for all four pairs of biological replicate samples using all non-control features present on the microarray. The Pearson correlation values for each sample pair indicate that the biological replicate samples are very highly correlated (ranging between 0.96 and 0.99) (Table 3). A Pearson correlation value of 1.0 means perfect correlation while 0 means no correlation and -1.0 denotes perfect anti-correlation. The replicates for each sample were then combined using an error-weighted average and each Vero subpool gene expression profile was then compared to Vero cells infected with parental DBAC vector (DAP) in order to identify differentially expressed transcripts (threshold of 1.5 fold difference).

Western Blot Analysis. 7b Vero cells were infected with indicated viral vectors at MOI of 1, 2, or 20. Cell lysates from infected cells and PC12 cells were harvested 24 hours post infection in 4X NuPage LDS buffer (Invitrogen) which was diluted to 1X prior to harvest. Cell lysates from approximately 100,000 cells were separated on a 4-12% SDS-Page gel (NuPage, Invitrogen) and transferred to a PVDF membrane. Standard immunoblotting protocols were followed for the detection of tyrosine hydroxylase and succinate dehydrogenase subunit D (Santa Cruz Biotechnology). Protein was visualized using HRP-conjugated secondary antibodies.

Polymerase chain reaction (PCR). The cDNA inserts were amplified from the HSV BAC cDNA library using primers specific for the HCMV promoter (GCGTGTACGGTGGGAGGTCTAT) and SV40 poly adenylation sequences (GGGGAGGTGTGGGAGGTTTT). PCR was done on a BIO-RAD iCycler IQ with the following thermal cycle: 94°C for 3 minutes, 35 cycles through 94°C for 30 seconds, and 61.7°C for 30 seconds, and 68°C for 1 minute or five minutes, followed by 1 cycle at 68°C for 5 minutes. Approximately 100 ng of template DNA was used for each reaction. Products from each PCR reaction were purified using Qiaquick PCR purification kit (Qiagen) with an additional 80% ethanol wash prior to elution.

Amplification of 1 kb fragments within four known genes contained within the library was done with the following thermal cycle: 94°C for 3 minutes, 35 cycles through 94°C for 30 seconds, 60°C for 30 seconds, and 68°C for 1 minute, followed by 1 cycle at 68°C for 5 minutes. Primers for individual genes were as follows: tyrosine hydroxylase F (CCTTGTCTCGGGCTGTAAAA) and R (CATTGAAGCTCTCGGACACA), cytochrome b F (CCGAAAATCTCACCCCCTAT) and R (TGTTCTACTGGTTGGCCTCC), Ikbkb F

(CTCCCTGACAAGCCTGCTAC) and R (TAAGCTGTCACAGGCACTGG), and chromogranin F (CTCACTACCGGGCTTCAGAG) and R (CCGCTATCTTCTGCAGTTCC). Approximately 10 ng of template DNA was used for each reaction. Products from each PCR reaction were purified using Qiaquick PCR purification kit (Qiagen) before further analysis.

Microarray Analysis of Library Inserts. PCR products from each of four individual 1 minute extension reactions were combined with PCR products generated by four 5 minute extension reactions to create four pseudo-biological replicates. Approximately 10 micrograms of DNA was chemically labeled at the guanine residue using the ULS labeling kit with Cy3 for Agilent gene expression arrays (catalog EA-023, Kreatech Biotechnology, Netherlands) according to manufacturer's instructions with the following modifications: 10 micrograms of DNA was combined with 10 µl of Cy3 in a 50 µl reaction volume. Following the labeling reaction, each 50 µl reaction was purified on one Kreapure column according to the provided protocol. The labeled cDNAs were stored at -20°C in the dark prior to shipment to Cogenics, Inc.

The cDNA was fragmented, and 3.3 micrograms of each labeled product was hybridized to an Agilent Whole Rat Genome Oligonucleotide Microarray in 4X44K format array. Hybridization, washing, staining and scanning were conducted using established procedures.

A given feature (probe) on the microarray was determined to be "well above background" if the measured mean signal intensity for the given feature was significantly greater than the corresponding background based on a 2-sided t-test. Furthermore, the background subtracted signal for the feature was greater than 2.6-times the standard deviation of the measured background levels. This approach enabled an array-by-array as well as a feature-by-feature determination of whether a given transcript was measured as "detected" in each sample

for all of the non-control probes present on the array. The results were tabulated in order to identify which transcripts were identified as "detected" in all 4 samples, 3 out of 4 samples, 2 out of 4 samples, 1 out of 4 samples, as well as not detected in any sample.

A Pearson correlation value using the normalized intensity values of all non-control probes present on the microarray was calculated for all pair-wise combinations of samples. In this experiment, the lowest correlation value was 0.985 and the highest was 0.993 (mean = 0.990). Cumulatively, these results indicate that the microarray data generated from these 4 samples is reproducible not only from the detected/non-detected assessment for each probe on the array, but also the correlation of the underlying intensity values.

Functional Analysis of Microarray Data. The networks and functional analyses were generated through the use of Ingenuity Pathways Analysis (Ingenuity® Systems, www.ingenuity.com).

The Functional Analysis identified the biological functions and/or diseases that were most significant to the data set. From the original microarray data report from Cogenics, Inc., a dataset was generated in which the mean intensity of each probe (from each of four biological replicates) was calculated and considered the expression value for each probe. Genes from the dataset that met the intensity cutoff of 100,000 and were associated with biological functions and/or diseases in the Ingenuity Pathways Knowledge Base were considered for the analysis. Fischer's exact test was used to calculate a p-value determining the probability that each biological function assigned to that data set is due to chance alone.

A network is a graphical representation of the molecular relationships between gene products. Genes or gene products are represented as nodes, and the biological relationship

between two nodes is represented as an edge (line). All edges are supported by at least 1 reference from the literature, from a textbook, or from canonical information stored in the Ingenuity Pathways Knowledge Base. Human, mouse, and rat orthologs of a gene are stored as separate objects in the Ingenuity Pathways Knowledge Base, but are represented as a single node in the network. The intensity of the node color (red) indicates the degree of intensity from the microarray. Nodes are displayed using various shapes that represent the functional class of the gene product. Edges are displayed with various labels that describe the nature of the relationship between the nodes (e.g., P for phosphorylation, T for transcription).

In order to generate networks, the data set containing gene identifiers and corresponding average intensity values was uploaded into in the application. Each gene identifier was mapped to its corresponding gene object in the Ingenuity Pathways Knowledge Base. An intensity cutoff of either 100,000 or a cutoff of gene identifiers "detected" in all four samples (see "well above background" description above) was set to identify genes whose expression was significantly differentially regulated. These genes, called focus genes, were overlaid onto a global molecular network developed from information contained in the Ingenuity Pathways Knowledge Base. Networks of these focus genes were then algorithmically generated based on their connectivity.

4.4 RESULTS

4.4.1 Infectious replication defective HSV vector genomes are maintained in bacteria as artificial chromosomes.

We engineered an HSV vector (d106) that is deleted for the essential immediate (IE) genes ICP4 and ICP27 [173] (Figure 13A). This vector was deleted for the coding sequences of ICP4 and ICP27, the two essential IE virus genes that are required for expression of the replication functions of HSV. In the absence of these viral functions, early and late viral genes are not expressed and the virus fails to replicate its DNA or produce virus particles. This vector also contains an expression cassette (HCMV:eGFP) introduced into the ICP27 locus to readily identify virus infected cells. This vector continues to express the remaining three IE gene functions ICP0, ICP22 and ICP47. ICP0 activity is of particular interest since this viral protein can prevent repression of non-HSV promoters, a requirement for expression of transgenes embedded in the vector genome and thus infection of non-complementing cells, which do not support virus replication, will fluoresce by eGFP expression. The vector was propagated on Vero (7b) cells that express the ICP4 and ICP27 genes in trans [185].

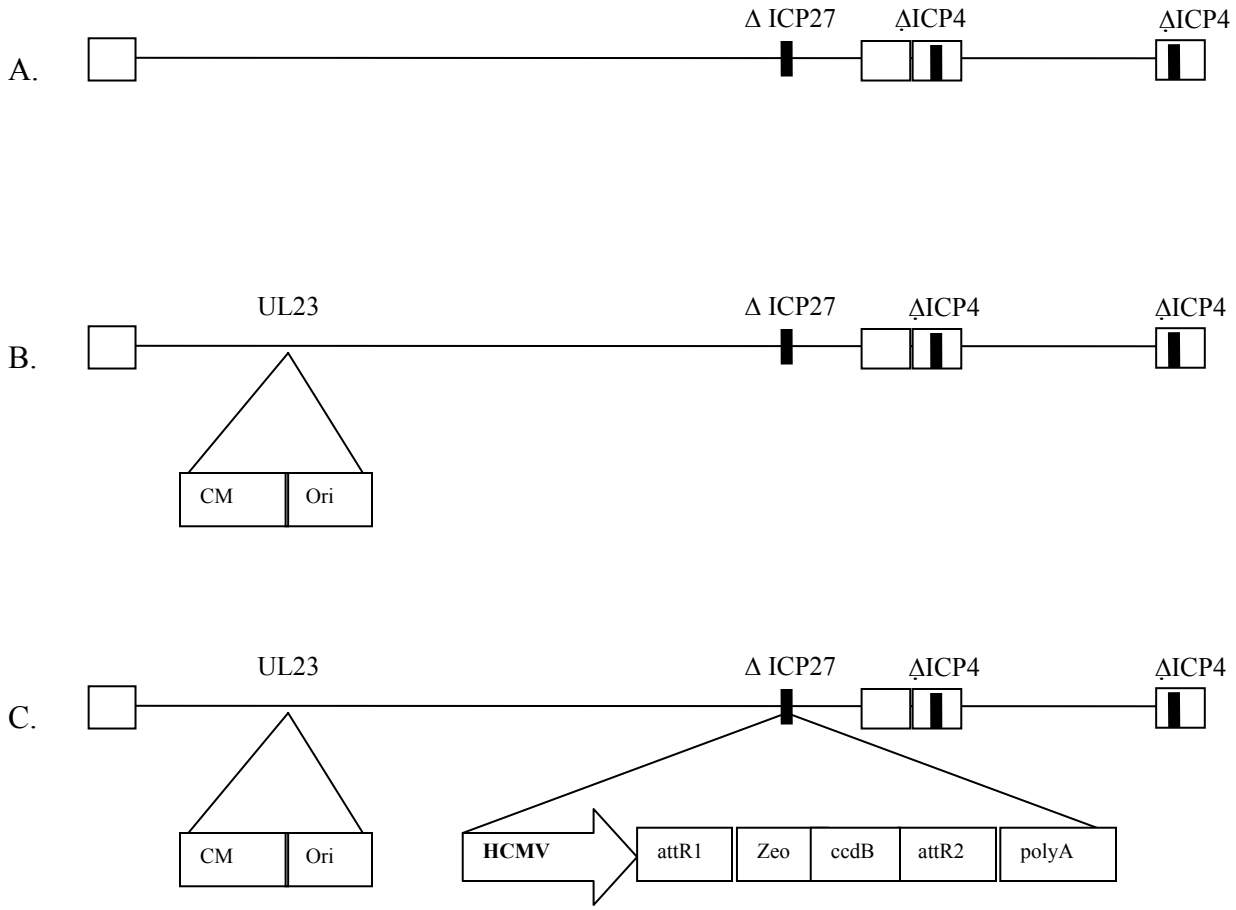

Figure 13. A bacterial artificial chromosome and the Gateway recombination system were engineered into the HSV vector backbone.

(A.) HSV vector d106 is deleted for both copies of ICP4 and the ICP27 locus was substituted for a reporter gene eGFP under the control of the HCMV promoter. (B.) DBAC was engineered by insertion of bacterial artificial chromosomal elements (origin of replication and chloramphenicol resistance) at the UL23 (tk) locus of d106 using homologous recombination. (C.) DBAC-Gate was engineered by homologous recombination of the Gateway recombination cassette into the ICP27 locus.

To propagate this infectious viral vector DNA in the E. coli strain DH10B, a bacterial artificial chromosome (bacterial origin and chloramphenicol gene) was introduced into the vector genome by homologous recombination at the thymidine kinase locus [186]. Recombinant viruses were selected using ganciclovir sensitivity (Figure 13B). The BAC plasmids proved to provide an ideal means of further manipulation of the vector genome and in particular, the generation of

recombinant vectors using an in vitro recombination system avoided the more difficult task of generating recombinants by marker transfer transfection methods in animal cells. Moreover, the analysis and storage of BAC recombinants was more efficient using bacteria. Transfection of purified BAC viral genomes into 7b cells provides a means of producing infectious herpesvirus particles when needed.

4.4.2 Engineering BAC vectors to contain the Gateway recombination system.

We exploited the Gateway directional recombination system (Invitrogen, Carlsbad, CA), to introduce a large number of cDNA clones into the HSV BAC genome. This was achieved using an in vitro recombination reaction involving commercially available donor (cDNA) and destination (BAC vector) plasmids. Directional recombination occurs through compatible recombination sites recognized by lamba phage integrase (Clonase), between which are positive and negative selectable markers that ensure highly efficient recombination upon transformation of recombinant BAC clones into bacteria.

The conversion of the HSV BAC vector into a "destination" plasmid required additional vector and bacteria strain engineering. Commercially available Gateway destination plasmids contain a negative selectable marker gene *ccd*B (controller of cell division or death B) that inhibits bacterial gyrase, resulting in cell death. To propagate death gene plasmids, Invitrogen provides a *ccd*B resistant bacterial strain DB3.1, a DH5α-derived strain containing the modified gyrase *gyr*A462 allele. However, there were no available bacterial strains that are *ccd*B resistant and also proficient for propagation of HSV BAC DNA. To generate this strain, global mutagenesis of the DH10B based bacterial strain GeneHogs (Invitrogen) and subsequent use of positive and negative selectable markers resulted in two strains that conferred *ccd*B resistance.

One of the strains, HerpesHogs, was further utilized to propagate *ccd*B-containing HSV BAC DNA.

The Gateway destination cassette was introduced into the HSV BAC genome by homologous recombination following co-transfection of complementing 7b cells. Clear plaque recombinants were identified by the replacement of the eGFP expression cassette at the ICP27 locus with the Gateway cassette (Figure 13C). The resulting HSV vector was termed DBAC-Gate and can be propagated in complementing 7b cells as infectious virus, or as a BAC in HerpesHogs bacteria.

4.4.3 Engineering DBAC-GATE to contain a library of expressed genes from PC12 cells.

We selected PC12 cells for initial experiments because this permanent line has attributes of neuronal cells and can be differentiated with neurotrophic factors. These cells are likely to express a wealth of genes that govern neuronal growth, signaling and differentiation pathways and provide a suitable host for later studies of gene functions. The PC12 cDNA library was first generated in a Gateway-based donor plasmid using the commercially available Cloneminer Kit (Invitrogen). During the reverse transcription of PC12 poly-adenylated RNA, gateway recombination sequences (*att*B1 and *att*B2) were incorporated at the 5' and 3' cDNA termini by linker ligation and primer design respectively. These recombination sites allowed for the efficient directional incorporation of the cDNAs into donor plasmids containing *att*P1 and *att*P2 sites during the in vitro BP recombination reaction, thereby generating recombinant plasmids with cDNAs flanked by *att*L1 and *att*L2 sites. The recombinant plasmids were then maintained in the DH5a bacterial strain following plasmid transformation. A limiting dilution of the entry plasmid containing bacteria demonstrated the presence of approximately 20 million individual

clones. The plasmid DNAs from 20 randomly picked bacterial clones were subjected to restriction digest to remove the cDNA inserts and size analysis revealed the presence of 20 different clones (size range of 1.5-6 kb) representing 20 different cDNAs (Table 2). The presence of 20 unique cDNAs was confirmed by DNA sequencing, the majority of which appeared to be full length (18/20). These data suggested that the starting library was complex.

Table 2. Sequence analysis of entry clones.
The plasmid DNA from 20 randomly picked bacterial clones was digested with restriction enzyme *Bsr*G1 to remove the cDNA inserts. Size analysis revealed the presence of 20 different clones (size range of 1.5-6 kb), and represented 20 different cDNAs.

PC12 Clone #	BsrG1 gel size	Seq Accession #	Expected Size	Full Length Y/N	Gene Product
1	1.0	BC087725	1.0	Y	Histone H3, 3B rat
2	1.5	NM_212496	3.3	N	DEAH box RNA helicase (only 2nd half of gene) rat
3	1.2	BC098059	1.2	Y	Meiotic recombination homologue REC14 rat
4	1.6	NM_031595	1.6	Y	Proteaosome 26S subunit Psmc3 rat
5	2.8	XM_215405	2.1	Y	5' Nucleotidase, cyto II Nt5c211 rat
6	2.1	NM_175843	2.1	Y	Binds PKCz and GABAc receptor- Sequestrome mouse (93%)
7	3.5	BC018491	3.6	Y	Transmembrane protein 30A-Mammary tumor
8	2.5	NM_053642	2.2	Y	Sterol-C5-desaturase (only 2nd half) rat
9	0.3	Reaction Failed			
10	2.5	BC055809	1.9	Y	Chromatin modifying protein 2B mouse (93%)
11	1.3	NM_177613	1.3	Y	cell division cycle cdc34 variant mouse (96%)
12	3.4	NM_198052	5.0	?	T-box 3 variant 2 Tbx3- Cardiac Differentiation mouse (93%) Unknown full length
13	1.7	NM_012545	5.1	Y	Dopa decarboxylase Dcd rat (clone is 1.7kb of 5' mRNA- variant)
14	3.0	AK087802	1.8	Y	Ubiquitin conjugating enzyme binding/ d10 cerebellum mouse (94%)
15	1.6	RN30CTR	1.6	Y	3-oxoacyl-CoA thiolase rat
16	2.4	NM_001007625	2.2	Y	Ependymin related protein Epdr2/ elevated in colorectal cancer rat
17	0.9	XM_344286	1.3	Y	DnaJ subfamily C (Hsp40) rat
18	2.4	XM_576107	2.1	Y	Hematopoietic progenitor protein homologue rat
19	4.7	NM_001011909	1.4	Y	Gpatch protein (Gpatc2) rat
20	2.4	BC083796	2.2	Y	Protein Kinase C binding protein Prcbp1 rat
21	3.9	XM_342595	1.5	Y	Syntaxin 16 (Imprint control) deletion in autosomal dominant pseudohypoparathyroidism
22	6.5	NM_019827	8.3	N	Glycogen synthase Gsk3b (only 2nd half) mouse (92%)
23	2.5	Tetracycline	2.5	Y	Positive control

The donor plasmid cDNA library was purified from the DH5a hosts and recombined into the DBAC-Gate HSV genome purified from the HerpesHogs strain using the in vitro LR recombination reaction. The LR reaction facilitated the directional exchange of genetic material between the *att*L sites in the donor plasmid library and *att*R sites in the HSV genome, and introduced each cDNA into an HSV genome under transcriptional control of the HCMV promoter. The recombinant vector was introduced into the *ccd*B sensitive DH10B cells resulting in the selection of bacteria containing the DBAC cDNA library. Each bacterium harbored a single copy plasmid representing a single recombinant cDNA-carrying virus genome. Approximately 5 million individual clones were detected using a limiting dilution of the HSV BAC cDNA containing DH10B bacteria.

DBAC library DNA was harvested and purified from the combined bacterial culture and transfected into complementing 7b cells. Titration of the virus library pool in 7b cells showed that the initial transfection produced 0.5-1 million individual pfu and expansion of this pool generated $4x10^7$ pfu. These infectious virus particles now represented the cDNA expression library that could be subsequently propagated in complementing cells where the individual cDNAs should be expressed. Moreover, the library gene products should be expressed following infection of a variety of non-complementing cells where virus gene expression is limited to the remaining IE genes in the vector; expression of other viral genes is prevented by the deletion of ICP4 and ICP27 from the vector genome.

4.4.4 The cDNA expression vectors were analyzed to confirm library complexity.

The large number of virus particles represented an unknown number of unique cDNAs. To estimate the complexity of our library we pool, we first determined whether the vector was

capable of expressing the cDNA both as mRNA in infected cells and as a transgene protein product. For this purpose, five random viral plaque forming units were isolated from the DBAC viral particle cDNA library were subjected to DNA sequence analysis. These five DBAC vectors contained the genes Prefoldin-5, a coiled-coil containing protein similar to myosin (RGD1306908), brix domain containing 2 (Bxdc2), an unknown sequence similar to amino acid aminotransferases (LOC363056, XM_343384), and dynactin 2. Individual DBAC vectors were propagated in 7b Vero cells to produce individual viral stocks. Equal amounts of each individual vector were mixed to generate a subpool of five known cDNA-containing virus particles, which was propagated on 7b cells once more for expansion. The pool of 5 known vectors was used to infect Vero cells such that each cell was infected with all 5 vectors at a total MOI of 10. At 24 h post infection, the infected cell mRNA was harvested and subjected to whole rat genome microarray analysis carried out at Cogenics Inc. Analysis of duplicate samples demonstrated >96% correlation (Table 3). Compared to the expression profile of cells infected with the parent vector, cells infected with the mix of five known cDNAs clearly demonstrate three highly expressed transcripts that were up-regulated 100-fold, and an additional two transcripts showed approximately 14-fold and 10-fold up-regulation (Figure 14A). These transcripts in fact correlate with the 5 sequenced genes that were present in the DBAC HSV subpool. This data suggest that expression from DBAC cDNA vectors is high in non-complementing Vero cells.

Table 3. Microarray analysis of Vero sample duplicates.
After infection of Vero cells with library vector subpools, the amount of genes with differential expression levels were calculated using thresholds of 1.5 and 5 fold (increase or decrease) when compared to Vero cells infected with the empty vector control. Pearson's correlation values were > 96% and demonstrated a high correlation between sample duplicates.

Sample Pair	Pearson's Correlation	Upregulated 1.5 fold	Upregulated 5 fold	Down-regulated -1.5 fold	Down-regulated -5 fold
Vero Empty Vector:	0.99481	N/A	N/A	N/A	N/A
Vero Mix 5:	0.99583	91	16	85	22
Vero Mix 100:	0.96544	428	295	96	19

A.

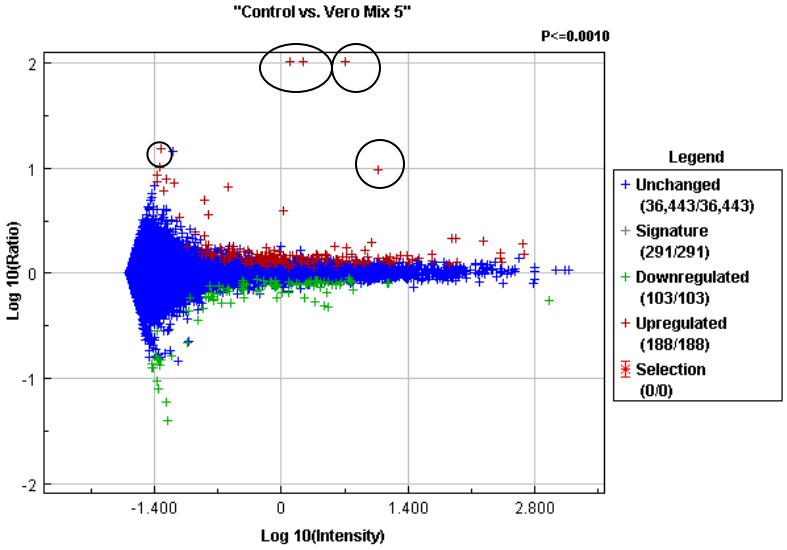

B.

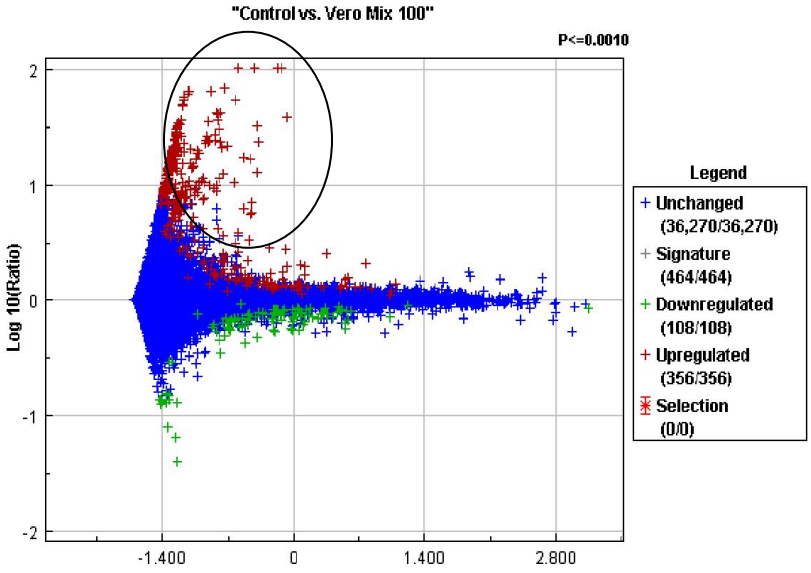

Figure 14. Microarray analysis of Vero cells infected with a subpools of five known or 100 cDNA-expressing HSV vectors show upregulation of gene products.

Log ratio plots depicting differential gene expression in Vero cells infected with five known (A.) or a mix of 100 unknown (B.) HSV cDNA vectors compared to Vero cells infected with the parent (empty) vector. The X-axis depicts the combined fluorescent intensity that was measured on the microarray while the Y-axis depicts the log ratio from the comparison. Each transcript is represented as a plus sign. The colors are based on the log-ratio p-value. The red denotes transcripts that are significantly upregulated by at least 1.5 fold compared to control (significance in this instance is defined as a log-ratio p-value less than 0.001), the green denotes transcripts that are significantly downregulated by -1.5 fold or less compared to control while the blue indicates those transcripts that are not significantly differentially expressed. Differentially regulated transcripts that are specifically expressed by an HSV cDNA library vector are circled in Figure A., while transcripts likely expressed by an HSV cDNA library vector are circled in Figure B.

An additional subpool of cDNA-containing HSV BAC vectors were generated by combining approximately 100 individual pfu (Mix 100) from the original DBAC library virus titration on 7b cells. This mix of 100 viral particles was further expanded in 7b cells. The subsequent stock was used to infect Vero cells at total MOI of 10 (individual vector MOI of 0.1). Log ratio plots from the comparison of the Mix 100 infection to the control vector infection shows a trend in which the number of upregulated genes increased, however the fold change of those upregulated genes was of a lower intensity than the vector mix of 5 known cDNAs (Figure 14B). Approximately 428 genes were upregulated at least 1.5 fold in the Vero Mix 100 microarray compared to the parental vector infection, which the majority (300) show at least a 5-fold upregulation (Table 3).

4.4.5 Protein Expression of cDNA containing HSV vectors

In order to verify protein expression from cDNA containing DBAC vectors, individual vectors were isolated from a titration of the Mix of 100 cDNA vectors on 7b cells. Several vectors were plaque purified and subjected to DNA sequence analysis which revealed two of the cDNA inserts as tyrosine hydroxylase and succinate dehydrogenase subunit D. The upregulated expression of

these two particular genes was observed in the microarray analysis of Vero cells infected with the Mix 100 subpool, demonstrating the expression of these genes from the HSV genome at the mRNA level. To demonstrate that the HSV cDNA library is capable of protein expression of the inserted cDNA sequence, complementing 7b cells were infected with each vector and the parent vector expressing only RFP. Western blot analysis of cell lysates showed the expression of tyrosine hydroxylase and succinate dehydrogenase subunit D from each respective infection (Figure 15). These proteins were also detected in PC12 cell lysates as expected since these cells were the original source of the cDNA.

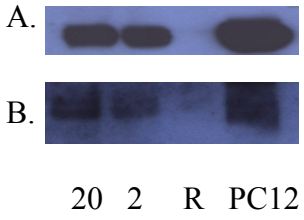

Figure 15. Clonally isolated library vectors express transgenes at the protein level.

Complementing 7b Vero cells were independently infected with two library vector isolates (A., HSV-Tyrosine hydroxylase; and B., HSV-succinate dehydrogenase subunit D) at MOI of 20 (20) and 2 (2), or an isogenic control vector, (R), expressing RFP from the Gateway locus, at an MOI of 1. PC12 cells were used as a positive control. Cell lysates were run on a 4-12% SDS-Page gel and western blots were performed using antibodes specific for tyrosine hydrogenase (A) or succinate dehydrogenase subunit D (B) (Santa Cruz Biotechnology).

4.4.6 Complexity of HSV BAC library DNA was directly examined using microarray analysis.

While the analysis of gene expression of a subpool of these library vectors in animal cells had suggested a level of diversity contained within the HSV cDNA library, there remained an

uncertainty as to how many unique genes this library contained. In order to more accurately determine which genes had been incorporated into the HSV BAC cDNA library, microarray analysis was used to identify the cDNAs directly from DBAC library genomic DNA rather than expression in animal cells. From this original stock of library-containing DBAC DNA, all cDNA inserts were amplified by PCR using unbiased primers which annealed to the HCMV promoter and the SV40 poly A sequences. PCR reactions varied in the amount of time allowed for extension and ranged from 1 minute to 5 minutes in order to enrich for cDNA of varying lengths (Figure 16A). The measured size range of cDNAs was 200 base pairs up greater than 5 kb.

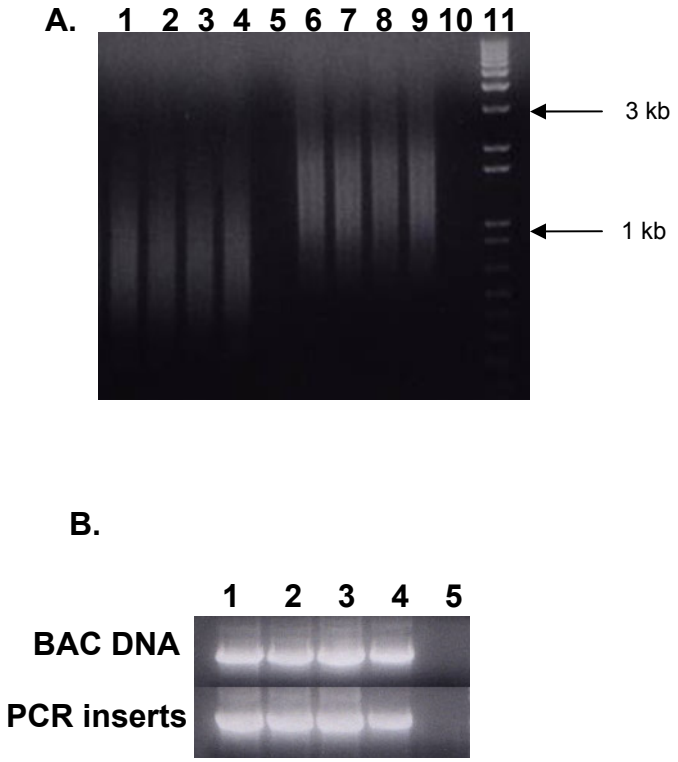

Figure 16. PCR amplification of cDNA library inserts and verification of known library components.

cDNA inserts were amplified from DBAC library genomic DNA using primers specific for the HCMV promoter and the SV40 poly-A sequences, and with varying extension times (lanes 1-4, 1 minute extension; lanes 6-9, 5 minute extension). (A.) 1/25 of each PCR reaction was run on a 1% agarose gel to reveal cDNAs of varying size (lane 11, DNA ladder). Arrows indicate approximate fragment size in kilobases (kb). (B.) Library components are

not lost during PCR amplification of cDNA inserts from DBAC library genomic DNA. Primers were designed to amplify 1 kb fragments within four individual genes known to be present in the library, tyrosine hydroxylase (lane 1), cytochrome b (lane 2), chromogranin (lane 3), and inhibitor of kappaB kinase-beta (lane 4). Water was used as a negative PCR control (lane 5). All four individual genes were detected using both the original DBAC library genomic DNA (top row) and the pool of PCR-amplified cDNA inserts (bottom row) as template DNA.

To verify that these PCR parameters had successfully amplified known library inserts (i.e. genes that had been upregulated in gene expression arrays in Figure 14B), primers were designed to detect 1 kb PCR products within the four genes tyrosine hydrogenase, inhibitor of kappaB kinase-beta (Ikbkb), cytochrome b, and chromogranin. These four genes were up-regulated by at least 5 fold in Vero cells infected with the Mix of 100 cDNA vector subpool (Table 5). As a positive control, these four genes were amplified from the original stock of DBAC library genomic DNA (Figure 16B, top row). We then sought to verify the retention of the four known genes in the PCR product pool generated from DBAC genomic library DNA. Figure 16B demonstrates that all four known genes were detected in the pool of PCR-amplified inserts as template DNA as well (bottom row). Prior to the amplification of Ikbkb, chromogranin, and cytochrome b from DBAC genomic library DNA in this experiment, it was unclear as to whether the up-regulation of these genes in the Vero gene expression array (Mix 100) was due to their presence in the cDNA library or simply a downstream transcriptional event induced by a vector-expressed cDNA. Collectively, this data confirmed that these four genes are present in the DBAC cDNA library. Furthermore, this data demonstrated that library genes were not lost during the unbiased PCR amplification of cDNA inserts and suggests that library complexity was not compromised during this step.

Individual PCR reactions that varied in extension times (1 minute and 5 minute) were pooled into four samples and treated as pseudo-biological replicates for downstream microarray analysis. PCR amplified cDNAs were chemically labeled with Cy3, fragmented, and hybridized

to whole rat genome microarray, carried out at Cogenics, Inc.

Table 4. Number of probes detected out of a total of 43,379 non-control probes present on the Agilent whole rat gene expression array.

Number of Samples in which Probe was Detected	Number of Probes Measured as Detected	Intensity Range
4 out of 4 samples	17,671	8116.8 – 658,704.5
3 out of 4 samples	1,989	6110.5 – 45,379.1
2 out of 4 samples	837	4887.6 – 18,926.3
1 out of 4 samples	791	2845.8 – 10,051.6
0 out of 4 samples, Not measured as detected	22,091	1506.1 – 8181.0

Table 5. Genes of interest detected in microarray of PCR products.
Mean intensity values detected in microarray of PCR products and fold increase of cDNA expression in gene expression microarray of Vero cells infected with Mix of 100 library vectors.

Genes of Interest	Mean Intensity	Fold Increase mRNA in Vero cells (Mix 100) compared to empty vector
Chromogranin	455662.93	5.78
Tyrosine Hydroxylase	412093.93	8.75
cytochrome b	405914.03	5.14
Succinate Dehydrogenase D	223972.60	40.9
Ikbkb	86523.05	16.25

Approximately 17,000 probes were detected in all four replicate samples, and an additional 1,989 probes were detected in 3 out of 4 replicate samples (Table 4). A total of 39,762 probes (92% of non-control probes) were identified consistently as detected in all four samples or not detected in any sample. The five genes that were examined by protein expression (Figure 15) or PCR (Figure 16) were detected in all four samples with intensities well above background (mean intensity, Table 5). As stated earlier, these five genes were also up-regulated (ranging from 5- to 40-fold) in Vero cells infected with the Mix of 100 library vectors (Table 5). These analyses confirmed that these five genes have successfully been incorporated into the

HSV BAC cDNA library, and further suggested that the HSV BAC cDNA library was diverse and contained many unique gene products.

Table 6. Analysis of detected probe IDs using various threshold criteria.
The entire dataset was analyzed using Ingenuity Pathways Analysis program using a threshold of probes detected in all four samples (per Cogenics, Inc. analysis), probe IDs detected at an intensity of 100,000 or higher, or probe IDs detected at an intensity of 214,748 or higher. The amount of probe IDs that were considered in the analysis was decreased as the threshold became more stringent. More than 50 percent of the total IDs in each case were mapped to a molecule in the Ingenuity knowledge base. IDs that are not mapped likely did not correspond to a known gene product. Genes that were eligible for functional analysis met the threshold criteria (column 1) and also had at least one functional annotation associated with that molecule in the Ingenuity knowledge Base.

Intensity Cutoff (Threshold)	Total IDs	Mapped IDs	Eligible Genes for Functional Analysis
All positive probes	17,671	10,263	4149
100,000	5404	3049	1508
214,748	1592	919	508

A functional analysis of the genes contained within this vector bearing library was generated through the use of Ingenuity Pathways Analysis (www.ingenuity.com). Using an intensity cutoff of 100,000, the number of genes that were eligible for functional analysis was limited to approximately 1500 genes, a manageable number of molecules to analyze according to guidelines provided by the program (Table 6). The molecules represent a diverse range of cellular functions, from cell signaling to skeletal and muscular disorders. The highest ranking biological functions which also contained at least 100 molecules are depicted in Figure 17A. A considerable amount of genes correlated with cellular growth and proliferation (Figure 17B) and cellular signaling (Figure 17C), which was expected since the source of genetic material for this cDNA library was a neuronal tumor cell type, the pheochromocytoma PC12 cell line. As one of the goals of this cDNA library construction was to generate a pool of molecules involved in cell signaling, we are confident that this library represents a diverse pool of genes that are likely involved in this as well as other functions.

A.

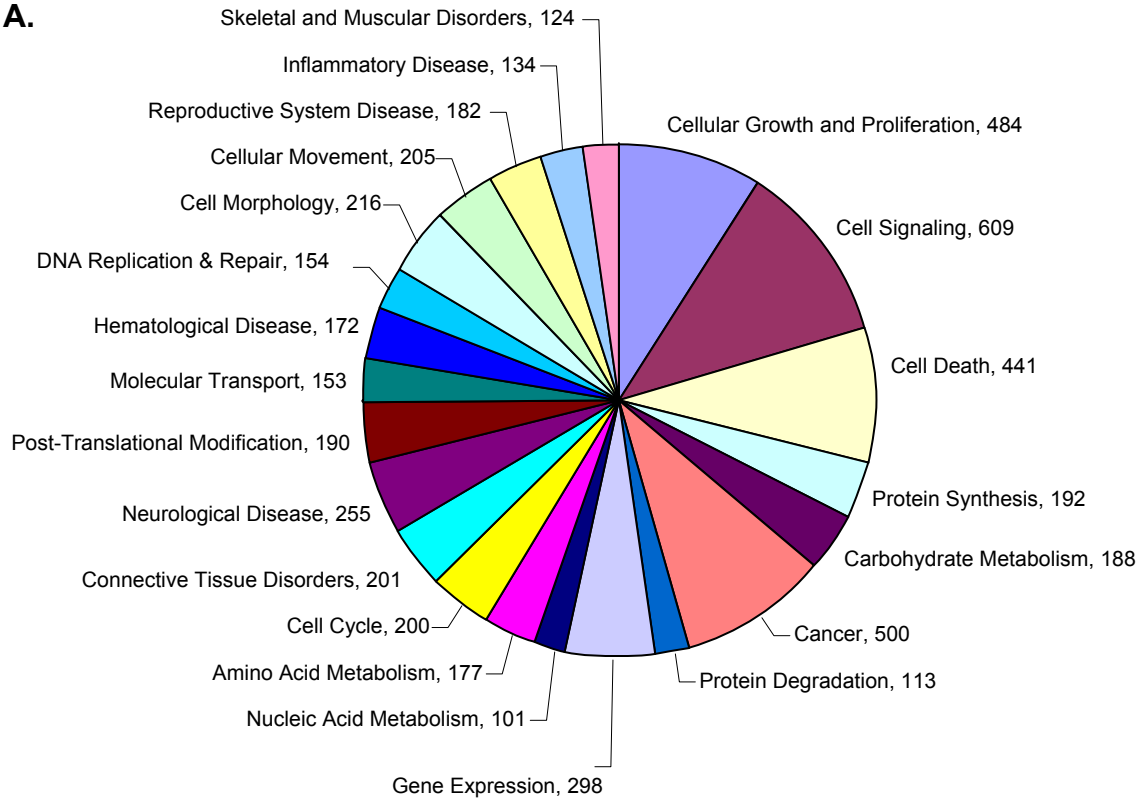

B. Cellular Growth

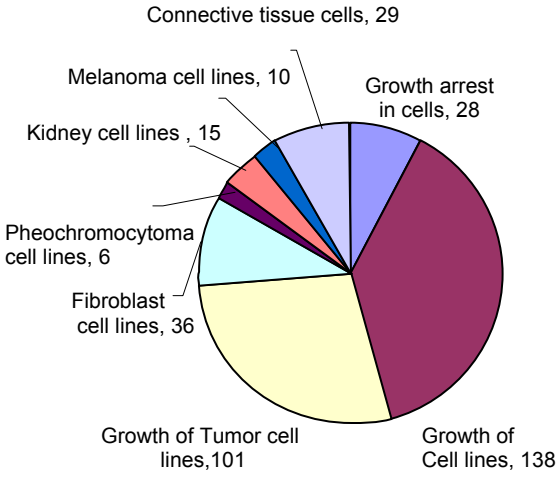

C. Cell Signaling

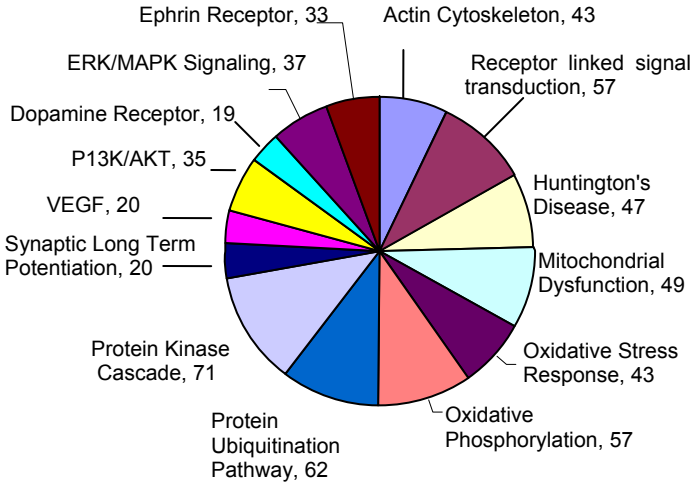

Figure 17. Relevant functions of top 1500 genes.

The functional analyses were generated through the use of Ingenuity Pathways Analysis, and identified the biological functions or diseases that were most significant to the data set. Genes from the dataset that met the intensity cutoff of 100,000 and were associated with biological functions or diseases in the Ingenuity Pathways Knowledge Base were considered for the analysis. (A.) The top 30 functional categories (and the number of genes associated) with the lowest p-value, and which contained at least 100 molecules ($P < 0.0003$) are depicted. Categories were not mutually exclusive, i.e. some molecules participated in more than one functional category. (B.) Functional analysis of 322 total molecules related to cellular growth. (C.) Functional analysis of 609 total molecules related to cellular signaling. Not all functional categories were depicted in this figure.

4.5 DISCUSSION

The overall goal of this of this work was to create a library of expressed genes by which genes that have a particular function, such as muscle differentiation, could be identified. The identification of such products can be a daunting task if standard methods such as transfection of cDNAs or retrovirus insertional mutagenesis are used as screening methods to identify these biological activities since, in the first case, limiting dilution experiments are required to identify genes from pools and in the second case, cell lines must be isolated and the insertion sites characterized. The use of HSV vectors for the screening stage has a number of advantages including the ability to create HSV vector cDNA libraries for testing in high throughput screens where virus plaquing will facilitate the capture of relevant genes. HSV also has a large transgene capacity and transduces stem cells and their derivatives with high efficiency. These features are essential to testing different gene products for their function in cellular differentiation.

The Gateway recombination system employs phage-lambda based site-specific recombination sites (*att*) that have been engineered to be compatible with one another and also provides unidirectional and irreversible recombination reactions. Manipulation of transgenes in vectors using the Gateway system makes cDNA library construction more efficient by maintaining gene orientation and reading frames during the transfer. We were able to

demonstrate the efficiency of incorporating full length cDNAs into our vectors using this system, as well as the expression of these genes at both the transcriptional and protein level. Furthermore, the amount and diversity of genes detected by microarray analysis suggests that the incorporation of cDNAs during these recombination reactions was efficient.

We have substantial preliminary data validating a selection system whereby TRPV1 delivered by an HSV vector and activated by chemical agonists prevents viral replication due to calcium overload-induced apoptosis. Thus virus recombinants carrying genes that either inhibit TRPV1 activation or function, or prevent apoptosis, will preserve cell viability and allow virus plaque formation. We have used this selective viral replication strategy with gene-encoded dominant-negative subunit of the TRPV1 ion channel, Poreless, to demonstrate that viral particles that harbor a gene encoded TRPV1 inhibitor could be selected from a pool of viral particles [187]. This co-infection strategy could be adapted so that negative regulators of TRPV1-mediated apoptosis could be identified from a library of HSV expressed cDNAs. Naturally-occurring gene-encoded ion channel regulators are most likely expressed by neuronal cell types and for this reason, PC12 cells were chosen as the source of expressed genes for the cDNA library. PC12 (rat pheochromocytoma) cells have been used as a model for neuronal differentiation since they are derived from the rat adrenal medulla and terminally differentiate in the presence of nerve growth factor. Indeed, functional analysis of the incorporated cDNAs demonstrated that these molecules participate in a wide variety of neuronal processes and signaling pathways (Figure 17).

The generation of this initial HSV-based library of expressed genes from PC12 cells was important in order to demonstrate that this task was feasible. The PC12 cell line was chosen because is easy to work with and likely expressed genes relevant to other applications described

above. However, the ultimate goal of this work was to provide a pool of genes from which regulators of cellular differentiation could be identified, namely those involved in early muscle differentiation. In this respect, the PC12 cell line would not have been the ideal source of genetic material, but rather a myogenic progenitor cell line or embryonic tissue (discussed below). Nevertheless, the ability to generate a library of expressed genes was clearly demonstrated and the methodology is in place to generate additional and more relevant gene libraries.

While most of the gene products contained within this cDNA library are akin to neuronal cell function, an in depth examination of these genes revealed several networks that contained genes involved in the regulation of muscle differentiation (Figure 18 and 19). Figure 18 depicts a network of molecules that have been directly or indirectly linked to the myogenic regulatory factors MyoD and Myf5, highlighted in blue, in the scientific literature. While MyoD and Myf5 were not detected in the cDNA library microarray analysis (intensities of 1791 and 5806 respectively), Id1 was detected with an intensity of greater than 315,000 (Appendix A). Id1 is a helix-loop-helix (HLH) domain-containing protein that can form heterodimers with basic HLH transcription factors, such as MyoD and Myf5. When bound to the myogenic regulatory factors, Id1 acts as a transcriptional repressor by reducing DNA binding ability. While Id1 can inhibit MyoD-mediated muscle development, MyoD has been shown to reduce the rate by which Id1 is degraded in co-transfection studies in Hela cells, which suggests a dynamic interplay between these two molecules [188]. In C2C12 mouse myoblast cells, it was shown that induction of Id1 expression not only blocks transcriptional activity of myogenin but also induces myogenin degradation by blocking formation of myogenin-E47 protein complexes, which stabilized myogenin in these cells [189]. Interestingly, in transgenic mice which over-express both

myogenin and Id1, Id1 caused an increase in the expression of MyoD and Myf5 mRNA in differentiated postmitotic mouse muscle fiber, which demonstrated that myogenic factors are influenced by mechanisms that maintain cellular homeostasis [190], and that genes related to these pathways are contained within the HSV cDNA library.

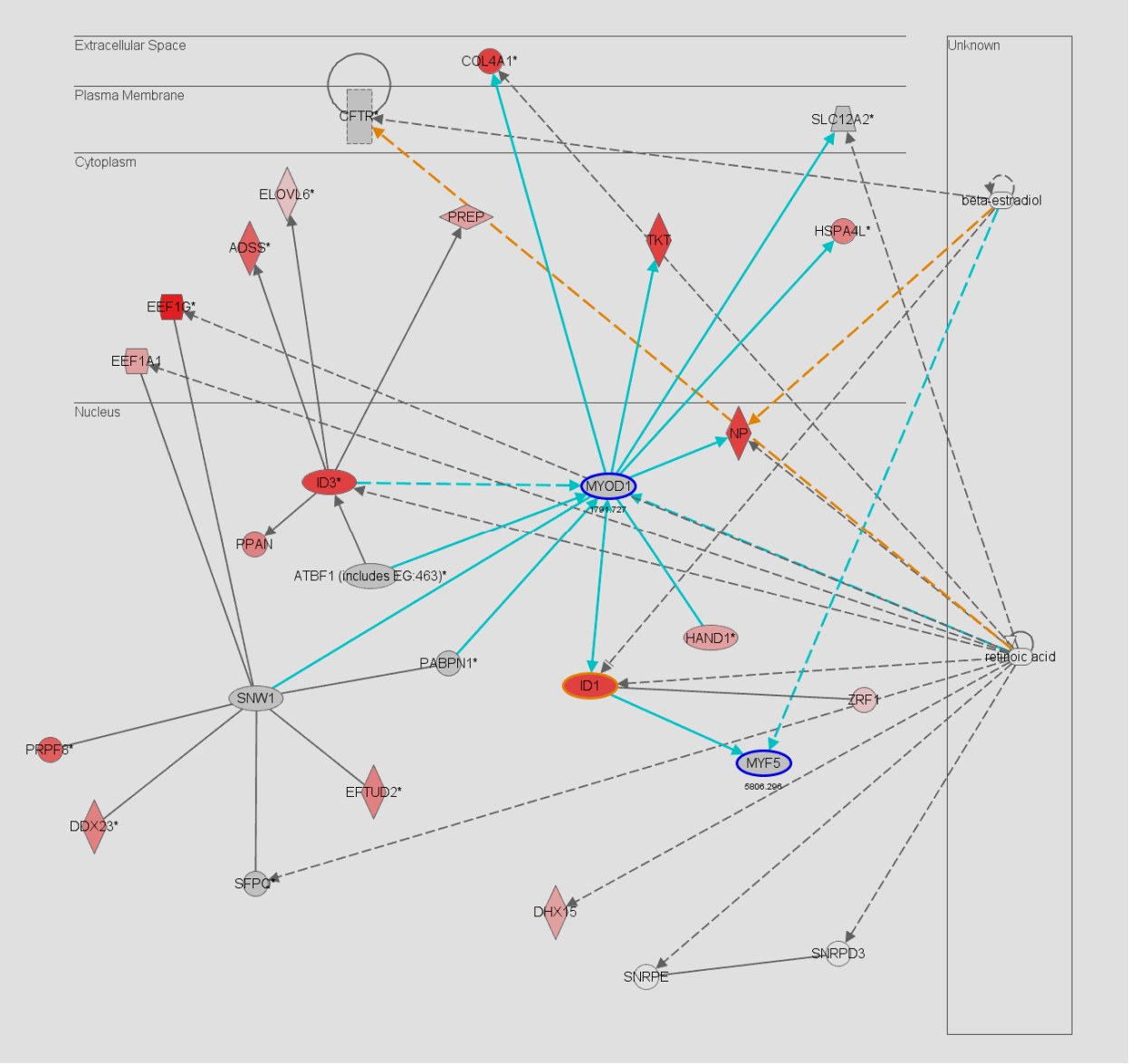

Figure 18. MyoD and Myf5 participated in a network of molecules contained in the HSV-based cDNA library.

The network depicting a graphical representation of the molecular relationships between gene products was generated in Ingenuity Pathways Analysis. An intensity cutoff of 100,000 was set to identify genes whose expression was significantly detected in the cDNA library. Genes are represented as nodes, and the biological relationship between two nodes is represented as an edge (line). All edges are supported by at least 1 reference from the literature, from a textbook, or from canonical information stored in the Ingenuity Pathways Knowledge Base. The myogenic regulatory factors MyoD (MYOD1) and Myf5 (MYF5) are highlighted in blue. The intensity of the node color indicates the degree of up-regulation (mean intensity) of the gene product. Gene descriptions and intensity values listed in Appendix 1.

A second network, in which myogenin participated, was identified during the examination of all probes that were considered "present" in four out of four sample replicates in the microarray analysis (Figure 19). While myogenin was not detected in the microarray (intensity of 10,910), molecules that interact with myogenin, such as Wnt11 (intensity of 83,000), creatine kinase (intensity of 146,238), and Cand2 (intensity of 25,920), were observed (Appendix B). In cultured mesenchymal adult stem cells from bone marrow of 2 month-old adult mouse, Wnt11 increased expression of sets of genes characteristic for cardiac and skeletal muscle cells, including myogenin, Myf5, MyoD and MRF4 [191], which otherwise would have not been expressed in this cell type. Another molecule detected in the microarray, creatine kinase, is important for the generation of energy that is required for muscle contraction. In crude extracts of C2C12 myoblast cells, myogenin was shown to bind to a DNA fragment containing sequences from the creatine kinase promoter [192]. Cand2 (also known as TIP120B) was recently identified as a novel myogenic regulator, in which its expression was induced in association with myogenic differentiation. Cand2 was shown to accelerate the myogenic differentiation of C2C12 cells, and suppress the ubiquitin-dependent degradation of myogenin [193]. The presence of genes in the HSV cDNA library that are related to the regulation of muscle differentiation confirmed the diverse nature of the library and also suggested that this library could be used for the identification of genes related to myogenic development.

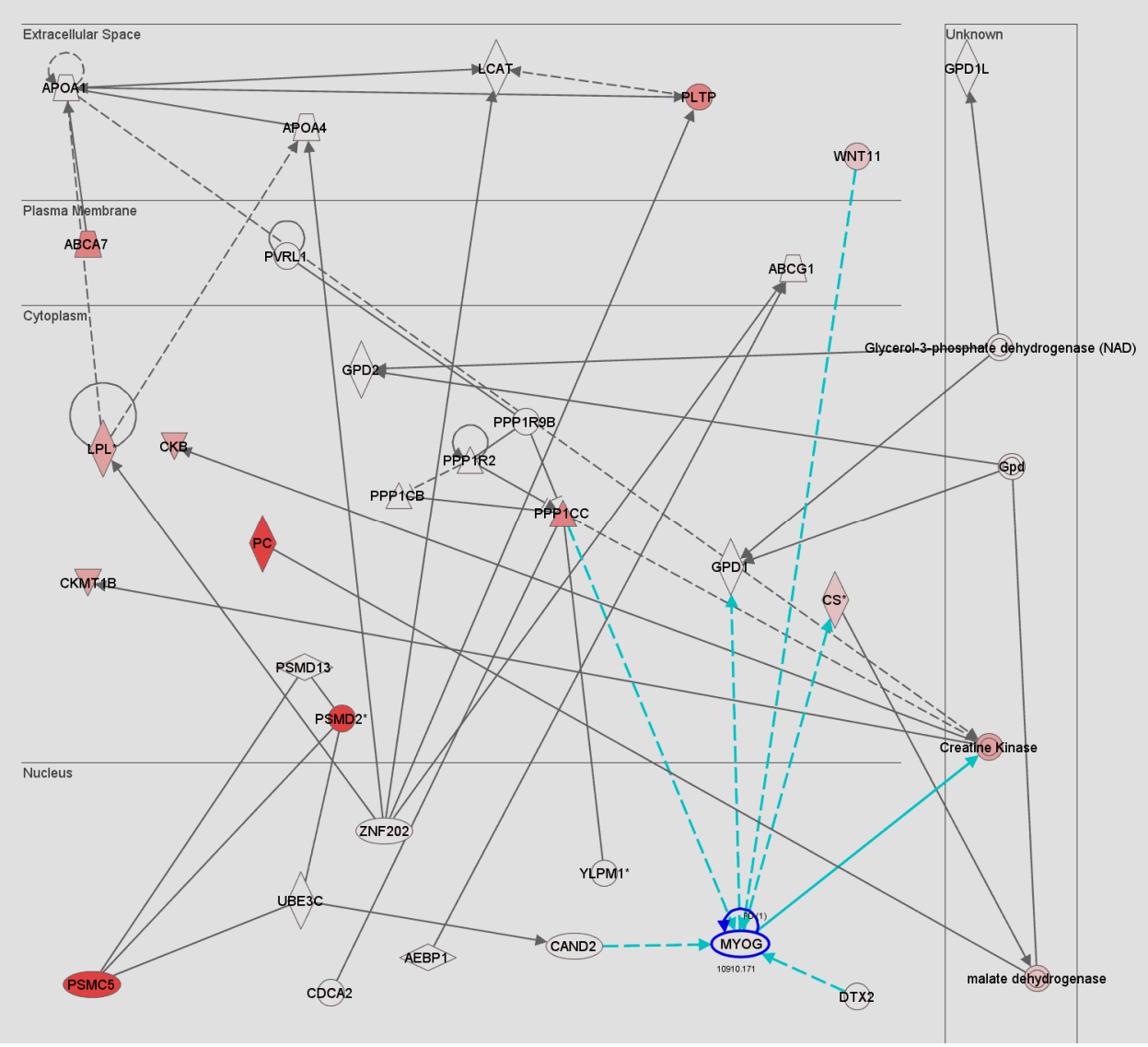

Figure 19. Myogenin participated in a network of molecules contained in the HSV-based cDNA library.

The network depicting a graphical representation of the molecular relationships between gene products was generated in Ingenuity Pathways Analysis using the dataset which included all genes that were detected in four out of four biological replicates as determined by the analysis at Cogenics, Inc. Genes are represented as nodes, and the biological relationship between two nodes is represented as an edge (line). All edges are supported by at least 1 reference from the literature, from a textbook, or from canonical information stored in the Ingenuity Pathways Knowledge Base. The myogenic regulatory factor Myogenin (MYOG) is highlighted in blue. The intensity of the node color (red) indicates the degree of up-regulation (mean intensity) of the gene product. Gene descriptions and intensity values listed in Appendix 2.

As stated above, the presence of muscle gene regulators within the recently engineered cDNA library may be useful in future studies, however, the development of additional and more

relevant cDNA libraries will provide more relevant tools for understanding early muscle development. Sources for potential myogenic activators include the embryo itself, explanted embryonic tissues, different stages of embryoid body development, or muscle progenitor cells. Embryonic stem cells are able to differentiate into skeletal muscle, and the step-wise progression of differentiation would likely contain genes that function at various stages of myogenic induction. In fact, genes that function in the regulation of many embryonic processes would likely be present in one or more stages of embryoid body differentiation. In this respect, a collective library of expressed genes during EB formation would be useful for studies of stem cell differentiation into other lineages as well. Furthermore, the method of selecting library gene functions based on virus replication can be applied broadly to genomics studies of stem cell differentiation, virus host-cell interactions, innate immune responses and brain biology.

5.0 CONDITIONAL REPLICATION OF AN HSV VECTOR UPON ACTIVATION OF AN EARLY MYOGENIC PROMOTER BY HOST CELLULAR FACTORS

5.1 INTRODUCTION

The activation of a developmental promoter during cell differentiation is likely dependent on a specific combination of environmental cues that are able to direct cellular transcription factors to that promoter sequence. Many myogenic promoters are activated by known transcription factors that are upstream in the muscle-specific cascade, such as the myogenin promoter, which is activated by a MyoD and MEF2 heterodimer. While some information about direct transcriptional activators is known, there remains many unknown elements that could potentially activate myogenic promoters naturally. Currently the mechanism by which many adult stem cells and embryonic stem cells are able to commit to the skeletal muscle lineage is unclear. Therein lies a critical need to unravel early muscle differentiation if progenitor populations are to be used in cell transplantation studies for the treatment of muscular dystrophy.

Pax3 is a transcription factor whose expression is activated early in myogenic development in the embryo. Its expression leads to the migration of limb precursor cells into the limb fields, where the progenitor cells then undergo extensive proliferation and differentiation into muscle fibers. Since it has been previously shown that Pax3 is able to induce the muscle specific gene cascade in several model systems [42, 43], induction of Pax3 expression would be

a useful target in order to identify upstream myogenic activating events. The activation of Pax3 expression through elements of the promoter is poorly understood. The essential promoter elements of Pax3 were studied in P19 embryonic carcinoma (EC) cells, which have been a model cell line to study myogenic induction, as they can be induced to differentiate into skeletal muscle cells when cultured as aggregates [194]. Researchers have identified two neural elements within the proximal 1.6 kb Pax3 promoter region that are necessary and sufficient for Pax3 expression in dorsal regions and the neural tube [195], however, this 1.6 kb promoter fragment failed to give expression of Pax3 in migrating myoblasts. Another group has identified upstream enhancer elements important for expression of Pax3, used by Tead2, a neural crest regulator of Pax3 [196]. Most recently, a hypaxial muscle promoter element approximately 5 kb upstream was identified in a Six1 and Six4 knock-out mouse [197]. This suggests that alternative elements in the Pax3 promoter are responsible for Pax3 expression during skeletal myogenesis and neural crest development.

In order to utilize the powerful genomics approach of selecting relevant genes from a newly generated HSV-based cDNA library, we sought to determine whether HSV replication could be dependent on the activation of a cellular promoter, namely Pax3. The HSV vector JDββHE was previously shown to be dependent on a single viral gene ICP4 for viral replication (Figure 6). By placing this essential viral gene under the control of the Pax3 promoter, activation of the Pax3 promoter would result in the expression of ICP4, thereby complementing viral replication of JDββHE. In this report, we demonstrate that an expression cassette containing the ICP4 coding sequence under the control of the Pax3 promoter is active in Pax3-expressing human rhabdomyosarcoma cells, and the level of ICP4 expression that results from this activation is sufficient for viral DNA replication. Furthermore, the addition of a known Pax3

activator, Tead2, was able to activate the Pax3p-ICP4 construct and support viral DNA replication in Vero cells which normally do not express Pax3 or support viral replication. We are able to conclude that the activation of a cellular promoter is sufficient drive viral replication, therefore we are confident that we can use this approach to select Pax3 activators from a pool of cDNA-expressing viral vectors, in which only vectors containing a Pax3 activator will be replication competent.

5.2 MATERIALS AND METHODS

Plasmid constructs. To generate the conditional ICP4 expression construct, a 2500 base pair fragment of the proximal murine Pax3 promoter [196] was amplified from D3 ES cell genomic DNA using the Pax3pF primer (AGAGAAGTGTCTGAACCCG) and Pax3pR primer (CGCAAATTATATCCAGGTG). The ICP4 coding sequence was excised from plasmid 4bla with *Sal*I and *Kpn*I and ligated into plasmid pSP72 at the *Sal*I and *Kpn*I sites to generate plasmid sp72-4. The Pax3 promoter fragment was enzymatically cleaved at the 5' and 3' ends using naturally occurring restriction sites *Pst*I and *BstE*II, respectively, and cloned into the *Pst*I and *BstE*II sites of sp72-4, such that the ICP4 coding sequence was under the control of the Pax3 promoter, to generate plasmid sp72-P4. Plasmid sp72-P4, also referred to as Pax3p-ICP4, was verified by DNA sequencing analysis (data not shown). The IL2-ICP4 expression construct contained the ICP4 coding sequence under the control of a drug inducible promoter (Ariad Biosystems). The ICP4 coding sequence was cloned into the multi-cloning site using the restriction sites *Sal*I and *Kpn*I. The Tead2 expression construct was a gift from Dr. Jonathan Epstein (University of Pennsylvania).

Cell culture and viral propagation. Human rhabdomyosarcoma cell line (R-sarcs) was obtained from ATCC (CCL-136) and maintained at > 30% confluence in DMEM supplemented with 10% FBS. Vero cells and 4BLA.4 cells were maintained in DMEM supplemented with 10% FBS. JDββHE virus was propagated on ICP4-complementing 4BLA.4 Vero cells, and stored at -80°C in 0.45 M NaCl with 10% glycerol.

Transfection and Infection Protocols. Two million actively proliferating R-sarc cells were transfected with plasmids Pax3p-ICP4, IL2-ICP4 or ECFP-N1 (Clontech) using lipofectamine (Invitrogen) in suspension for 1 hour. Cells were plated in 6 well culture dishes (Falcon) at $1x10^6$ cells/well and maintained in DMEM supplemented with 10% FBS four hours later. The following day, transfected R-sarc monolayers were infected with JDββHE ($5x10^6$ TU per well, MOI of 5) in 100 µl volume for 1.5 hours with agitation. Three days post infection, DNA from duplicate wells were harvested using DNEasy genomic DNA purification kit (Qiagen) and eluted in 30 µl TE.

One million actively proliferating Vero cells or 4BLA.4 cells were transfected with plasmids EGFP-N1 (Clontech) alone, Pax3p-ICP4 and EGFP-N1 (1:1 ratio), or Pax3p-ICP4 and Tead2 (1:1 ratio) using lipofectamine (Invitrogen) in suspension for 1 hour. Cells were plated at in 6 well culture dishes (Falcon) at $1x10^6$ cells/well and maintained in DMEM supplemented with 10% FBS four hours later. The following day, transfected monolayers were infected with JDββHE ($2x10^6$ TU per well, MOI of 2) in 100 µl volume for 1.5 hours with agitation. Two days post infection, DNA from duplicate wells were harvested using DNEasy genomic DNA purification kit (Qiagen) and eluted in 30 µl TE.

Quantitative PCR. Quantitative PCR (Q-PCR) analysis was performed using Taqman Universal master mix and primers and probes specific for UL1, a single copy gene present in the HSV genome. Primer and probe sequences provided upon request. Two microliters (1/15) of each DNA sample was subject to PCR. Q-PCR was done on a BIO-RAD iCycler IQ with the following thermal cycle: 95°C for 3 minutes, 40 cycles through 95°C for 30 seconds, and 60°C for 30 seconds. Duplicate wells for each sample were averaged. Changes in expression were calculated from threshold cycle (Ct) values where relative copy number = $2^{-\Delta\Delta Ct}$ [171]. Expression levels were normalized to internal control 18S [172]. There was no UL1 amplification from negative controls (mock infected cells and water).

5.3 RESULTS

In order to utilize the powerful selection mechanism by which viral replication could capture a relevant gene product, viral replication must be engineered to be conditional upon a cellular event, such as the activation of a promoter. As early embryonic events that trigger muscle differentiation are largely unknown, the myogenic promoter of Pax3 was used to demonstrate that the activation of this promoter by cellular factor(s) could result in viral replication. We have previously shown that the viral vector JDββHE depends on a single IE gene ICP4 for viral replication (Figure 6). By placing the essential viral gene ICP4 behind a PCR-amplified fragment of the Pax3 promoter, we have generated an ICP4 expression construct that is conditional upon Pax3 promoter activation. In this manner, viral replication, triggered by ICP4 expression, is then conditional upon the activation of this promoter (Figure 20).

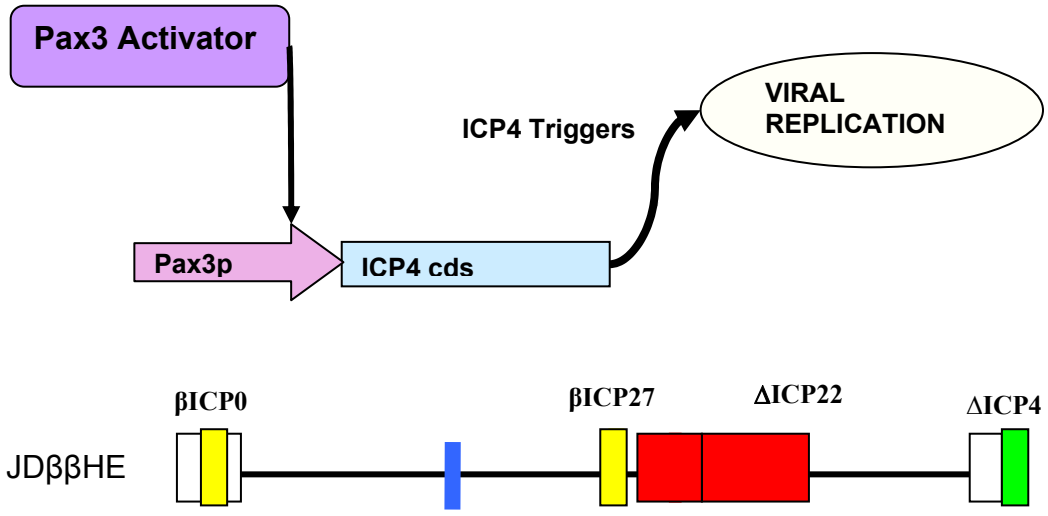

Figure 20. Schematic of condition viral replication.

The concept of conditional viral replication is depicted in this figure. The viral vector JDββHE requires only ICP4 in order to replicate. The ICP4 coding sequence was placed under the control of a 2.5 kb PCR amplified fragment of the proximal Pax3 promoter. Upon the introduction of an activator of the Pax3 promoter, ICP4 is expressed. ICP4 then activates the remainder of the HSV gene cascade and viral replication proceeds. In the absence of a Pax3 activator, ICP4 would not be expressed and the HSV gene cascade would remain silent.

Since not much is known regarding the promoter elements responsible for the expression of Pax3 in skeletal muscle progenitor cells, the Pax3p-ICP4 construct was designed to include known transcriptional activation sequences (within the proximal 1.6 kb Pax3 promoter) that have been previously shown to control Pax3 expression in neural crest cells [196]. The source of expressed genes that were incorporated into the HSV cDNA library was the PC12 neuronal tumor cell line, and this library likely contains natural genes (in the context of neural crest development) that activate this fragment of Pax3 promoter. Pax3 expression is also expressed during the differentiation of embryonic stem cells, however, it is expressed in a transient manner. For this reason, a cell line that constitutively expressed Pax3 was desired to test the Pax3p-ICP4 expression construct.

Human rhabdomyosarcoma cells (R-sarcs), derived from a pediatric alveolar striated muscle cancer, express a Pax3 fusion protein in which the N-terminal portion of Pax3, including the DNA binding domain, is fused to the C-terminal portion of Forkhead transcription factor protein [198]. The resulting fusion protein, Pax3-FKHR, is expressed constitutively in human rhabdomyosarcoma cells, and also has higher transcriptional activity [199]. We hypothesized that this rhabdomyosarcoma cell line expressed a factor or combination of factors that were able to activate the Pax3 promoter, and that the Pax3p-ICP4 construct would be active in this cell type. To test this hypothesis, ICP4 expression constructs were transfected into these cells, and then the cells were infected with JDββHE. The level of viral replication was considered a read-out of Pax3 promoter activation and was measured by quantitative PCR using primers and probes specific for a single copy gene in the HSV genome, UL1.

In addition to the Pax3p-ICP4 construct, unrelated expression constructs ECFP-N1, which contains the eCFP reporter gene under the control of the HCMV IE promoter, and IL2p-ICP4, in which the ICP4 coding sequence was placed under the control of a drug-inducible promoter, were used as negative controls for viral replication. After transfection, cells were infected with JDββHE at an MOI of 5 and viral replication was allowed to proceed for three days before DNA was harvested for analysis.

The amount of viral replication that had occurred in these cells was determined by quantitative PCR for HSV genomes. The level of viral DNA detected in R-sarcs transfected with the Pax3p-ICP4 construct was approximately 40-fold higher than cells transfected with CFP or the unrelated promoter construct IL2p-ICP4 (Figure 21). The low level of HSV genomes that were detected in R-sarcs transfected with CFP or IL2p-ICP4 plasmids represented the level of input genomes. The significant increase of HSV genomes present in cells transfected with the

Pax3p-ICP4 construct suggested that ICP4 was indeed expressed and we were able to conclude that the Pax3 promoter was active in this cell type. The amount of ICP4 that was induced in this cell type was also sufficient to induce viral DNA replication. We did not observe complete lysis or the appearance of plaques the infected cell monolayer in any sample, likely due to the incomplete transduction efficiency of liposome-mediated transfection (< 60 %, data not shown). Nevertheless, the data suggest that the activation of a cellular promoter (Pax3) by cellular component(s) was able to induce viral replication.

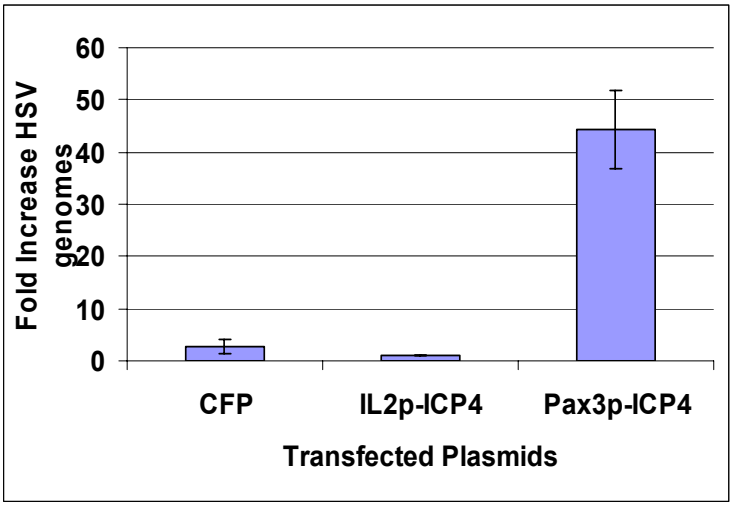

Figure 21. Rhabdomyosarcoma cells conditionally support viral replication.

One million R-sarc cells were transfected with indicated plasmids in duplicate. One day post transfection, R-sarcs were infected in monolayer with JDββHE at an MOI of 5, and infection proceeded for three days. Total DNA was harvested from the cells and supernatant and the amount of viral DNA replication was measured using quantitative PCR for the single copy HSV gene, UL1. UL1 levels were normalized to an internal control 18S, and graph represents copy number of UL1 relative to a standard curve using HSV genomic DNA.

A second transient transfection assay was used to determine whether the Pax3p-ICP4 construct could support viral replication conditionally upon the introduction of a known Pax3 activator, Tead2. The Pax3 promoter fragment that was amplified to generate the Pax3p-ICP4 construct contained known DNA binding elements that are sufficient for Tead2 mediated Pax3

gene expression as shown by Dr. Jonathan Epstein and colleagues [196]. Similar to the transient transfection assay in R-sarc cells, Vero cells and ICP4-complementing 4BLA.4 cells were transfected with eGFP alone, the Pax3p-ICP4 construct with eGFP at a 1:1 ratio, or the Pax3p-ICP4 construct with a Tead2 expression plasmid at a 1:1 ratio. The transfected cells were then infected with JDββHE at an MOI of 2 (TU) and the infection progressed for 2 days, when total DNA was harvested and the level of viral replication (amount of HSV genomes) was measured by quantitative PCR. As shown in Figure 22, as we expected, viral replication progressed in ICP4 complementing 4BLA.4 cells (positive control, relative value set at 1.00) and did not progress in Vero cells (negative control), both transfected with eGFP alone. Replication did not significantly increase in Vero or 4BLA.4 cells tranfected with the Pax3p-ICP4 construct in the presence of eGFP. However, in the presense of the Tead2 expression plasmid, a five fold increase in viral replication was observed in Vero cells transfected with the Pax3p-ICP4 construct two days post infection. Similarly, a 1.9 fold increase of viral DNA replication was observed in ICP4-complementing 4BLA.4 cells transfected with Tead2 and the Pax3p-ICP4 construct. In this experiment, the Pax3p-ICP4 construct was conditionally activated in Vero cells in the presence of Tead2, and this transient activation supported viral replication in cells that do not normally support viral replication. In addition, an increase in viral replication was observed in cells that do support viral replication (4BLA.4) in the presence of the Pax3p-ICP4 construct and Tead2.

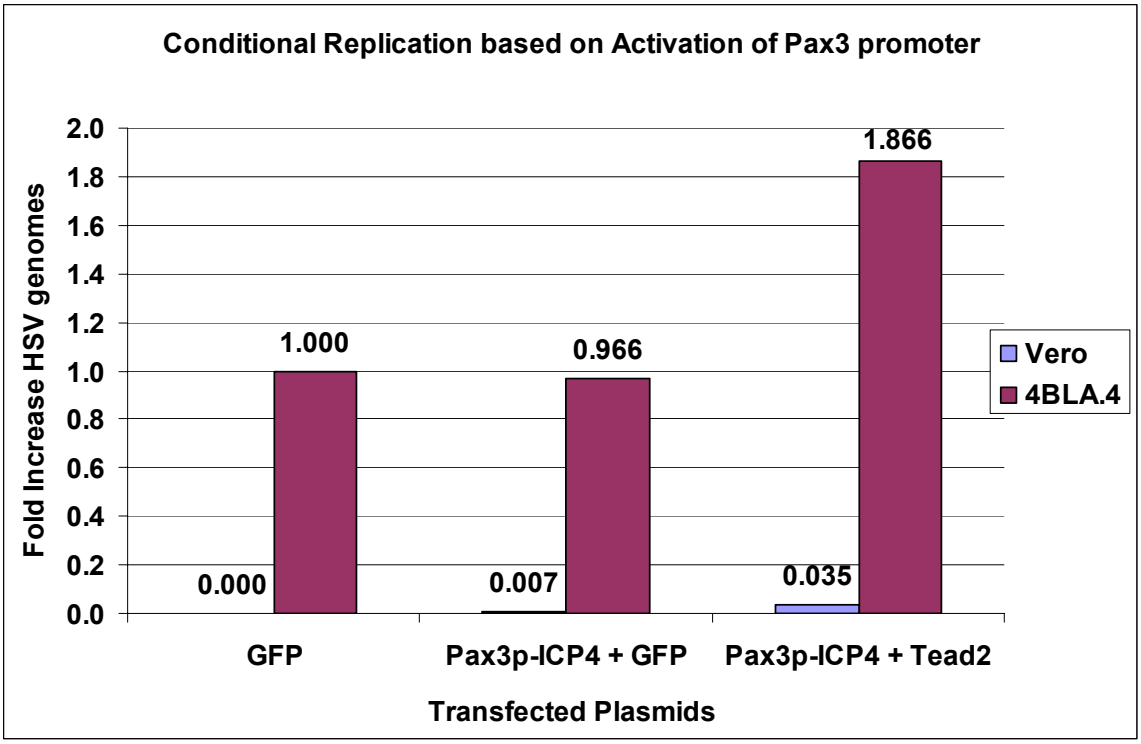

Figure 22. Conditional viral replication based on activation of the Pax3 promoter.

One million Vero cells or 4BLA.4 cells were transfected with indicated plasmids (1:1 ratio if two plasmids) in duplicate. One day post transfection, cell monolayers were infected with JDββHE at an MOI of 2, and infection proceeded for two days. Total DNA was harvested from the cells and supernatant and the amount of viral DNA replication was measured using quantitative PCR for the single copy HSV gene, UL1. UL1 levels were normalized to an internal control 18S, and graph represents copy number of UL1 relative to a standard curve using HSV genomic DNA. The level of viral replication in 4BLA.4 cells transfected with eGFP was arbitrarily set at 1.

5.4 DISCUSSION

In this brief report, we have shown that viral replication can be engineered to be conditional upon the activation of a cellular promoter by factors present in a host cell or encoded by exogenous plasmid DNA. The early myogenic promoter of Pax3, in the form of an ICP4 reporter plasmid, was activated in transient transfection studies in human rhabdomyosarcoma cells, which constitutively express a Pax3 fusion protein. The activation of the Pax3 promoter was able to produce sufficient levels of ICP4 to initiate viral DNA replication, as observed by

PCR analysis. An additional transient transfection experiment demonstrated that the addition of a known Pax3 activator Tead2 was sufficient to activate the Pax3p-ICP4 construct and support viral DNA replication in Vero cells, which normally do not express Pax3 or support viral replication (Figure 22). While we did not observe cell lysis in either case, the lack of uniform transduction of the Pax3p-ICP4 construct is likely a bottleneck for viral replication and spread of infectious virus to neighboring cells. A slight increase in viral DNA replication was observed in Vero cells transfected with the Pax3p-ICP4 construct alone, but transfection results in high plasmid copy number that may not act as transcriptionally silent as if one copy of ICP4 was in the context of genomic DNA. These transient experiments nevertheless demonstrated proof of principle that viral replication could be conditionally dependent on the activation of a cellular promoter.

Conditional replication has been explored previously in the construction of an oncolytic HSV viral vector, in which lytic replication was dependent on the activation of a cellular promoter. A tissue-specific promoter, Nestin-1, was highly active in several human glioma cell lines and was therefore used to control the expression of an essential HSV gene, γ34.5, in the genome of the vector. The high activity of the Nestin-1 promoter from within the viral genome facilitated lytic viral replication in human glioma cells, yet was non toxic to normal brain tissue [200]. In a similar strategy, by placing the essential viral gene ICP4 under the control of a myogenic promoter, the JDββHE viral vector would be able to replicate and lyse the infected cell only if an activator of the myogenic promoter was present. Furthermore, the myogenic activator could be a gene encoded within the HSV genome itself, which is hypothesized in the case of recently produced HSV cDNA library, such that viral replication would progress only if a Pax3 activator was expressed by a library vector.

Like the aforementioned study, the insertion of the Pax3p-ICP4 construct into the JDββHE vector backbone would generate a vector that was replication-competent only in cells which expressed a Pax3 activator. Preliminary data using a JDββ-Pax3p-ICP4 vector suggests that the Pax3 promoter is silent in Vero cells (no viral replication), while replication in ICP4-complementing cells is retained. This vector may be used to test for the presence of Pax3 activators during embryonic stem cell differentiation by infecting embryoid body cells over a specified time course. The detection of infectious virus around day 7 or 8 of embryoid body formation, for example, would suggest that day 7 embryoid bodies express a factor or combination of factors that activate the Pax3 promoter naturally. Furthermore, information regarding the presence of Pax3 activators, or activators of other differentiation-related or tissue-specific promoters, over the course of ES cell differentiation would be of great use to the stem cell field. The HSV genome is attractive in this context because its large genome can accommodate large promoter fragments up to 15 kb. The ability to propagate the HSV genome in bacteria as a bacterial artificial chromosome also facilitates the ease of recombination of these large genomic fragments into the genome.

The goal of this research project was to develop a selective replication system by which activators of early muscle gene promoters could be identified from a recently produced HSV cDNA library. While transient transfection of the Pax3p-ICP4 construct was sufficient to induce viral replication in Pax3-expressing cells, a more uniform distribution of the Pax3p-ICP4 construct, such as the insertion into the host cellular genome itself, would be necessary to identify novel gene regulators from a pool of cDNA-expressing vectors. A stable cell line, in which the ICP4 coding sequence was targeted to the natural Pax3 locus, would provide additional promoter elements as well as a higher level of controlled regulation. A stable cell line

such as this could be used to select for Pax3 activators from the pool of cDNA expressing vectors, in which the viral-encoded cDNA would activate the natural Pax3 promoter, and trigger viral replication in that cell. Viral-mediated lysis of the cell would then release progeny virus into the supernatant, an immediate "capture" of the biologically relevant gene product. The life cycle of library vectors which contain cDNAs that do not function as Pax3 activators would be arrested at the earliest stages of infection, since the lack of immediate early (ICP4) gene expression prevents early and late viral gene expression.

6.0 SUMMARY OF THESIS AND FUTURE DIRECTIONS

Muscular dystrophy is a devastating disease in which no treatment or cure exists. A promising therapy for muscular dystrophy is the transplantation of cells that are able to contribute to existing muscle fibers or generate new muscle fibers. While several cell populations have been shown to demonstrate this phenomenon in mouse models, the mechanism by which these cells are able to differentiate into myogenic cells is largely unknown. Our current understanding of muscle differentiation lacks sufficient information regarding the earliest stages of myogenesis, partly due to the inaccessibility of and difficulty using early embryos at this stage. In recent years, the ability of embryonic stem cells to generate cells of various lineages has become a convenient model system to study differentiation. These cells are able to proliferate indefinitely in culture and their differentiation pathways mimic those that occur in the embryo. A detailed method to commit ES cells to a particular lineage has the potential to inhibit teratoma formation that is observed when pluripotent ES-derived cells are transplanted into recipient animals. This dissertation focuses on the development of tools that can be used to study the effect of muscle gene expression in ES cells, as well as tools that can be used to identify genes that participate in the activation of early muscle promoters in a selective replication strategy. The future use of this selection method to identify gene products that specifically activate an early myogenic promoter would lead to the testing of these gene products

for their ability to induce downstream myogenic gene expression and differentiation. In this manner, a better understanding of early muscle differentiation can be achieved and applied to the use of stem cells in transplantation studies using muscular dystrophy models.

In chapter three, the engineering and characterization of a replication defective HSV vector that would be useful for the delivery of genes to embryonic stem cells and their derivatives was described. The features of this vector are as follows:

1) The deletion of ICP4, ICP22 and the conversion of the immediate early gene ICP27 to the early gene class by promoter exchange generated a vector, JDββHE, which was non-toxic to ES cells and the differentiation of ES cells into all three germ layers, yet was dependent on a single IE gene ICP4 for replication.

2) In the vector JDββHE, the conversion of the immediate early gene ICP0 to the early gene class by promoter exchange greatly reduced the expression of this gene to levels that are sufficient for high levels of transgene expression from the viral genome, yet not sufficient to induce cell cycle arrest and ICP0-mediated toxicity.

3) The vector JDββHE provided a high level of gene expression from both an HSV encoded (ICP0) promoter and the HCMV IE promoter. Gene expression from HSV, including the expression of eGFP and Pax3, was provided in a transient manner, which reflected the expression pattern of many developmental genes.

4) Embryonic stem cells as well as embryoid body derived cells are permissive to JDββHE infection and expression of transgenes from both the ICP0 promoter and the HCMV IE promoter.

In conclusion, chapter three demonstrates the use of a replication defective vector to express a developmentally regulated gene, Pax3, in embryonic stem cells and cells of the embryoid body. The HSV vector does not integrate into or otherwise alter the host chromosomal DNA and the viral genome is progressively lost during cell division. The availability of a vector that can be used to deliver genes during the course of ES cell differentiation will be indispensable in the study of gene function in these differentiated cell types and will likely contribute to the overall understanding of muscle differentiation which is necessary for the development of cell based therapies for muscular dystrophy.

Chapter four of this dissertation describes the construction of a library of expressed genes in HSV viral vectors to be used in the identification of novel genes that function to activate early myogenic promoters or regulate ion channels. The findings from this study are listed below:

1) The HSV genome was modified to contain a bacterial origin of replication in order to utilize highly efficient bacterial resistant genes and the Gateway recombination system (Invitrogen), which facilitated the efficient in vitro recombination of cDNAs into vector genomes in a manner which maintained gene orientation.

2) Following infection of tissue culture cells, HSV cDNA library vectors expressed gene products at both the transcriptional and protein levels.

3) Microarray analysis of PCR-amplified inserts demonstrated the presence of at least 15,000 unique genes, some of which participate in biological functions related to muscle differentiation, such as Id1 and Cand2.

In conclusion, chapter four demonstrates the successful introduction of more than 15,000 unique genes into HSV gene expression vectors and provides a pool from which relevant genes can be identified. While this particular library was generated from neuronal tumor cell line PC12, it provides the methodology necessary to generate more relevant cDNA libraries from myogenic progenitor cells or differentiating embryonic stem cells. Additional gene expression libraries will be necessary in order to provide a pool of expressed genes that are more likely to contribute to the differentiation of stem cells into skeletal muscle.

In chapter five, a conditional replication strategy was developed by which the recently produced HSV cDNA library could be used to identify genes that activate early myogenic promoters. This study exploited the characteristic of the JDββHE vector in which viral replication can be restored upon the introduction of the essential viral gene ICP4. By placing this essential viral gene under the control of the early myogenic promoter Pax3, viral replication was then conditional upon the activation of this cellular promoter. In transient transfection studies using a human rhabdomyosarcoma cell line, this Pax3p-ICP4 construct was activated and the amount of ICP4 that was expressed was sufficient to induce viral DNA replication, which demonstrated that viral replication could be dependent on the activation of a cellular promoter by host cell factor(s). In a similar manner, cDNA library vectors that express a Pax3 activator, in the presence of the Pax3-ICP4 construct, would be able to replicate in cells which did not possess an endogenous Pax3 activator, such as embryonic stem cells.

While the above described transient transfection approach was successful in demonstrating proof of principle, the inefficient method of transfection would not likely be used to identify Pax3 activators from the pool of HSV cDNA library vectors. The generation of an ES cell line with the ICP4 gene placed at the natural Pax3 locus would provide a more biologically relevant situation in which additional promoter elements could be utilized. In fact, many myogenic enhancer elements are found more than 5 kb upstream of the transcriptional start site [201]. Future studies include the generation of this knock-in ES cell line, which can then be used to identify novel Pax3 activators from the recently generated HSV cDNA library. Only those library vectors containing gene products that activate the Pax3 promoter in this cell line would replicate, lyse the host cell, and be released into the supernatant. The natural HSV lytic life cycle provides a means to capture the vector which expresses the gene with promoter activating functions, and results in the release of a biologically relevant gene within a gene delivery vehicle. This vector would be immediately available for downstream functional analysis in ES cells or other models of muscle differentiation.

This system is extremely versatile and can be easily applied to all aspects of ES and adult stem cell differentiation in which the essential viral gene is placed under the control of any developmental promoters such as early cardiomyocyte promoters, hematopoetic promoters, or neuronal promoters (Figure 23). In this manner, cDNA library expression vectors could be screened for activators of many lineage-specific promoters. The generation and screening of additional differentiation-related cDNA libraries could potentially identify many useful genes which can tested for the ability to commit ES cells or their derivates into specific lineages.

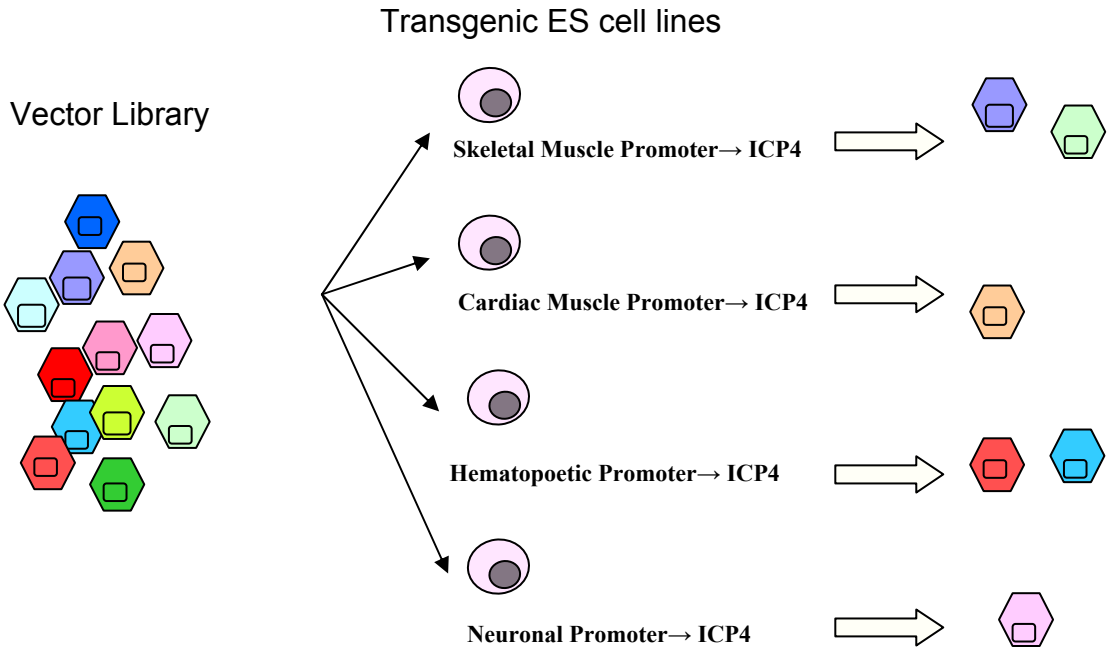

Figure 23. Broad applications of the selective replication system in stem cell differentiation.

A pool of cDNA expressing HSV vectors could be used to identify activators of various developmentally regulated promoters, in which the essential viral gene ICP4 has been inserted into the natural locus of a desired target gene. A vector library can be simultaneously used to infect various transgenic ES cell lines, which would result in the release of differential viral progeny that is functionally relevant to each specific application.

In conclusion, the focus of this dissertation was to create and characterize tools that can facilitate studies of gene function in stem cells, and also the identification of novel genes that influence ES cell differentiation into the muscle lineage. A better understanding of stem cell commitment to the muscle lineage will undoubtedly lead to the generation of therapeutic cell-based treatments for muscular dystrophy.

APPENDIX A

NETWORK OF LIBRARY-CONTAINED GENES ASSOCIATED WITH MYOD AND MYF5

Name	Synonyms	Description	Family	Entrez (Rat)	Intensity
EEF1G	EF-1 GAMMA	Eukaryotic translation elongation factor 1 gamma	translation regulator	293725	468455.48
TKT	p68, TKT1	transketolase (Wernicke-Korsakoff syndrome)	enzyme	64524	346052.55
ID1	ID, ID-1H, ID125A, Idb1	inhibitor of DNA binding 1, dominant negative helix-loop-helix protein	transcription regulator	25261	315346.23
NP	Np-1, Np-2, PNP, PUNP	nucleoside phosphorylase	enzyme	290029	310280.65
ID3	HEIR-1, IDB3	inhibitor of DNA binding 3, dominant negative helix-loop-helix protein	transcription regulator	25585	297890.73
COL4A1	arresten, BRU	collagen, type IV, alpha 1	Other	290905	295462.15
PRPF8	DBF3/PRP8, PRPC8, RP13, Sfprp8l, U5-220	PRP8 pre-mRNA processing factor 8 homolog (S. cerevisiae)	Other	287530	261565.73
ADSS	ADEH, ADS, Adss1, ADSS2	adenylosuccinate synthase	enzyme	289276	254907.90
PPAN	BXDC3, SSF, SSF1, SSF2	peter pan homolog (Drosophila)	Other	298699	187097.03

EFTUD2	p116, snRNP C U5, Snrp116, Snu114	Elongation factor Tu GTP binding domain containing 2	enzyme	287739	184972.82
HSPA4L	94kDa, APG-1	Heat shock 70kDa protein 4-like	Other	294993	183447.73
DDX23	prp28, PRPF28, U5-100K, U5-100KD	DEAD (Asp-Glu-Ala-Asp) box polypeptide 23	enzyme	300208	175372.53
HAND1	EHAND, Ehand1, Th1, Thing1	heart and neural crest derivatives expressed 1	transcription regulator	59112	147836.43
DHX15	DBP1, DD15, DDX15, DEAH9, HRH2, PRP43	DEAH (Asp-Glu-Ala-His) box polypeptide 15	enzyme	289693	129158.58
EEF1A1	CCS-3, EEF-1, EEF1A, Eef1a2, EF-Tu, PTI1, SI	Eukaryotic translation elongation factor 1 alpha 1	translation regulator	171361	123322.40
PREP	PE, PEP, Prolyl Oligopeptidase, rPop	Prolyl endopeptidase	peptidase	83471	119414.19
ELOVL6	Face, FAE, LCE, Lce2, rELO2	ELOVL family member 6, elongation of long chain fatty acids	enzyme	171402	116129.65
ZRF1	DNAJC2, MIDA1, MPHOSPH11, MPP11, Zrf2, ZUO1	zuotin related factor 1	Other	116456	107450.03
ATBF1	Atbf1, ATBT, WBP9, ZFHX3	AT-binding transcription factor 1	transcription regulator	307829	70789.46
PABPN1	mPABII, OPMD, PAB2, PABN1, PABP2, Pabp3	Poly(A) binding protein, nuclear 1	Other	116697	69507.43
SNW1	Bx42, Prp45, SKIIP, SKIP, SNW1 protein	SNW domain containing 1	transcription regulator	500695	50114.95
SFPQ	Nono, POMP100, PSF	splicing factor proline/glutamine-rich	Other	252855	26222.77
SLC12A2	BSC, BSC2, mBSC2, NKCC1, sy-ns	solute carrier family 12 (ion transporters), member 2	transporter	83629	15089.57
MYF5	B130010J22Rik, Myf5_predicted	myogenic factor 5	transcription regulator	299766	5806.30
CFTR	CF, CFTR/MRP, MRP7, TNR-CFTR	cystic fibrosis transmembrane conductance regulator	ion channel	24255	1829.96

MYOD1	MD1, MYF3, MYOD, PUM	myogenic differentiation 1	transcription regulator	337868	1791.73
beta-estradiol	1,3,5(10)-estratriene-3,17beta-diol	chemical	chemical - endogenous mammalian	-	0.00
retinoic acid	all-trans retinoic acid	chemical	chemical - endogenous mammalian	-	0.00
SNRPD3	SNRNP SM D3	small nuclear ribonucleoprotein D3 polypeptide 18kDa	Other	-	0.00
SNRPE	B-raf, Sm protein E, SME, SNRNP SM E, snRNP-E	small nuclear ribonucleoprotein polypeptide E	Other	685587	0.00

APPENDIX B

NETWORK OF LIBRARY-CONTAINED GENES ASSOCIATED WITH MYOGENIN

Name	Synonyms	Description	Family	Entrez (Rat)	Intensity
PSMC5	p45, S8, SUG1, TBP10, TRIP1	proteasome 26S subunit, ATPase, 5	transcription regulator	81827	386622.52
PC	PCB, Pcx, Pyr	pyruvate carboxylase	enzyme	25104	374853.23
PSMD2	S2, TEG-190, Tex190, TRAP-2	proteasome 26S subunit, non-ATPase, 2	other	287984	353931.05
ABCA7	Abc51, ABCA-SSN, ABCX	ATP-binding cassette, sub-family A (ABC1), member 7	transporter	299609	260400.20
PPP1CC	Pp-1g, PP1, PP1 GAMMA, PP1 GAMMA1, PP1C GAMMA, Ppp1cc1	protein phosphatase 1, catalytic subunit, gamma isoform	phosphatase	24669	234359.15
PLTP	OD107, Pltp_predicted	phospholipid transfer protein	other	296371	229134.15
CKB	B-CK, Ck-3, CKBB, Ckbr, Creatine kinase b chain, RATCKBR	creatine kinase, brain	kinase	24264	187114.48
LPL	Lipase, LIPD, Lipoprotein lipase 1	lipoprotein lipase	enzyme	24539	148385.98
CKMT1B	CKMT, CKMT1, mi-CK, Mt-CK, ScCKmit, UbCKmit, UMTCK	creatine kinase, mitochondrial 1B	kinase	29593	146238.85
CS	Cis	citrate synthase	enzyme	170587	95366.58

WNT11	HWNT11	wingless-type MMTV integration site family, member 11	other	140584	83144.96
UBE3C	Ubiquitin Protein Isopeptide Ligase E3	ubiquitin protein ligase E3C	enzyme	362294	67035.69
PPP1R9B	Neb2, NEURABIN II, Neurabin2, PPP1R6, PPP1R9, SPINO, SPINOPHILIN,	protein phosphatase 1, regulatory (inhibitor) subunit 9B	other	84686	66415.47
PPP1CB	PP-1B, PP-1D, Pp1 Beta, Pp1 delta, PP1-C BETA II, PPP1C DELTA, PPP1CD	protein phosphatase 1, catalytic subunit, beta isoform	phosphatase	25594	58033.50
ABCG1	ABC8, White, WHITE1	ATP-binding cassette, sub-family G (WHITE), member 1	transporter	85264	57589.36
PPP1R2	I-2, INHIBITOR 2, IPP-2	protein phosphatase 1, regulatory (inhibitor) subunit 2	phosphatase	192361	44093.74
GPD2	Alpha-gpd, GDH2, Gdm1, Gpd-m, GPDH, mtGPDH, TISP38	glycerol-3-phosphate dehydrogenase 2 (mitochondrial)	enzyme	25062	43942.63
YLPM1	Nuclear protein ZAP3, ZAP	YLP motif containing 1	other	299199	39944.46
AEBP1	ACLP, Aebp1_predicted	AE binding protein 1	peptidase	305494	35380.53
LCAT	Lecithin Acyltransferase	lecithin-cholesterol acyltransferase	enzyme	24530	32641.70
ZNF202	Zfp202, ZKSCAN10	zinc finger protein 202	transcription regulator	500981	30427.45
CAND2	TIP120B, Tp120b	cullin-associated and neddylation-dissociated 2 (putative)	transcription regulator	192226	25920.56
APOA1	Ai, ALP-1, Apo1a, APOA-I, Brp-14, HDLA1, LP(A-I), Ltw-1, Lvtw-1, Sep-1, Sep-2	apolipoprotein A-I	transporter	25081	23016.32
DTX2	Deltex2, RNF58	deltex homolog 2 (Drosophila)	other	304591	23008.56

PSMD13	26S Proteasome Subunit p40.5, HSPC027, p40.5, Psmd13_predicted, S11	proteasome 26S subunit, non-ATPase, 13	peptidase	365388	22575.64
GPD1L	RGD1560123_predicted	glycerol-3-phosphate dehydrogenase 1-like	enzyme	363159	18679.09
GPD1	Gdc-1, Glycerolphosphate Dehydrogenase, Gopdh, Gpd3, GPDH	glycerol-3-phosphate dehydrogenase 1 (soluble)	enzyme	60666	15509.70
PVRL1	CD111, CLPED1, ED4, HIgR, HVEC, NECTIN-1, Nectin1 alpha, PRR1, PVRR1	poliovirus receptor-related 1 (herpesvirus entry mediator C)	other	192183	15111.88
APOA4	Acl, APOA-IV, Apoc4	apolipoprotein A-IV	transporter	25080	13103.47
CDCA2	Repo-Man	cell division cycle associated 2	other	305984	12590.50
MYOG	MG, MYF4, myo, myogenic factor 4	myogenin (myogenic factor 4)	transcription regulator	29148	10910.17
Creatine Kinase	adenosine triphosphate-creatine transphosphorylase, ATP:creatine N-phosphotransferase	-	group	-	0.00
Glycerol-3-phosphate dehydrogenase (NAD)	alpha-glycerol phosphate dehydrogenase (NAD)	-	group	-	0.00
Gpd	alpha-glycerophosphate dehydrogenase	-	group	-	0.00
malate dehydrogenase	(S)-malate:NAD oxidoreductase, L-malate dehydrogenase	-	group	-	0.00

BIBLIOGRAPHY

1. Bradley, D.M., E.P. Parsons, and A.J. Clarke, *Experience with screening newborns for Duchenne muscular dystrophy in Wales.* Bmj, 1993. **306**(6874): p. 357-60.
2. CDC, *National Center on Birth Defects and Developmental Disabilities.* 2006.
3. NINDS, *Muscular Dystrophy: Hope Through Research*. 2007, NIH.
4. Hoogerwaard, E.M., et al., *Cardiac involvement in carriers of Duchenne and Becker muscular dystrophy.* Neuromuscul Disord, 1999. **9**(5): p. 347-51.
5. Greenberg, C.R., et al., *Three years' experience with neonatal screening for Duchenne/Becker muscular dystrophy: gene analysis, gene expression, and phenotype prediction.* Am J Med Genet, 1991. **39**(1): p. 68-75.
6. Radley, H.G., et al., *Duchenne muscular dystrophy: focus on pharmaceutical and nutritional interventions.* Int J Biochem Cell Biol, 2007. **39**(3): p. 469-77.
7. Wong, B.L. and C. Christopher, *Corticosteroids in Duchenne muscular dystrophy: a reappraisal.* J Child Neurol, 2002. **17**(3): p. 183-90.
8. Brooke, M.H., et al., *Clinical investigation of Duchenne muscular dystrophy. Interesting results in a trial of prednisone.* Arch Neurol, 1987. **44**(8): p. 812-7.
9. Mendell, J.R., et al., *Randomized, double-blind six-month trial of prednisone in Duchenne's muscular dystrophy.* N Engl J Med, 1989. **320**(24): p. 1592-7.
10. Louis, M., et al., *Effect of creatine supplementation on skeletal muscle of mdx mice.* Muscle Nerve, 2004. **29**(5): p. 687-92.
11. Folkers, K. and R. Simonsen, *Two successful double-blind trials with coenzyme Q10 (vitamin Q10) on muscular dystrophies and neurogenic atrophies.* Biochim Biophys Acta, 1995. **1271**(1): p. 281-6.
12. Snow, M.H., *An autoradiographic study of satellite cell differentiation into regenerating myotubes following transplantation of muscles in young rats.* Cell Tissue Res, 1978. **186**(3): p. 535-40.
13. Patel, K. and H. Amthor, *The function of Myostatin and strategies of Myostatin blockade-new hope for therapies aimed at promoting growth of skeletal muscle.* Neuromuscul Disord, 2005. **15**(2): p. 117-26.
14. Sitnik, R., et al., *Novel point mutations in the dystrophin gene.* Hum Mutat, 1997. **10**(3): p. 217-22.
15. Bulman, D.E., et al., *Point mutation in the human dystrophin gene: identification through western blot analysis.* Genomics, 1991. **10**(2): p. 457-60.
16. Politano, L., et al., *Gentamicin administration in Duchenne patients with premature stop codon. Preliminary results.* Acta Myol, 2003. **22**(1): p. 15-21.
17. Barton-Davis, E.R., et al., *Aminoglycoside antibiotics restore dystrophin function to skeletal muscles of mdx mice.* J Clin Invest, 1999. **104**(4): p. 375-81.

18. De Angelis, F.G., et al., *Chimeric snRNA molecules carrying antisense sequences against the splice junctions of exon 51 of the dystrophin pre-mRNA induce exon skipping and restoration of a dystrophin synthesis in Delta 48-50 DMD cells.* Proc Natl Acad Sci U S A, 2002. **99**(14): p. 9456-61.
19. Wilton, S.D., et al., *Specific removal of the nonsense mutation from the mdx dystrophin mRNA using antisense oligonucleotides.* Neuromuscul Disord, 1999. **9**(5): p. 330-8.
20. Fletcher, S., et al., *Dystrophin expression in the mdx mouse after localised and systemic administration of a morpholino antisense oligonucleotide.* J Gene Med, 2006. **8**(2): p. 207-16.
21. Sakamoto, M., et al., *Micro-dystrophin cDNA ameliorates dystrophic phenotypes when introduced into mdx mice as a transgene.* Biochem Biophys Res Commun, 2002. **293**(4): p. 1265-72.
22. Dickson, G., et al., *Recombinant micro-genes and dystrophin viral vectors.* Neuromuscul Disord, 2002. **12 Suppl 1**: p. S40-4.
23. Scott, J.M., et al., *Viral vectors for gene transfer of micro-, mini-, or full-length dystrophin.* Neuromuscul Disord, 2002. **12 Suppl 1**: p. S23-9.
24. Watchko, J., et al., *Adeno-associated virus vector-mediated minidystrophin gene therapy improves dystrophic muscle contractile function in mdx mice.* Hum Gene Ther, 2002. **13**(12): p. 1451-60.
25. Christ, B. and C.P. Ordahl, *Early stages of chick somite development.* Anat Embryol (Berl), 1995. **191**(5): p. 381-96.
26. Goulding, M., A. Lumsden, and A.J. Paquette, *Regulation of Pax-3 expression in the dermomyotome and its role in muscle development.* Development, 1994. **120**(4): p. 957-71.
27. Jostes, B., C. Walther, and P. Gruss, *The murine paired box gene, Pax7, is expressed specifically during the development of the nervous and muscular system.* Mech Dev, 1990. **33**(1): p. 27-37.
28. Pourquie, O., et al., *Control of somite patterning by signals from the lateral plate.* Proc Natl Acad Sci U S A, 1995. **92**(8): p. 3219-23.
29. Amthor, H., et al., *The importance of timing differentiation during limb muscle development.* Curr Biol, 1998. **8**(11): p. 642-52.
30. Wagner, J., et al., *Compartmentalization of the somite and myogenesis in chick embryos are influenced by wnt expression.* Dev Biol, 2000. **228**(1): p. 86-94.
31. Dietrich, S., et al., *The role of SF/HGF and c-Met in the development of skeletal muscle.* Development, 1999. **126**(8): p. 1621-9.
32. Epstein, J.A., et al., *Pax3 modulates expression of the c-Met receptor during limb muscle development.* Proc Natl Acad Sci U S A, 1996. **93**(9): p. 4213-8.
33. Bladt, F., et al., *Essential role for the c-met receptor in the migration of myogenic precursor cells into the limb bud.* Nature, 1995. **376**(6543): p. 768-71.
34. Tajbakhsh, S., et al., *Redefining the genetic hierarchies controlling skeletal myogenesis: Pax-3 and Myf-5 act upstream of MyoD.* Cell, 1997. **89**(1): p. 127-38.
35. Tajbakhsh, S. and M.E. Buckingham, *Mouse limb muscle is determined in the absence of the earliest myogenic factor myf-5.* Proc Natl Acad Sci U S A, 1994. **91**(2): p. 747-51.
36. Tajbakhsh, S., et al., *Differential activation of Myf5 and MyoD by different Wnts in explants of mouse paraxial mesoderm and the later activation of myogenesis in the absence of Myf5.* Development, 1998. **125**(21): p. 4155-62.

37. Maroto, M., et al., *Ectopic Pax-3 activates MyoD and Myf-5 expression in embryonic mesoderm and neural tissue.* Cell, 1997. **89**(1): p. 139-48.
38. Stockdale, F.E. and H. Holtzer, *DNA synthesis and myogenesis.* Exp Cell Res, 1961. **24**: p. 508-20.
39. Megeney, L.A. and M.A. Rudnicki, *Determination versus differentiation and the MyoD family of transcription factors.* Biochem Cell Biol, 1995. **73**(9-10): p. 723-32.
40. Petropoulos, H. and I.S. Skerjanc, *Beta-catenin is essential and sufficient for skeletal myogenesis in P19 cells.* J Biol Chem, 2002. **277**(18): p. 15393-9.
41. Rudnicki, M.A., et al., *MyoD or Myf-5 is required for the formation of skeletal muscle.* Cell, 1993. **75**(7): p. 1351-9.
42. Ridgeway, A.G. and I.S. Skerjanc, *Pax3 is essential for skeletal myogenesis and the expression of Six1 and Eya2.* J Biol Chem, 2001. **276**(22): p. 19033-9.
43. Schmidt, M., M. Tanaka, and A. Munsterberg, *Expression of (beta)-catenin in the developing chick myotome is regulated by myogenic signals.* Development, 2000. **127**(19): p. 4105-13.
44. Tassabehji, M., et al., *Mutations in the PAX3 gene causing Waardenburg syndrome type 1 and type 2.* Nat Genet, 1993. **3**(1): p. 26-30.
45. Franz, T., et al., *The Splotch mutation interferes with muscle development in the limbs.* Anat Embryol (Berl), 1993. **187**(2): p. 153-60.
46. Daston, G., et al., *Pax-3 is necessary for migration but not differentiation of limb muscle precursors in the mouse.* Development, 1996. **122**(3): p. 1017-27.
47. Pritchard, C., G. Grosveld, and A.D. Hollenbach, *Alternative splicing of Pax3 produces a transcriptionally inactive protein.* Gene, 2003. **305**(1): p. 61-9.
48. Peault, B., et al., *Stem and progenitor cells in skeletal muscle development, maintenance, and therapy.* Mol Ther, 2007. **15**(5): p. 867-77.
49. Schmalbruch, H. and U. Hellhammer, *The number of nuclei in adult rat muscles with special reference to satellite cells.* Anat Rec, 1977. **189**(2): p. 169-75.
50. Schmalbruch, H. and U. Hellhammer, *The number of satellite cells in normal human muscle.* Anat Rec, 1976. **185**(3): p. 279-87.
51. Asakura, A., M. Komaki, and M. Rudnicki, *Muscle satellite cells are multipotential stem cells that exhibit myogenic, osteogenic, and adipogenic differentiation.* Differentiation, 2001. **68**(4-5): p. 245-53.
52. Seale, P., A. Asakura, and M.A. Rudnicki, *The potential of muscle stem cells.* Dev Cell, 2001. **1**(3): p. 333-42.
53. Heslop, L., J.E. Morgan, and T.A. Partridge, *Evidence for a myogenic stem cell that is exhausted in dystrophic muscle.* J Cell Sci, 2000. **113 (Pt 12)**: p. 2299-308.
54. Morgan, J.E., et al., *Long-term persistence and migration of myogenic cells injected into pre-irradiated muscles of mdx mice.* J Neurol Sci, 1993. **115**(2): p. 191-200.
55. Morgan, J.E., R.M. Fletcher, and T.A. Partridge, *Yields of muscle from myogenic cells implanted into young and old mdx hosts.* Muscle Nerve, 1996. **19**(2): p. 132-9.
56. Partridge, T.A., et al., *Conversion of mdx myofibres from dystrophin-negative to -positive by injection of normal myoblasts.* Nature, 1989. **337**(6203): p. 176-9.
57. Morgan, J.E., E.P. Hoffman, and T.A. Partridge, *Normal myogenic cells from newborn mice restore normal histology to degenerating muscles of the mdx mouse.* J Cell Biol, 1990. **111**(6 Pt 1): p. 2437-49.

58. Huard, J., et al., *Utilization of an antibody specific for human dystrophin to follow myoblast transplantation in nude mice.* Cell Transplant, 1993. **2**(2): p. 113-8.
59. Huard, J., et al., *Human myoblast transplantation: preliminary results of 4 cases.* Muscle Nerve, 1992. **15**(5): p. 550-60.
60. Law, P.K., et al., *Myoblast transfer therapy for Duchenne muscular dystrophy.* Acta Paediatr Jpn, 1991. **33**(2): p. 206-15.
61. Law, P.K., et al., *Dystrophin production induced by myoblast transfer therapy in Duchenne muscular dystrophy.* Lancet, 1990. **336**(8707): p. 114-5.
62. Hoffman, E.P., et al., *Somatic reversion/suppression of the mouse mdx phenotype in vivo.* J Neurol Sci, 1990. **99**(1): p. 9-25.
63. Miller, R.G., et al., *Myoblast implantation in Duchenne muscular dystrophy: the San Francisco study.* Muscle Nerve, 1997. **20**(4): p. 469-78.
64. Gussoni, E., et al., *Normal dystrophin transcripts detected in Duchenne muscular dystrophy patients after myoblast transplantation.* Nature, 1992. **356**(6368): p. 435-8.
65. Morandi, L., et al., *Lack of mRNA and dystrophin expression in DMD patients three months after myoblast transfer.* Neuromuscul Disord, 1995. **5**(4): p. 291-5.
66. Asakura, A., et al., *Myogenic specification of side population cells in skeletal muscle.* J Cell Biol, 2002. **159**(1): p. 123-34.
67. Gussoni, E., et al., *Dystrophin expression in the mdx mouse restored by stem cell transplantation.* Nature, 1999. **401**(6751): p. 390-4.
68. Bachrach, E., et al., *Muscle engraftment of myogenic progenitor cells following intraarterial transplantation.* Muscle Nerve, 2006. **34**(1): p. 44-52.
69. Qu-Petersen, Z., et al., *Identification of a novel population of muscle stem cells in mice: potential for muscle regeneration.* J Cell Biol, 2002. **157**(5): p. 851-64.
70. Huard, J., B. Cao, and Z. Qu-Petersen, *Muscle-derived stem cells: potential for muscle regeneration.* Birth Defects Res C Embryo Today, 2003. **69**(3): p. 230-7.
71. Cao, B., et al., *Muscle stem cells differentiate into haematopoietic lineages but retain myogenic potential.* Nat Cell Biol, 2003. **5**(7): p. 640-6.
72. Lee-Pullen, T.F., et al., *Superior survival and proliferation after transplantation of myoblasts obtained from adult mice compared with neonatal mice.* Transplantation, 2004. **78**(8): p. 1172-6.
73. Minasi, M.G., et al., *The meso-angioblast: a multipotent, self-renewing cell that originates from the dorsal aorta and differentiates into most mesodermal tissues.* Development, 2002. **129**(11): p. 2773-83.
74. Sampaolesi, M., et al., *Cell therapy of alpha-sarcoglycan null dystrophic mice through intra-arterial delivery of mesoangioblasts.* Science, 2003. **301**(5632): p. 487-92.
75. Dellavalle, A., et al., *Pericytes of human skeletal muscle are myogenic precursors distinct from satellite cells.* Nat Cell Biol, 2007. **9**(3): p. 255-67.
76. Gussoni, E., et al., *Long-term persistence of donor nuclei in a Duchenne muscular dystrophy patient receiving bone marrow transplantation.* J Clin Invest, 2002. **110**(6): p. 807-14.
77. Sherwood, R.I., et al., *Determinants of skeletal muscle contributions from circulating cells, bone marrow cells, and hematopoietic stem cells.* Stem Cells, 2004. **22**(7): p. 1292-304.
78. Prockop, D.J., *Marrow stromal cells as stem cells for nonhematopoietic tissues.* Science, 1997. **276**(5309): p. 71-4.

79. Conboy, I.M. and T.A. Rando, *The regulation of Notch signaling controls satellite cell activation and cell fate determination in postnatal myogenesis.* Dev Cell, 2002. **3**(3): p. 397-409.
80. Dezawa, M., et al., *Bone marrow stromal cells generate muscle cells and repair muscle degeneration.* Science, 2005. **309**(5732): p. 314-7.
81. Rohwedel, J., et al., *Muscle cell differentiation of embryonic stem cells reflects myogenesis in vivo: developmentally regulated expression of myogenic determination genes and functional expression of ionic currents.* Dev Biol, 1994. **164**(1): p. 87-101.
82. Evans, M.J. and M.H. Kaufman, *Establishment in culture of pluripotential cells from mouse embryos.* Nature, 1981. **292**(5819): p. 154-6.
83. Martin, G.R., *Isolation of a pluripotent cell line from early mouse embryos cultured in medium conditioned by teratocarcinoma stem cells.* Proc Natl Acad Sci U S A, 1981. **78**(12): p. 7634-8.
84. Thomson, J.A., et al., *Embryonic stem cell lines derived from human blastocysts.* Science, 1998. **282**(5391): p. 1145-7.
85. Keller, G.M., *In vitro differentiation of embryonic stem cells.* Curr Opin Cell Biol, 1995. **7**(6): p. 862-9.
86. Smith, A.G., *Embryo-derived stem cells: of mice and men.* Annu Rev Cell Dev Biol, 2001. **17**: p. 435-62.
87. Smith, A.G., et al., *Inhibition of pluripotential embryonic stem cell differentiation by purified polypeptides.* Nature, 1988. **336**(6200): p. 688-90.
88. Williams, R.L., et al., *Myeloid leukaemia inhibitory factor maintains the developmental potential of embryonic stem cells.* Nature, 1988. **336**(6200): p. 684-7.
89. Niwa, H., et al., *Self-renewal of pluripotent embryonic stem cells is mediated via activation of STAT3.* Genes Dev, 1998. **12**(13): p. 2048-60.
90. Ying, Q.L., et al., *BMP induction of Id proteins suppresses differentiation and sustains embryonic stem cell self-renewal in collaboration with STAT3.* Cell, 2003. **115**(3): p. 281-92.
91. Amit, M., et al., *Clonally derived human embryonic stem cell lines maintain pluripotency and proliferative potential for prolonged periods of culture.* Dev Biol, 2000. **227**(2): p. 271-8.
92. Xu, C., et al., *Feeder-free growth of undifferentiated human embryonic stem cells.* Nat Biotechnol, 2001. **19**(10): p. 971-4.
93. Xu, R.H., et al., *BMP4 initiates human embryonic stem cell differentiation to trophoblast.* Nat Biotechnol, 2002. **20**(12): p. 1261-4.
94. Xu, R.H., et al., *Basic FGF and suppression of BMP signaling sustain undifferentiated proliferation of human ES cells.* Nat Methods, 2005. **2**(3): p. 185-90.
95. Amit, M. and J. Itskovitz-Eldor, *Derivation and spontaneous differentiation of human embryonic stem cells.* J Anat, 2002. **200**(Pt 3): p. 225-32.
96. Heins, N., et al., *Derivation, characterization, and differentiation of human embryonic stem cells.* Stem Cells, 2004. **22**(3): p. 367-76.
97. Niwa, H., *How is pluripotency determined and maintained?* Development, 2007. **134**(4): p. 635-46.
98. Nichols, J., et al., *Formation of pluripotent stem cells in the mammalian embryo depends on the POU transcription factor Oct4.* Cell, 1998. **95**(3): p. 379-91.

99. Yuan, H., et al., *Developmental-specific activity of the FGF-4 enhancer requires the synergistic action of Sox2 and Oct-3.* Genes Dev, 1995. **9**(21): p. 2635-45.
100. Rodda, D.J., et al., *Transcriptional regulation of nanog by OCT4 and SOX2.* J Biol Chem, 2005. **280**(26): p. 24731-7.
101. Kuroda, T., et al., *Octamer and Sox elements are required for transcriptional cis regulation of Nanog gene expression.* Mol Cell Biol, 2005. **25**(6): p. 2475-85.
102. Chambers, I., et al., *Functional expression cloning of Nanog, a pluripotency sustaining factor in embryonic stem cells.* Cell, 2003. **113**(5): p. 643-55.
103. Mitsui, K., et al., *The homeoprotein Nanog is required for maintenance of pluripotency in mouse epiblast and ES cells.* Cell, 2003. **113**(5): p. 631-42.
104. Turksen, K., *Embryonic stem cells : methods and protocols*. Methods in molecular biology ; v. 185. 2002, Totowa, N.J.: Humana Press. xvi, 499 , [8] of col. plates.
105. Martin, G.R. and M.J. Evans, *Differentiation of clonal lines of teratocarcinoma cells: formation of embryoid bodies in vitro.* Proc Natl Acad Sci U S A, 1975. **72**(4): p. 1441-5.
106. Coucouvanis, E. and G.R. Martin, *Signals for death and survival: a two-step mechanism for cavitation in the vertebrate embryo.* Cell, 1995. **83**(2): p. 279-87.
107. Fraichard, A., et al., *In vitro differentiation of embryonic stem cells into glial cells and functional neurons.* J Cell Sci, 1995. **108 (Pt 10)**: p. 3181-8.
108. Bain, G., et al., *Embryonic stem cells express neuronal properties in vitro.* Dev Biol, 1995. **168**(2): p. 342-57.
109. Strubing, C., et al., *Differentiation of pluripotent embryonic stem cells into the neuronal lineage in vitro gives rise to mature inhibitory and excitatory neurons.* Mech Dev, 1995. **53**(2): p. 275-87.
110. Doetschman, T.C., et al., *The in vitro development of blastocyst-derived embryonic stem cell lines: formation of visceral yolk sac, blood islands and myocardium.* J Embryol Exp Morphol, 1985. **87**: p. 27-45.
111. Schmitt, R.M., E. Bruyns, and H.R. Snodgrass, *Hematopoietic development of embryonic stem cells in vitro: cytokine and receptor gene expression.* Genes Dev, 1991. **5**(5): p. 728-40.
112. Wiles, M.V. and G. Keller, *Multiple hematopoietic lineages develop from embryonic stem (ES) cells in culture.* Development, 1991. **111**(2): p. 259-67.
113. Keller, G., et al., *Hematopoietic commitment during embryonic stem cell differentiation in culture.* Mol Cell Biol, 1993. **13**(1): p. 473-86.
114. Palacios, R., E. Golunski, and J. Samaridis, *In vitro generation of hematopoietic stem cells from an embryonic stem cell line.* Proc Natl Acad Sci U S A, 1995. **92**(16): p. 7530-4.
115. Kennedy, M., et al., *A common precursor for primitive erythropoiesis and definitive haematopoiesis.* Nature, 1997. **386**(6624): p. 488-93.
116. Maltsev, V.A., et al., *Cardiomyocytes differentiated in vitro from embryonic stem cells developmentally express cardiac-specific genes and ionic currents.* Circ Res, 1994. **75**(2): p. 233-44.
117. Maltsev, V.A., et al., *Embryonic stem cells differentiate in vitro into cardiomyocytes representing sinusnodal, atrial and ventricular cell types.* Mech Dev, 1993. **44**(1): p. 41-50.

118. Kouskoff, V., et al., *Sequential development of hematopoietic and cardiac mesoderm during embryonic stem cell differentiation.* Proc Natl Acad Sci U S A, 2005. **102**(37): p. 13170-5.
119. Kubo, A., et al., *Development of definitive endoderm from embryonic stem cells in culture.* Development, 2004. **131**(7): p. 1651-62.
120. Leahy, A., et al., *Use of developmental marker genes to define temporal and spatial patterns of differentiation during embryoid body formation.* J Exp Zool, 1999. **284**(1): p. 67-81.
121. Fehling, H.J., et al., *Tracking mesoderm induction and its specification to the hemangioblast during embryonic stem cell differentiation.* Development, 2003. **130**(17): p. 4217-27.
122. Haub, O. and M. Goldfarb, *Expression of the fibroblast growth factor-5 gene in the mouse embryo.* Development, 1991. **112**(2): p. 397-406.
123. Varlet, I., J. Collignon, and E.J. Robertson, *nodal expression in the primitive endoderm is required for specification of the anterior axis during mouse gastrulation.* Development, 1997. **124**(5): p. 1033-44.
124. Park, C., et al., *A hierarchical order of factors in the generation of FLK1- and SCL-expressing hematopoietic and endothelial progenitors from embryonic stem cells.* Development, 2004. **131**(11): p. 2749-62.
125. Nakano, T., H. Kodama, and T. Honjo, *Generation of lymphohematopoietic cells from embryonic stem cells in culture.* Science, 1994. **265**(5175): p. 1098-101.
126. Klug, M.G., M.H. Soonpaa, and L.J. Field, *DNA synthesis and multinucleation in embryonic stem cell-derived cardiomyocytes.* Am J Physiol, 1995. **269**(6 Pt 2): p. H1913-21.
127. Klug, M.G., et al., *Genetically selected cardiomyocytes from differentiating embronic stem cells form stable intracardiac grafts.* J Clin Invest, 1996. **98**(1): p. 216-24.
128. Nishikawa, S.I., et al., *Progressive lineage analysis by cell sorting and culture identifies FLK1+VE-cadherin+ cells at a diverging point of endothelial and hemopoietic lineages.* Development, 1998. **125**(9): p. 1747-57.
129. Yamashita, J., et al., *Flk1-positive cells derived from embryonic stem cells serve as vascular progenitors.* Nature, 2000. **408**(6808): p. 92-6.
130. Dang, S.M., et al., *Controlled, scalable embryonic stem cell differentiation culture.* Stem Cells, 2004. **22**(3): p. 275-82.
131. Lee, S.H., et al., *Efficient generation of midbrain and hindbrain neurons from mouse embryonic stem cells.* Nat Biotechnol, 2000. **18**(6): p. 675-9.
132. Kim, J.H., et al., *Dopamine neurons derived from embryonic stem cells function in an animal model of Parkinson's disease.* Nature, 2002. **418**(6893): p. 50-6.
133. Lumelsky, N., et al., *Differentiation of embryonic stem cells to insulin-secreting structures similar to pancreatic islets.* Science, 2001. **292**(5520): p. 1389-94.
134. Gouon-Evans, V., et al., *BMP-4 is required for hepatic specification of mouse embryonic stem cell-derived definitive endoderm.* Nat Biotechnol, 2006. **24**(11): p. 1402-11.
135. Dekel, I., et al., *Conditional conversion of ES cells to skeletal muscle by an exogenous MyoD1 gene.* New Biol, 1992. **4**(3): p. 217-24.
136. Shani, M., et al., *The consequences of a constitutive expression of MyoD1 in ES cells and mouse embryos.* Symp Soc Exp Biol, 1992. **46**: p. 19-36.

137. Dinsmore, J., et al., *Embryonic stem cells differentiated in vitro as a novel source of cells for transplantation.* Cell Transplant, 1996. **5**(2): p. 131-43.
138. Lakshmipathy, U., et al., *Efficient transfection of embryonic and adult stem cells.* Stem Cells, 2004. **22**(4): p. 531-43.
139. Lorenz, P., U. Harnack, and R. Morgenstern, *Efficient gene transfer into murine embryonic stem cells by nucleofection.* Biotechnol Lett, 2004. **26**(20): p. 1589-92.
140. Ma, H., et al., *Mouse embryonic stem cells efficiently lipofected with nuclear localization peptide result in a high yield of chimeric mice and retain germline transmission potency.* Methods, 2004. **33**(2): p. 113-20.
141. Kawabata, K., et al., *Efficient gene transfer into mouse embryonic stem cells with adenovirus vectors.* Mol Ther, 2005. **12**(3): p. 547-54.
142. Cherry, S.R., et al., *Retroviral expression in embryonic stem cells and hematopoietic stem cells.* Mol Cell Biol, 2000. **20**(20): p. 7419-26.
143. Smith-Arica, J.R., et al., *Infection efficiency of human and mouse embryonic stem cells using adenoviral and adeno-associated viral vectors.* Cloning Stem Cells, 2003. **5**(1): p. 51-62.
144. Burton, E.A., et al., *Multiple applications for replication-defective herpes simplex virus vectors.* Stem Cells, 2001. **19**(5): p. 358-77.
145. Sandri-Goldin, R.M. and G.E. Mendoza, *A herpesvirus regulatory protein appears to act post-transcriptionally by affecting mRNA processing.* Genes Dev, 1992. **6**(5): p. 848-63.
146. Sandri-Goldin, R.M., M.K. Hibbard, and M.A. Hardwicke, *The C-terminal repressor region of herpes simplex virus type 1 ICP27 is required for the redistribution of small nuclear ribonucleoprotein particles and splicing factor SC35; however, these alterations are not sufficient to inhibit host cell splicing.* J Virol, 1995. **69**(10): p. 6063-76.
147. Roizman, B., R.J. Whitley, and C. Lopez, *The Human herpesviruses*. 1993, New York: Raven Press. xi, 433.
148. Fields, B.N., et al., *Fields' virology*. 4th ed. 2001, Philadelphia: Lippincott Williams & Wilkins. 2 v. (xix, 3087, 72).
149. Everett, R.D., *Construction and characterization of herpes simplex virus type 1 mutants with defined lesions in immediate early gene 1.* J Gen Virol, 1989. **70 (Pt 5)**: p. 1185-202.
150. Cai, W., et al., *The herpes simplex virus type 1 regulatory protein ICP0 enhances virus replication during acute infection and reactivation from latency.* J Virol, 1993. **67**(12): p. 7501-12.
151. Sacks, W.R. and P.A. Schaffer, *Deletion mutants in the gene encoding the herpes simplex virus type 1 immediate-early protein ICP0 exhibit impaired growth in cell culture.* J Virol, 1987. **61**(3): p. 829-39.
152. Everett, R.D., A. Orr, and M. Elliott, *High level expression and purification of herpes simplex virus type 1 immediate early polypeptide Vmw110.* Nucleic Acids Res, 1991. **19**(22): p. 6155-61.
153. Everett, R.D., M. Meredith, and A. Orr, *The ability of herpes simplex virus type 1 immediate-early protein Vmw110 to bind to a ubiquitin-specific protease contributes to its roles in the activation of gene expression and stimulation of virus replication.* J Virol, 1999. **73**(1): p. 417-26.

154. Maul, G.G., H.H. Guldner, and J.G. Spivack, *Modification of discrete nuclear domains induced by herpes simplex virus type 1 immediate early gene 1 product (ICP0).* J Gen Virol, 1993. **74 (Pt 12)**: p. 2679-90.
155. Lomonte, P., K.F. Sullivan, and R.D. Everett, *Degradation of nucleosome-associated centromeric histone H3-like protein CENP-A induced by herpes simplex virus type 1 protein ICP0.* J Biol Chem, 2001. **276**(8): p. 5829-35.
156. Everett, R.D., et al., *Specific destruction of kinetochore protein CENP-C and disruption of cell division by herpes simplex virus immediate-early protein Vmw110.* Embo J, 1999. **18**(6): p. 1526-38.
157. Parkinson, J., S.P. Lees-Miller, and R.D. Everett, *Herpes simplex virus type 1 immediate-early protein vmw110 induces the proteasome-dependent degradation of the catalytic subunit of DNA-dependent protein kinase.* J Virol, 1999. **73**(1): p. 650-7.
158. Boutell, C., S. Sadis, and R.D. Everett, *Herpes simplex virus type 1 immediate-early protein ICP0 and is isolated RING finger domain act as ubiquitin E3 ligases in vitro.* J Virol, 2002. **76**(2): p. 841-50.
159. Van Sant, C., et al., *The infected cell protein 0 of herpes simplex virus 1 dynamically interacts with proteasomes, binds and activates the cdc34 E2 ubiquitin-conjugating enzyme, and possesses in vitro E3 ubiquitin ligase activity.* Proc Natl Acad Sci U S A, 2001. **98**(15): p. 8815-20.
160. Wu, N., et al., *Prolonged gene expression and cell survival after infection by a herpes simplex virus mutant defective in the immediate-early genes encoding ICP4, ICP27, and ICP22.* J Virol, 1996. **70**(9): p. 6358-69.
161. Samaniego, L.A., L. Neiderhiser, and N.A. DeLuca, *Persistence and expression of the herpes simplex virus genome in the absence of immediate-early proteins.* J Virol, 1998. **72**(4): p. 3307-20.
162. Preston, C.M. and M.J. Nicholl, *Repression of gene expression upon infection of cells with herpes simplex virus type 1 mutants impaired for immediate-early protein synthesis.* J Virol, 1997. **71**(10): p. 7807-13.
163. Preston, C.M., R. Mabbs, and M.J. Nicholl, *Construction and characterization of herpes simplex virus type 1 mutants with conditional defects in immediate early gene expression.* Virology, 1997. **229**(1): p. 228-39.
164. Chen, J. and S. Silverstein, *Herpes simplex viruses with mutations in the gene encoding ICP0 are defective in gene expression.* J Virol, 1992. **66**(5): p. 2916-27.
165. Cai, W. and P.A. Schaffer, *Herpes simplex virus type 1 ICP0 regulates expression of immediate-early, early, and late genes in productively infected cells.* J Virol, 1992. **66**(5): p. 2904-15.
166. Hobbs, W.E., et al., *Efficient activation of viral genomes by levels of herpes simplex virus ICP0 insufficient to affect cellular gene expression or cell survival.* J Virol, 2001. **75**(7): p. 3391-403.
167. Tompers, D.M. and P.A. Labosky, *Electroporation of murine embryonic stem cells: a step-by-step guide.* Stem Cells, 2004. **22**(3): p. 243-9.
168. Kosaka, Y., et al., *Lentivirus-based gene delivery in mouse embryonic stem cells.* Artif Organs, 2004. **28**(3): p. 271-7.
169. Krisky, D.M., et al., *Deletion of multiple immediate-early genes from herpes simplex virus reduces cytotoxicity and permits long-term gene expression in neurons.* Gene Ther, 1998. **5**(12): p. 1593-603.

170. Niranjan, A., et al., *Treatment of rat gliosarcoma brain tumors by HSV-based multigene therapy combined with radiosurgery.* Mol Ther, 2003. **8**(4): p. 530-42.
171. Livak, K.J. and T.D. Schmittgen, *Analysis of relative gene expression data using real-time quantitative PCR and the 2(-Delta Delta C(T)) Method.* Methods, 2001. **25**(4): p. 402-8.
172. Murphy, C.L. and J.M. Polak, *Differentiating embryonic stem cells: GAPDH, but neither HPRT nor beta-tubulin is suitable as an internal standard for measuring RNA levels.* Tissue Eng, 2002. **8**(4): p. 551-9.
173. Hobbs, W.E., 2nd and N.A. DeLuca, *Perturbation of cell cycle progression and cellular gene expression as a function of herpes simplex virus ICP0.* J Virol, 1999. **73**(10): p. 8245-55.
174. Hancock, M.H., J.A. Corcoran, and J.R. Smiley, *Herpes simplex virus regulatory proteins VP16 and ICP0 counteract an innate intranuclear barrier to viral gene expression.* Virology, 2006. **352**(1): p. 237-52.
175. Yao, F. and P.A. Schaffer, *An activity specified by the osteosarcoma line U2OS can substitute functionally for ICP0, a major regulatory protein of herpes simplex virus type 1.* J Virol, 1995. **69**(10): p. 6249-58.
176. Itskovitz-Eldor, J., et al., *Differentiation of human embryonic stem cells into embryoid bodies compromising the three embryonic germ layers.* Mol Med, 2000. **6**(2): p. 88-95.
177. Goins, W.F., et al., *Herpes simplex virus type 1 vector-mediated expression of nerve growth factor protects dorsal root ganglion neurons from peroxide toxicity.* J Virol, 1999. **73**(1): p. 519-32.
178. Chattopadhyay, M., et al., *In vivo gene therapy for pyridoxine-induced neuropathy by herpes simplex virus-mediated gene transfer of neurotrophin-3.* Ann Neurol, 2002. **51**(1): p. 19-27.
179. Puskovic, V., et al., *Prolonged biologically active transgene expression driven by HSV LAP2 in brain in vivo.* Mol Ther, 2004. **10**(1): p. 67-75.
180. Samaniego, L.A., N. Wu, and N.A. DeLuca, *The herpes simplex virus immediate-early protein ICP0 affects transcription from the viral genome and infected-cell survival in the absence of ICP4 and ICP27.* J Virol, 1997. **71**(6): p. 4614-25.
181. Rice, S.A., et al., *Herpes simplex virus immediate-early protein ICP22 is required for viral modification of host RNA polymerase II and establishment of the normal viral transcription program.* J Virol, 1995. **69**(9): p. 5550-9.
182. Torrente, Y., et al., *Intraarterial injection of muscle-derived CD34(+)Sca-1(+) stem cells restores dystrophin in mdx mice.* J Cell Biol, 2001. **152**(2): p. 335-48.
183. Payne, T.R., et al., *Regeneration of dystrophin-expressing myocytes in the mdx heart by skeletal muscle stem cells.* Gene Ther, 2005. **12**(16): p. 1264-74.
184. Huard, J., et al., *High efficiency of muscle regeneration after human myoblast clone transplantation in SCID mice.* J Clin Invest, 1994. **93**(2): p. 586-99.
185. Marconi, P., et al., *Replication-defective herpes simplex virus vectors for gene transfer in vivo.* Proc Natl Acad Sci U S A, 1996. **93**(21): p. 11319-20.
186. Schmeisser, F. and J.P. Weir, *Cloning of replication-incompetent herpes simplex viruses as bacterial artificial chromosomes to facilitate development of vectors for gene delivery into differentiated neurons.* Hum Gene Ther, 2006. **17**(1): p. 93-104.
187. Srinivasan, R., et al., *An HSV vector system for selection of ligand-gated ion channel modulators.* Nat Methods, 2007. **4**(9): p. 733-9.

188. Trausch-Azar, J.S., et al., *Ubiquitin-Proteasome-mediated degradation of Id1 is modulated by MyoD.* J Biol Chem, 2004. **279**(31): p. 32614-9.
189. Vinals, F. and F. Ventura, *Myogenin protein stability is decreased by BMP-2 through a mechanism implicating Id1.* J Biol Chem, 2004. **279**(44): p. 45766-72.
190. Gundersen, K., et al., *Overexpression of myogenin in muscles of transgenic mice: interaction with Id-1, negative crossregulation of myogenic factors, and induction of extrasynaptic acetylcholine receptor expression.* Mol Cell Biol, 1995. **15**(12): p. 7127-34.
191. Schulze, M., et al., *Mesenchymal stem cells are recruited to striated muscle by NFAT/IL-4-mediated cell fusion.* Genes Dev, 2005. **19**(15): p. 1787-98.
192. Puri, P.L., et al., *p300 is required for MyoD-dependent cell cycle arrest and muscle-specific gene transcription.* Embo J, 1997. **16**(2): p. 369-83.
193. Shiraishi, S., et al., *TBP-interacting protein 120B (TIP120B)/cullin-associated and neddylation-dissociated 2 (CAND2) inhibits SCF-dependent ubiquitination of myogenin and accelerates myogenic differentiation.* J Biol Chem, 2007. **282**(12): p. 9017-28.
194. Goulding, M.D., et al., *Pax-3, a novel murine DNA binding protein expressed during early neurogenesis.* Embo J, 1991. **10**(5): p. 1135-47.
195. Natoli, T.A., et al., *Positive and negative DNA sequence elements are required to establish the pattern of Pax3 expression.* Development, 1997. **124**(3): p. 617-26.
196. Milewski, R.C., et al., *Identification of minimal enhancer elements sufficient for Pax3 expression in neural crest and implication of Tead2 as a regulator of Pax3.* Development, 2004. **131**(4): p. 829-37.
197. Grifone, R., et al., *Six1 and Six4 homeoproteins are required for Pax3 and Mrf expression during myogenesis in the mouse embryo.* Development, 2005.
198. Downing, J.R., et al., *Multiplex RT-PCR assay for the differential diagnosis of alveolar rhabdomyosarcoma and Ewing's sarcoma.* Am J Pathol, 1995. **146**(3): p. 626-34.
199. Relaix, F., et al., *The transcriptional activator PAX3-FKHR rescues the defects of Pax3 mutant mice but induces a myogenic gain-of-function phenotype with ligand-independent activation of Met signaling in vivo.* Genes Dev, 2003. **17**(23): p. 2950-65.
200. Kambara, H., et al., *An oncolytic HSV-1 mutant expressing ICP34.5 under control of a nestin promoter increases survival of animals even when symptomatic from a brain tumor.* Cancer Res, 2005. **65**(7): p. 2832-9.
201. Brown, C.B., et al., *Identification of a hypaxial somite enhancer element regulating Pax3 expression in migrating myoblasts and characterization of hypaxial muscle Cre transgenic mice.* Genesis, 2005. **41**(4): p. 202-9.